FRIEDRICH-SCHILLER-
UNIVERSITÄT
JENA

UNIVERSITÄTS
KLINIKUM
jena

DISSERTATION

zur Erlangung des akademischen Grades doctor
rerum naturalium (Dr. rer. nat.)

Unravelling the therapeutic potential of erythropoietin signaling in hemolytic-uremic syndrome in mice – A preclinical work-up from model establishment to an interventional study

---

vorgelegt dem Rat der Medizinischen Fakultät
der Friedrich-Schiller-Universität Jena von

Sophie Dennhardt

Jena, 15.11.2022

Gutachter *(akademischer Grad, Vor- und Nachname sowie Wirkungsort)*

1. **Prof. Dr. Sina M. Coldewey, PhD, Universitätsklinikum Jena**
2. **Prof. Dr. Carsten Hoffmann, Universitätsklinikum Jena**
3. **Prof. Dr. Christoph Thiemermann, PhD, Queen Mary Universität London**

Tag der öffentlichen Verteidigung: 17.10.2023

Table of Content

Abbreviations

A

AKI	*acute kidney injury*
ARA290	*pyroglutamate helix B surface peptide*

C

CEPO	*carbamylated EPO, carbamylated EPO*
CERA	*continuous erythropoiesis receptor activator*
CKD	*chronic kidney disease*
CXCL	*chemokine (C-X-C motif) ligand*

D

D-	*diarrhea-negative*
D+	*diarrhea-positive*
D1 domain	*membrane-distal domain*
D2 domain	*membrane-proximal domain*
DAMPs	*danger-associated molecular patterns*
DGKE	*diacylglycerol kinase epsilon*
DNA	*deoxyribonucleic acid*

E

EHEC	*enterohemorrhagic Escherichia coli*
EMA	*European Medicines Agency*
eNOS	*endothelial nitric oxide synthase*
EPO	*erythropoietin*
EPO-R	*erythropoietin receptor*
ESAs	*erythropoiesis stimulating agents*

F

FDA	*U.S. Food and Drug Administration*

G

Gb3	*globotriaosylceramide receptor*
GSK3β	*glycogen synthase kinase 3β*

H

Hb	*hemoglobin*
HIV	*human immunodeficiency virus*

HUS	*hemolytic-uremic syndrome*
I	
i.p.	*intraperitoneally*
i.v.intravenous	
IRR	*innate repair receptor*
J	
JAK2	*Janus-like kinase 2*
L	
LDH	*lactate dehydrogenase*
LPS	*lipopolysaccharide*
M	
MAHA	*microangiopathic hemolytic anemia*
MAPK	*mitogen-activated protein kinases*
N	
NF-κB	*nuclear-factor 'kappa-light-chain-enhancer' of activated B-cells*
P	
pHBSP	*pyroglutamate helix B surface peptide*
PI3Ks	*phosphoinositide 3-kinases*
R	
RBC	*red blood cell*
ROS	*reactive oxygen species*
S	
STAT	*signal transducer and activator of transcription*
STEC	*Shiga-toxin-producing enterohemorrhagic E. coli*, *Shiga-toxin-producing enterohemorrhagic E. coli*
STEC-HUS	*HUS caused by Shiga-toxin-producing Escherichia coli*
Stx	*Shiga toxin*
T	
TM	*thrombomodulin*
TMAs	*thrombotic microangiopathies*
TNF-α	*tumor-necrosis factor α*
B	
βCR	*β-common receptor*

Summary

Typical hemolytic-uremic syndrome (HUS) occurs as a severe complication of an infection with enterohemorrhagic *Escherichia coli* (EHEC) and is one of the major causes of acute and chronic renal failure in children. HUS is clinically characterized by a symptom triad comprised of acute kidney injury (AKI), microangiopathic hemolytic anemia and thrombocytopenia. There is no approved specific therapy, intensive care is provided supportively. Erythropoietin (EPO), a hematopoietic hormone, confers tissue-protective effects that attenuated AKI in several other conditions such as sepsis. The tissue-protective effects of EPO are mediated via a heteromer of the EPO receptor (EPO-R) and the β-common receptor. This receptor can also be selectively activated by non-hematopoietic structure analogs of EPO such as pyroglutamate helix B surface peptide (pHBSP). The overall objective of this thesis was the preclinical assessment of the potential of EPO and pHBSP in the treatment of HUS. Firstly, two murine models of HUS have been established and extensively characterized by laboratory chemistry as well as histology and immunohistochemistry (manuscript I). Thereby, it was demonstrated that a single high dose of Shiga toxin (Stx) applied to the tail vein of mice resulted in an acute disease progression with prerenal mechanisms of AKI prevailing. In contrast, three sublethal doses of Stx on days 0, 3 and 6 of the experiment induced subacute disease progression with predominantly intrarenal mechanisms of AKI. In the following manuscript, EPO plasma levels of different species with HUS (humans, pigs, mice) were measured and an interventional study with EPO and pHBSP was performed applying the subacute model of HUS (manuscript II). Significant increases in plasma EPO were observed in all three species during HUS indicating a role of EPO signaling in the pathogenesis. EPO or pHBSP treatment in mice suffering from experimental HUS improved 7-day survival and reduced oxidative stress in the kidneys. pHBSP attenuated oxidative and nitrosative stress, stabilized tubular epithelial barriers and reduced the expression of KIM-1. Within the framework of this thesis, two relevant murine models suitable for the performance of preclinical interventional studies have been established. In the context of such a preclinical study, it was demonstrated that the modulation of the EPO/β-common-receptor axis attenuates disease severity in HUS. Thereby, this thesis provides the preclinical groundwork for further examinations in the repurposing of EPO and the implementation of pHBSP for the treatment of HUS.

Zusammenfassung

Das typische hämolytisch-urämische Syndrom (HUS) stellt eine schwerwiegende Komplikation einer Infektion mit enterohämorrhagischen *Escherichia coli* (EHEC) dar und ist eine der häufigsten Ursachen für akutes und chronisches Nierenversagen im Kindesalter. Klinisch gekennzeichnet ist das HUS durch eine Symptomtrias aus akutem Nierenversagen, mikroangiopathischer hämolytischer Anämie sowie Thrombozytopenie. Eine zugelassene, spezifische Therapie steht nicht zur Verfügung, die intensivmedizinische Behandlung erfolgt ausschließlich supportiv. Erythropoietin (EPO), ein hämatopoietisch wirkendes Hormon, besitzt zusätzliche gewebeprotektive Effekte, welche in verschiedenen Krankheitsbildern, unter anderem der Sepsis, ein akutes Nierenversagen verhindern konnten. Diese gewebeprotektiven Effekte beruhen auf der Aktivierung eines Heteromers aus EPO-Rezeptor und *β-common*-Rezeptor, der selektiv auch durch nicht-hämatopoietische Strukturanaloga des EPOs wie zum Beispiel das *pyroglutamate helix B surface peptide* (pHBSP) reguliert werden kann. In der vorliegenden Arbeit sollte das Potential von EPO und pHBSP in der Therapie des HUS präklinisch untersucht werden. Dazu wurden zunächst zwei murine Modelle des HUS etabliert und umfassend laborchemisch sowie histologisch und immunhistochemisch charakterisiert (Manuskript I). Dabei zeigte sich, dass die einmalige, hochdosierte Applikation von Shiga-Toxin (Stx) über die Schwanzvene zu einem akuten Verlauf der Erkrankung mit vordergründig prärenalen Mechanismen des akuten Nierenversagens führte. Im Gegensatz dazu führten drei sublethale Dosen an den Tagen 0, 3 und 6 zu einem eher subakuten Verlauf, bei dem intrarenale Mechanismen des Nierenversagens im Vordergrund stehen. Anschließend wurden die EPO-Plasmaspiegel verschiedener Spezies (Mensch, Schwein und Maus) mit HUS bestimmt und im subakuten Modell des HUS eine Interventionsstudie mit EPO und pHBSP durchgeführt (Manuskript II). In allen drei Spezies zeigten sich signifikant erhöhte EPO-Plasmaspiegel im Rahmen einer HUS-Erkrankung, welche auf eine Rolle des EPO-Signalweges in der Pathogenese hindeutet. Die Behandlung von Mäusen, die an experimentellem HUS litten, mit EPO oder pHBSP verbesserte das 7-Tage-Überleben und reduzierte den oxidativen Stress in der Niere. pHBSP verhinderte oxidativen und nitrosativen Stress in der Niere vollkommen, stabilisierte die tubuläre epitheliale Barriere und reduzierte die Expression von KIM-1. Insgesamt wurden im Rahmen dieser Arbeit zwei relevante murine Modelle des HUS etabliert, die sich für

die Durchführung präklinischer Interventionsstudien eignen. Im Rahmen einer solchen präklinischen Studie konnte gezeigt werden, dass die pharmakologische Modulation der *EPO/ß-common*-Rezeptorachse die Krankheitsschwere im HUS deutlich reduziert. Damit liefert diese Arbeit den präklinischen Grundstein für weitere Untersuchungen zur Umwidmung von EPO und zur Verwendung von pHBSP für die Therapie des HUS.

1. Introduction

1.1 Hemolytic-uremic syndrome (HUS)

1.1.1 Definition and clinical presentation of STEC-HUS

The hemolytic-uremic syndrome belongs to the thrombotic microangiopathies (TMAs) and is clinically defined by a symptomatic trias of microangiopathic hemolytic anemia (MAHA), thrombocytopenia and acute kidney injury (AKI). HUS was first described in 1955 by Gasser and Gautier (Gasser *et al.* 1955). Historically, the differentiation of HUS was carried out exclusively according to clinical presentation into diarrhea-positive (D+) or diarrhea-negative (D-) HUS. This original classification was revised and adapted manifold, so that to date the classification of HUS varies widely throughout the literature. However, in 2016, the International Haemolytic Uraemic Syndrome group introduced a new classification based on the etiology of HUS (Loirat *et al.* 2016). Briefly, four clusters of causes for the development of HUS were identified: HUS associated with underlying diseases or conditions (e. g. auto-immune diseases, malignancies or drug abuse), infection-associated HUS, cobalamin-C-defect HUS and atypical HUS that can be associated with genetic mutations in the complement pathway, diacylglycerol kinase epsilon (DGKE or without identified mutations (Loirat *et al.* 2016). Infection-induced HUS includes HUS caused by viruses such as influenza or the human immunodeficiency virus (HIV) and bacteria such as enterohemorrhagic *Escherichia coli* (EHEC), specifically those strains of EHEC producing the main virulence factor Shiga toxin (Stx, termed STEC) or *Staphylococcus pneumonia*.

This thesis addresses HUS caused by STECs (STEC-HUS) that accounts for approximately 85-90% of worldwide annual HUS cases (Constantinescu *et al.* 2004). Between 2 and 12 days after the onset of acute gastroenteritis, the three key symptoms of STEC-HUS (MAHA, thrombocytopenia and AKI) develop in 5-15% of patients with STEC-infection (Tarr *et al.* 2005). In 1983, Karmali *et al.* identified Stx as the main virulence factor responsible for STEC-HUS (Karmali *et al.* 1983). Stx occurs in two main subtypes called Stx1 and Stx2 (Mayer *et al.* 2012), the latter is more frequently associated with clinical outbreaks (Boerlin *et al.* 1999). STEC-HUS patients present with typical symptoms of renal failure such as high blood pressure, edema, oliguria, emesis and nausea as well as acute pallor (Gasser *et al.* 1955). Extrarenal complications may include myocardial (Thayu *et al.* 2003), neurological (Bauer *et al.*

2014), pancreatic (Robitaille *et al.* 1997) and respiratory (Piastra *et al.* 2004) involvement. Although the mortality of STEC-HUS decreased to 1-5% owing to progresses in supportive care, there is still a vast amount of up to one third of HUS survivors suffering from long-term sequela (Garg *et al.* 2003).

1.1.2 Epidemiology of STEC-HUS

Usually, STEC infections occur as individual cases that are conferred by the ingestion of undercooked meat, contaminated water or vegetables (Gerber *et al.* 2002) or by smear infection after contact with animals or infected persons (Goode *et al.* 2009). Although the incidence of STEC-infections is rather low in the European Union (1.5 per 100,000 inhabitants in 2020 (EFSA 2021)), they ranked in fourth position regarding reported foodborne gastrointestinal infections and foodborne outbreaks caused by bacterial agents in 2020 (EFSA 2021). Approximately 5–15% of STEC infections result in HUS (Byrne *et al.* 2015, Cummings *et al.* 2002, Jenssen *et al.* 2014, Lynn *et al.* 2005). These individual cases most frequently affect children under the age of 5 years (Byrne *et al.* 2015), e.g. 68% of the 2020 STEC-HUS cases in Germany occurred in children under 5 years (RKI 2021). Although HUS is a rather rare disease, food contamination can result in large unpredictable outbreaks such as the one observed 2011 in Northern Germany. During outbreaks, HUS incidence can rise to 20% of all STEC-infections and the age distribution can change substantially (Frank *et al.* 2011, RKI 2012). For example, STEC-HUS incidence in Germany was one magnitude higher than usual in the year of the 2011 outbreak (1.1 per 100,000 inhabitants in 2011 (RKI 2012) versus 0.07 in 2020 (RKI 2021)). In contrast, the general STEC-HUS incidence in Argentina, a country with extensive cattle-farming, was 0.67 in 2020 (MDS 2021).

1.1.3 Pathogenesis of STEC-HUS

After ingestion, STEC bacteria colonize the terminal ileum (Chong *et al.* 2007) and subsequently attach to colonic enterocytes forming attachment and effacing lesions (Jerse *et al.* 1991). Classical STEC strains are non-invasive (McKee and O'Brien 1995), thus they remain in the intestine and bacteremia is only sporadically observed (Chiurchiu *et al.* 2003, Manton *et al.* 2000) or associated with novel hybrid STEC strains (Soysal *et al.* 2016). Different mechanisms how Stx crosses the intestinal barrier and reaches the kidney are discussed to date. However, it is clear that endothelial injury is one of the most crucial steps in the pathophysiology of human HUS. To date, four different mechanisms of Stx-induced endothelial injury were

identified: I) direct toxicity of Stx via interaction with the globotriaosylceramide receptor (Gb3), II) immune cell activation and transmigration, III) generation of reactive oxygen species (ROS) and VI) induction of a pro-coagulant phenotype. A scanning electron microscopy study demonstrated that the damage conferred to the endothelium by Stx2 comprises apoptotic nature (Bauwens *et al.* 2011). This is in line with the ribotoxic effect of Stx resulting in an inhibition of protein translation and thereby apoptosis (Endo *et al.* 1987).

Activated neutrophils are key mediators of the kidney pathophysiology observed in HUS as they were shown to confer damage to both the endothelium (Forsyth *et al.* 1989, Fitzpatrick *et al.* 1992, Fernandez *et al.* 2007) as well as the glomerular basement membrane (Davies *et al.* 1978). Neutrophil invasion to the kidney is a histopathological feature commonly observed in human HUS patients (Inward *et al.* 1997) but also occurs in mice (Rutjes *et al.* 2002). Neutrophil activation positively correlates with elevated levels in plasma soluble thrombomodulin (TM) indicating a direct link between neutrophil activation and endothelial damage (Ishikawa *et al.* 2000). The key drivers of neutrophil migration to the kidney appear to be chemokine (C-X-C motif) ligand 1 and 2 (CXCL1 and CXCL2) as neutralization of these chemokines in the murine model reduced neutrophil invasion to the glomeruli by 85 % (Roche *et al.* 2007). The role of neutrophils in HUS pathophysiology is further undermined by the observation that in granulocyte-depleted mice, renal damage in response to Stx2 challenge is restricted to mild tubular lesions (Fernandez *et al.* 2006). Activated neutrophils can further contribute to renal damage by their enhanced tendency to the spontaneous release of neutrophil extracellular traps (a process known as NETosis) as these networks composed of deoxyribonucleic acid (DNA), histones and proteins activate immune cells and might accelerate the formation of thrombi (Ramos *et al.* 2016). The immune response in HUS is not limited to the activation of neutrophils but also includes other immune cells, however, their role in HUS pathogenesis is less well understood (Exeni *et al.* 2018). Interestingly, tissue-resident macrophages in the kidney appear to play a critical role in neutrophil recruitment as their depletion in HUS significantly reduced CXCL1 and 2 and consequently neutrophil invasion (Lill *et al.* 2021).

ROS are known to play an important role in the development of endothelial injury. Gomez *et al.* demonstrated that Stx2 induces an oxidative imbalance and an increased

ROS production by neutrophils, which may be one of the major sources of oxidative stress during HUS (Gomez *et al.* 2013).

The pro-coagulant, pro-thrombotic phenotype of endothelial cells induced by Stx2 exposition is thought to be multifactorial and is not only created by the aforementioned mechanisms. Stx-mediated apoptosis results in a release of danger-associated molecular patterns (DAMPs), e.g. histone DAMPs that were shown to induce endothelial dysfunction in two distinct cells lines in a study by Mayer *et al.* (Mayer *et al.* 2015). Furthermore, Stx2 in combination with tumor-necrosis factor α (TNF-α) is able to decrease the surface expression of TM in human endothelial glomerular cells through a mechanism that is not completely explained by Stx2-mediated inhibition of protein synthesis (Fernandez *et al.* 2003).

1.1.4 Therapy of STEC-HUS

Although the connection between STEC infections and the development of HUS was revealed already in 1985 by Karmali *et al.* (Karmali *et al.* 1985), to date there is no specific treatable target known in STEC-HUS. Treatment is limited to supportive therapy, including volume replacement and management of blood pressure. In more severe cases, renal replacement therapy is required. Although plasmapheresis has been proposed to improve outcome in several studies, randomized control trials and meta-analyses found no benefit of plasmapheresis over supportive standard of care (Dundas *et al.* 2001, Michael *et al.* 2009, Tarr *et al.* 2005). The use of antibiotics is also highly controversial: Several types of stress induced by antibiotics mediate the entry of the *stx*-carrying phage into the lytic cycle thereby increasing Stx production (McGannon *et al.* 2010). However, this effect appears to be dependent on the class of antibiotics and mainly associated with beta-lactams (Kakoullis *et al.* 2019). In contrast, the use of azithromycin has been shown to be beneficial in mice in two independent studies (Amran *et al.* 2013, Ohara *et al.* 2002) and also appears to reduce the long-term shedding of STECs in patients surviving HUS (Nitschke *et al.* 2012).

1.2 Animal models of STEC-HUS

1.2.1 Rodent models

Both mice and rats lack glomerular expression of Gb3 receptors (Rutjes *et al.* 2002). Nonetheless, several rodent HUS models are described in the literature. In mice, in comparison to Stx1, Stx2 administered intravenously preferentially targets murine

kidneys, where it binds to proximal and distal tubuli resulting in dilatation whereas glomeruli are unaffected (Rutjes *et al.* 2002). Initially, glomerular changes in murine models of HUS appeared to be dependent from co-application of lipopolysaccharide (LPS) (Ikeda *et al.* 2004, Keepers *et al.* 2006). Ikeda *et al.* introduced a model were they observed a significant elevation in blood urea nitrogen, proteinuria and ultrastructural changes in glomeruli (Ikeda *et al.* 2004). In the model proposed by Keepers *et al.*, similar ultrastructural changes were detected in the glomeruli and furthermore also fibrin and thrombi deposition (Keepers *et al.* 2006). However, Sauter *et al.* published a model in which three sublethal doses of endotoxin-free Stx2 administered intraperitoneally (*i.p.*) were sufficient to provoke glomerular damage (Sauter *et al.* 2008).

In rats, direct perfusion of the kidney with Stx1 in the living animal resulted in extensive tubular injury, massive leukocyte infiltration and apoptosis in the renal medulla as well as platelet aggregation in glomeruli and medullary capillaries (Yamamoto *et al.* 2005). Extensive tubular injury with mainly unaltered glomeruli was also the main finding in models in that Stx1 or 2 were administered *i.p.* (Sugatani *et al.* 2002, Zhao *et al.* 2002). Two studies where Stx2 was co-administered with LPS indicated that the glomerular changes such as glomerular mesangial proliferation (Silberstein *et al.* 2011) and mesangiolysis as well as changes in podocyte protein expression patterns (Ochoa *et al.* 2012) were mainly induced by LPS.

1.2.2 Large animal models

Rabbits are naturally susceptible to STEC infection and develop HUS-like symptoms (Garcia *et al.* 2002). Hence, they appear to be an appropriate model organisms for EHEC infection and Stx intoxication. Surprisingly, inoculation of rabbits with the classical human pathogen EHEC O157:H7 86-24 failed to induce kidney pathology (Panda *et al.* 2010, Zangari *et al.* 2014) whereas the inoculation with EHEC O153:HJ led to classical signs of HUS (Garcia *et al.* 2006). Similar as in humans, the severity of HUS-like symptoms in rabbits seems to be influenced by the Stx variant: While intravenous (*i.v.*) injection of Stx1 induces only mild symptoms of kidney dysfunction (Richardson *et al.* 1992), *i.v.* injection of Stx2 induces classical HUS-associated renal lesions and severe clinical symptoms (Garcia *et al.* 2008).

Although pigs are difficult to manage due to their size, they are ideal models for kidney disease as their macroscopic kidney anatomy resembles the human one. Systemically,

pigs inoculated with STEC develop edema and the main histological finding are segmental arteriolar smooth muscle cell lesions (Matise *et al.* 1999). Inoculation of gnotobiotic piglets with the EHEC strains O157:H7 and O26:H11 results in glomerular endothelial damage in all and TMA in most of the inoculated animals (Gunzer *et al.* 2002). Interestingly, the strain responsible for the 2011 outbreak in Northern Germany - O104:H4 - induced milder symptoms of kidney injury in comparison to O157:H7 in gnotobiotic piglets (Wöchtl *et al.* 2017).

The extent and nature of kidney damage in non-human primates following Stx-challenge is highly variable. In one study, Stx1-challenged baboons developed renal failure due to severe tubular injury (Taylor *et al.* 1999). In contrast, another study found HUS-like symptoms only after co-challenge with Stx1 and LPS (Siegler *et al.* 2001). Juvenile baboons challenged with Stx2 *i.v.* developed acute kidney injury (Stearns-Kurosawa *et al.* 2011), indicating that the type of Stx might play a role in HUS pathogenesis in non-human primates. However, the effects of Stx-challenge in baboons widely varied also in two studies directly comparing the effects of Stx1 and Stx2. Siegler *et al.* observed no clinical signs of HUS in baboons challenged with Stx1 and TMA only in the Stx2-challenged animals (Siegler *et al.* 2003). Stearns-Kurosawa *et al.* observed severe damage to the glomerular filtration barrier following Stx1-challenge and only minor tubular injury, but severe acute tubulointerstitial injury with no damage to the glomeruli in Stx2-challenged animals (Stearns-Kurosawa *et al.* 2013).

1.3 Erythropoietin (EPO)

1.3.1 Structure and function

Although its existence and function was already postulated in 1906 (Carnot and Deflandre), the primary structure of human erythropoietin (EPO) was not resolved until 1986 (Lai *et al.* 1986). As a member of the type I cytokine superfamily, EPO is characterized by a globular structure formed by 4 α-helices (Jelkmann 2004). The glycoprotein consists of 165 amino acids and has a molecular weight of 30.4 kDa when synthesized in the kidneys. Interestingly, the level of glycosylation of EPO varies depending on the organ of its origin: While renal EPO contains four polysaccharide chains that are capped by sialic acid, EPO from the brain is poorly sialated (Masuda *et al.* 1994). Plasma half-life and thereby also mode of action is determined by the

degree of sialation: Renal EPO has a half-life of 5-6 h allowing for endocrine function whereas the poorly sialated EPO from other organs has a half-life of only a few minutes resulting in paracrine-autocrine function (Tsuda *et al.* 1990). EPO interacts with its receptor via two distinct binding sites (Syed *et al.* 1998). The first one is a high-affinity binding site with a dissociation constant of ~1 nM (Syed *et al.* 1998) comprised of a common motif for cytokine:cytokine receptor interaction (Clackson and Wells 1995). The second one is a low-affinity binding site with a dissociation constant of approximately 1 µM (~1000-fold lower; (Philo *et al.* 1996)).

For decades, EPO was mainly recognized for its hematopoietic function. Erythropoiesis is controlled by EPO via a classical negative feedback loop. A declining number of red blood cells results in relative hypoxia, which is detected by renal interstitial cells and leads to the release of EPO from these cells into the circulation. Once it reaches the bone marrow, EPO interacts with proerythrocytes that are expressing the EPO receptor (EPO-R) during a brief time period of their maturation (Koury *et al.* 2002). The binding of EPO to its receptor triggers signaling cascades that result in the prevention of programmed cell-death of the proerythrocytes. These proerythrocytes allow the body to adapt to hypoxia, anemia or profound blood loss. Another small fraction of erythroid precursors (burst-forming and colony-forming unit erythroids) continuously expresses the EPO-R and is thereby responsive to EPO (Lacombe and Mayeux 1999). However, if EPO is not present in the circulation, these cells are undergoing apoptosis (Lacombe and Mayeux 1999). This fraction allows the precise replacement of senescent erythrocytes (approximately 1% of total erythrocyte population per day). Next to its main function in erythropoiesis, EPO has several other effects in the circulation, e. g. the stimulation of platelet formation and an increase in P- and E-selectin expression (Allegra *et al.* 1999, Heinisch *et al.* 2012). These effects are associated with an increased risk for thrombosis.

A second key function of EPO was discovered more recently, when Cerami and Brines uncovered the tissue-protective role of a second type of EPO receptors, a heterodimer of an EPO-R and a β-common receptor (βCR) subunit which was termed the “innate repair receptor” (IRR;(Brines *et al.* 2004)).

1.3.2 EPO receptors and pleiotropic signaling

The EPO-R is a 484 amino acid glycoprotein belonging to the superfamily of cytokine type I receptors (Bazan 1990). Two immunoglobulin-like domains are forming the

extracellular region of EPO-R. Four conserved cysteine residues in the membrane-distal (D1) domain are forming disulfide bonds stabilizing the D1 structure (Livnah *et al.* 1996, Syed *et al.* 1998). A short hinge links the D1 domain to the membrane-proximal (D2) domain at a 90° angle. The tertiary structure of EPO-R is stabilized by the conserved WSXWS motif located in the D2 domain (Hilton *et al.* 1996, Livnah *et al.* 1996, Syed *et al.* 1998). EPO-binding to its receptor is hypothesized to occur sequentially; first, the high affinity binding site of EPO interacts with one EPO-R molecule, afterwards the low affinity site attaches to the second EPO-R molecule (Matthews *et al.* 1996). Despite asymmetric EPO-binding of the two EPO-R subunits, they appear to function similar in regards to the activation of down-stream signaling (Zhang *et al.* 2009). About 300-1000 receptors are found on the surface of erythroid progenitor cells and cell lines of erythroid origin. Upon ligand binding, homodimerization of the EPO-R results in phosphorylation and thereby activation of the receptor-associated tyrosine kinase Janus-like kinase 2 (JAK2). Interestingly, the mode of dimerization appears to be critical, as some agonists also induce EPO-R homodimerization without or only weak activation of downstream signaling (Livnah *et al.* 1998, Livnah *et al.* 1996). This might be explained by the fact that EPO binding to EPO-R induces a distinct conformation of the receptor in which the angle between D1 domains is ~120° and the D2 domains are positioned in the same plane (Livnah *et al.* 1996, Syed *et al.* 1998). Complete autophosphorylation and thereby activation of JAK2 might depend on this receptor conformation (Watowich 2011). This hypothesis is further underlined by the fact that both a mutated form of EPO (R103A, mutation in the site 2 binding loop) and EPO-R mutated in either binding site 1 or 2 for EPO failed to induce down-stream signaling in hematopoietic cells (Matthews *et al.* 1996, Zhang *et al.* 2009). Down-stream signaling of the EPO-R receptor involves signal transducer and activator of transcription 1, 3 and 5 (STAT1, 3 and 5), however, it can also activate several mitogen-associated protein kinases (MAPK) such as MAPK1 and 3 (also known as Erk1/2) or p38 (Richmond *et al.* 2005).

In contrast, the IRR which is a heteromer of an EPO-R and a βCR subunit is activated in a paracrine-autocrine manner by higher doses of locally produced EPO (1-2 nmol/l (Anagnostou *et al.* 1990)). The βCR is comparably large as it comprises of a duplicated extracellular portion as well as a long intracellular tail. The receptor is shared by hematopoietic type I cytokines (interleukins 3 and 5, granulocyte macrophage-colony-stimulating factor) (Brines and Cerami 2012). Ligand specificity is conferred by

disulfide bonds to the specific cytokine receptor subunit (Mirza *et al.* 2010). The IRR mediates tissue-protection in a variety of tissues including heart (Guan *et al.* 2020), kidney (Kitamura *et al.* 2008), brain (Brines *et al.* 2004) and peripheral nervous system (Loesch *et al.* 2010). However, the receptor is also expressed on some cells of the immune system, especially on subsets of macrophages (Nairz *et al.* 2011). Assembly of the IRR is enhanced in lipid rafts (Saulle *et al.* 2009) and favoured by a surplus in βCR subunits which are usually expressed as dimers (Carr *et al.* 2001). Interestingly, the formation of the IRR is further enhanced in the presence of its ligands as it has been shown for carbamylated EPO (CEPO) (Guan *et al.* 2020). Signaling via the IRR down-stream of JAK2 is mediated via three different major survival pathways: (I) STATs (Ahmet *et al.* 2011, Ueba *et al.* 2010), (II) phosphoinositide 3-kinases (PI3Ks) (Coldewey *et al.* 2013, Patel *et al.* 2011, Ueba *et al.* 2010) and (III) MAPK (Patel *et al.* 2011, Ueba *et al.* 2010). The latter pathways cumulate in the inhibition of glycogen synthase kinase 3β (GSK3β), not only inhibiting nuclear-factor 'kappa-light-chain-enhancer' of activated B-cells (NF-κB) and thereby inflammation but also stabilizing mitochondria and thereby inhibit apoptosis (Brines and Cerami 2012). Furthermore, PI3Ks are also critically involved in the generation of nitric oxide by inducing endothelial nitric oxide synthase (eNOS) resulting in an increase in regional blood flow (Ahmet *et al.* 2011). STAT-induced pathways mediate the expression of pro-survival factors, the inhibition of apoptosis and tissue-restorative functions such as the activation of neural stem cell differentiation (Ahmet *et al.* 2011).

1.3.3 EPO and its derivatives as erythropoiesis stimulating agents

The U.S. Food and Drug Administration (FDA) lists the following indications for EPO therapy: anemia caused by chronic kidney disease (CKD), chemotherapy against cancer or zidovidune treatment against HIV-infection and to reduce the need of red blood cell transfusions in surgery patients (FDA; Reference ID: 4160848; (Bilenker *et al.* 2002)). Similar indications are listed by the European Medicines Agency (EMA; EMEA/H/C/000726). However, the so-called off-label use of EPO is very common comprising up to 50% of total EPO use (Guan *et al.* 2020, Bilenker *et al.* 2002), e. g. in cancer patients whose anemia was not caused by chemotherapy (Guan *et al.* 2020), secondary anemia occurring in chronic diseases (Guan *et al.* 2020) and in patients who decline red blood cell transfusions (such as Jehova’s witnesses (Agapidou *et al.* 2014, Menkis *et al.* 2012)).

EPO for therapeutic use is always produced in a recombinant manner allowing the production of several so called next generation EPO compounds or erythropoiesis stimulating agents (ESAs) that are modifications of the original genetic sequence of EPO. These next generation compounds include for example darbepoetin α and continuous erythropoiesis receptor activator (CERA). Darbepoetin α has a three times higher plasma half-life then recombinant EPO as its degree of sialation was increased by the exchange of five amino acids (Hudson and Sameri 2002). CERA is modified with a polyethylenglycopolymer that increases the molecular mass and further exceeds plasma half-life of darbepoetin α approximately five-fold (Macdougall 2005). Both ESAs are approved for therapy of anemia.

1.3.4 Non-hematopoietic EPO-derived peptides

The discovery of EPOs tissue-protective effects and the IRR prompted in the development of several non-hematopoietic compounds that were derived from the structure of EPO but designed to exclusively bind the IRR (Brines *et al.* 2008).

Carbamylated EPO (CEPO) contains carbamyl-residues that are increasing its affinity for the IRR (Coleman *et al.* 2006). Although initially developed for neuroprotection, a preclinical study also demonstrated that CEPO outperforms EPO in the treatment of AKI (Togel *et al.* 2016). Safety and pharmacokinetics trials have been performed in patients with acute ischemic stroke (NCT00756249, NCT00870844) and Friedreich's ataxia (NCT01016366), however, only the results of the latter clinical trial have been published. Although CEPO was well-tolerated, unfortunately there were no therapeutic benefits compared with the placebo (Boesch *et al.* 2014).

The pyroglutamate helix B surface peptide (pHBSP, also known as ARA290 or cibinetide) was introduced in 2008 by Brines *et al.* (Brines *et al.* 2008). It mimics the aqueous surface of EPO's helix B that is not involved in binding the EPO-R and therefore exclusively activates tissue-protective signaling pathways via the βcR-axis without inducing erythropoiesis and thereby being free of the risk of increased thrombosis (Brines *et al.* 2008). Although its plasma half-life is only about 2 min (Brines *et al.* 2008), pHBSP has demonstrated protective effects in various animal models of serious conditions such as ischemic myocardial injury (Ahmet *et al.* 2011), acute kidney injury (Patel *et al.* 2012) and traumatic brain injury (Robertson *et al.* 2013). Furthermore, successful phase two clinical trials have been performed using pHBSP as a therapeutic against neuropathic pain associated with sarcoidosis (Culver *et al.*

2017) and neuropathy and metabolic dysfunction associated with type II diabetes (Brines *et al.* 2015). Due to the promising preclinical effects and the progression into clinical studies, pHBSP was chosen to be further assessed as a potential therapeutic for HUS in this thesis.

1.3.5 The role of EPO in HUS

Anemia usually results in an increase of EPO plasma levels as the body tries to correct anemia by an increase in erythropoiesis. It therefore stands to reason that EPO levels in HUS should also increase due to MAHA resulting from the massive loss of erythrocytes. However, EPO levels in HUS patients have not been routinely studied to date. There is one clinical report from pediatric HUS patients indicating that EPO plasma levels in this condition are elevated (Exeni *et al.* 1998). Yet, this elevation is disproportionally low when compared to the EPO levels in anemia of other etiologies (Exeni *et al.* 1998). Several mechanisms might contribute to this surprising observation. For example, it has been shown before that pro-inflammatory cytokines might suppress the production of EPO (Jelkmann 1998). Furthermore, the HUS-characteristic damage to the kidney might result in renal anemia (Exeni *et al.* 1998). At this point, it appears unexpected that EPO is not approved for the therapy of HUS-associated anemia. This might be due to the fact that clinical evidence is low and the two studies performed in pediatric HUS patients showed conflicting results. While Pape *et al.* observed a reduced need for red blood cell transfusion in EPO-treated children with HUS (Pape *et al.* 2009), Balestracci *et al.* could not verify this observation in a larger case-control study (Balestracci *et al.* 2015) and a pilot randomized controlled trial (Balestracci *et al.* 2022).

2. Aim of thesis

Overall, this thesis aimed to further assess the pathophysiology of the hemolytic-uremic syndrome, examine the role of erythropoietin signaling in disease progression and determine the potential of EPO and pHBSP as therapeutics in HUS. To date, there is still no specific therapy for HUS and treatable targets are lacking. As it is a rare disease, randomized control trials are difficult to perform in HUS and there is an urgent need for reliable preclinical models to perform interventional studies.

Specific objectives:

I) Establish clinically relevant murine models of HUS (Manuscript I).

II) Characterize these models in-depth by laboratory chemistry, histology and immunohistochemistry (Manuscript I).

III) Examine the status of endogenous EPO levels in different species suffering from HUS (Manuscript II).

IV) Assess the therapeutic potential of EPO and pHBSP in a clinically relevant preclinical murine model (Manuscript II).

3. Manuscripts

Manuscript I:

S. Dennhardt*, W. Pirschel*, B. Wissuwa, C. Daniel, F. Gunzer, S. Lindig, A. Medyukhina, M. Kiehntopf, W. W. Rudolph, P. F. Zipfel, M. Gunzer, M. T. Figge, K. Amann, S. M. Coldewey, Modeling Hemolytic-Uremic Syndrome: In-Depth Characterization of Distinct Murine Models Reflecting Different Features of Human Disease. *Front Immunol* **9**, 1459 (2018). *Authors contributed equally.

Manuscript II:

Dennhardt S, Pirschel W, Wissuwa B, Imhof D, Daniel C, Kielstein JT, Hennig-Pauka I, Amann K, Gunzer F, Coldewey SM. Targeting the innate repair receptor axis *via* erythropoietin or pyroglutamate helix B surface peptide attenuates hemolytic-uremic syndrome in mice. *Front Immunol*. **13,** 1010882 (2022).

3.1 Manuscript I

Manuskript Nr. I

Titel des Manuskriptes: Modeling Hemolytic-Uremic Syndrome: In-Depth Characterization of Distinct Murine Models Reflecting Different Features of Human Disease

Autoren: S. Dennhardt, W. Pirschel, B. Wissuwa, C. Daniel, F. Gunzer, S. Lindig, A. Medyukhina, M. Kiehntopf, W. W. Rudolph, P. F. Zipfel, M. Gunzer, M. T. Figge, K. Amann, S. M. Coldewey

Bibliographische Informationen: Dennhardt S, Pirschel W, Wissuwa B, Daniel C, Gunzer F, Lindig S, Medyukhina A, Kiehntopf M, Rudolph WW, Zipfel PF, Gunzer M, Figge MT, Amann K, Coldewey SM. Modeling Hemolytic-Uremic Syndrome: In-Depth Characterization of Distinct Murine Models Reflecting Different Features of Human Disease. Front Immunol. 2018 Jun 25;9:1459. doi: 10.3389/fimmu.2018.01459. PMID: 29988557; PMCID: PMC6026657.

D**er Kandidat / Die Kandidatin ist** (bitte ankreuzen)

☐ Erstautor/-in, ☒ Ko-Erstautor/-in, ☐ Korresp. Autor/-in, ☐ Koautor/-in.

Status: publiziert

Anteile (in %) der Autoren / der Autorinnen an der Publikation (anzugeben ab 20%)

Autor/-in	**Konzeptionell**	**Datenanalyse**	**Experimentell**	**Verfassen des Manuskriptes**	**Bereitstellung von Material**
S. Dennhardt		40	40	40	
W. Pirschel		30	30		
B. Wissuwa	20	20	20		
C. Daniel					
F. Gunzer					
S. Lindig					
A. Medyukhina					
M. Kiehntopf					
W.W. Rudolph					
P.F. Zipfel					
M. Gunzer					
M. T. Figge					
K. Amann					
S. M. Coldewey	80			40	90

frontiers in Immunology

ORIGINAL RESEARCH
published: 25 June 2018
doi: 10.3389/fimmu.2018.01459

Modeling Hemolytic-Uremic Syndrome: In-Depth Characterization of Distinct Murine Models Reflecting Different Features of Human Disease

Sophie Dennhardt[1,2,3†], Wiebke Pirschel[1,2†], Bianka Wissuwa[1,2], Christoph Daniel[4], Florian Gunzer[5], Sandro Lindig[1], Anna Medyukhina[6], Michael Kiehntopf[7], Wolfram W. Rudolph[5], Peter F. Zipfel[8], Matthias Gunzer[9], Marc Thilo Figge[3,6,10], Kerstin Amann[4] and Sina M. Coldewey[1,2,3]*

[1] Department of Anesthesiology and Intensive Care Medicine, Jena University Hospital, Jena, Germany, [2] Septomics Research Center, Jena University Hospital, Jena, Germany, [3] Center for Sepsis Control and Care, Jena University Hospital, Jena, Germany, [4] Department of Nephropathology, Friedrich-Alexander University (FAU) Erlangen-Nürnberg, Erlangen, Germany, [5] Institute of Medical Microbiology and Hygiene/Institute of Virology, TU Dresden, Dresden, Germany, [6] Applied Systems Biology, Leibniz Institute for Natural Product Research and Infection Biology, Hans Knöll Institute, Leibniz-Association, Jena, Germany, [7] Department of Clinical Chemistry and Laboratory Medicine, Jena University Hospital, Jena, Germany, [8] Department of Infection Biology, Leibniz Institute for Natural Product Research and Infection Biology, Jena, Germany, [9] Institute for Experimental Immunology and Imaging, University Hospital, University Duisburg-Essen, Essen, Germany, [10] Friedrich Schiller University (FSU) Jena, Jena, Germany

OPEN ACCESS

Edited by:
Tobias Schuerholz, Universitätsmedizin Rostock, Germany

Reviewed by:
Steven L. Spitalnik, Columbia University, United States
Lara Campana, University of Edinburgh, United Kingdom

***Correspondence:**
Sina M. Coldewey
sina.coldewey@med.uni-jena.de

[†]These authors have contributed equally to this work.

Specialty section:
This article was submitted to Inflammation, a section of the journal Frontiers in Immunology

Received: *06 January 2018*
Accepted: *12 June 2018*
Published: *25 June 2018*

Citation:
Dennhardt S, Pirschel W, Wissuwa B, Daniel C, Gunzer F, Lindig S, Medyukhina A, Kiehntopf M, Rudolph WW, Zipfel PF, Gunzer M, Figge MT, Amann K and Coldewey SM (2018) Modeling Hemolytic-Uremic Syndrome: In-Depth Characterization of Distinct Murine Models Reflecting Different Features of Human Disease. Front. Immunol. 9:1459. doi: 10.3389/fimmu.2018.01459

Diarrhea-positive hemolytic-uremic syndrome (HUS) is a renal disorder that results from infections with Shiga-toxin (Stx)-producing *Escherichia coli*. The aim of this study was to establish well-defined refined murine models of HUS that can serve as preclinical tools to elucidate molecular mechanisms of disease development. C57BL/6J mice were subjected to different doses of Stx2 purified from an *E. coli* O157:H7 patient isolate. Animals received 300 ng/kg Stx2 and were sacrificed on day 3 to establish an acute model with fast disease progression. Alternatively, mice received 25 ng/kg Stx2 on days 0, 3, and 6, and were sacrificed on day 7 to establish a subacute model with moderate disease progression. Indicated by a rise in hematocrit, we observed dehydration despite volume substitution in both models, which was less pronounced in mice that underwent the 7-day regime. Compared with sham-treated animals, mice subjected to Stx2 developed profound weight loss, kidney dysfunction (elevation of plasma urea, creatinine, and neutrophil gelatinase-associated lipocalin), kidney injury (tubular injury and loss of endothelial cells), thrombotic microangiopathy (arteriolar microthrombi), and hemolysis (elevation of plasma bilirubin, lactate dehydrogenase, and free hemoglobin). The degree of complement activation (C3c deposition), immune cell invasion (macrophages and T lymphocytes), apoptosis, and proliferation were significantly increased in kidneys of mice subjected to the 7-day but not in kidneys of mice subjected to the 3-day regime. However, glomerular and kidney volume remained mainly unchanged, as assessed by 3D analysis of whole mount kidneys using CD31 staining with light sheet fluorescence microscopy. Gene expression analysis of kidneys revealed a total of only 91 overlapping genes altered in both Stx2 models. In conclusion, we have developed two refined mouse models with different disease progression, both leading to hemolysis, thrombotic microangiopathy, and acute kidney dysfunction and damage as key clinical features of human HUS. While intrarenal changes (apoptosis, proliferation, complement deposition, and

immune cell invasion) mainly contribute to the pathophysiology of the subacute model, prerenal pathomechanisms (hypovolemia) play a predominant role in the acute model. Both models allow the further study of the pathomechanisms of most aspects of human HUS and the testing of distinct novel treatment strategies.

Keywords: hemolytic-uremic syndrome, Shiga toxin, enterohemorrhagic *E. coli*, *Escherichia coli*, acute kidney injury, mouse models, Shiga-toxin-producing *Escherichia coli*

INTRODUCTION

Hemolytic-uremic syndrome (HUS) is a form of thrombotic microangiopathy that mainly affects the kidneys. Initial renal endothelial cell damage is a common pathological feature of all HUS variants, of which the causes may differ (1). Infection-induced HUS can develop as a serious systemic complication following infections with distinct pathogens, including Shiga-toxin (Stx)-producing *Escherichia coli* (STEC) (2, 3) or pneumococcal-surface protein-C-expressing *Streptococcus pneumoniae* (4) whereas atypical or genetic HUS results from autoimmune or genetic defects, leading to altered complement regulation (5).

Hemolytic-uremic syndrome is the leading cause of acute renal failure in children (6), in which the proportion of STEC-HUS is estimated as 85–90% in comparison to atypical HUS with 5–10% and *S. pneumoniae*-HUS with approximately 5% (4, 7). The prognosis of atypical HUS has markedly improved as administration of a humanized monoclonal antibody against complement C5 allows the reversal of renal pathology and, thus, the prevention of end-stage renal disease (8). By contrast, the pathophysiological principles of infection-associated HUS are less well understood and specific biomarkers and prognosis-improving treatable targets are not available to date. However, a large outbreak of HUS caused by Stx2-producing O104:H4 *E. coli* in Germany in 2011 emphasized the impact of this pathogen on public health. A total of 3,861 cases, including 54 deaths, were reported within 2 months, of which 845 developed HUS, consuming tremendous resources in critical care units across Northern Germany (9). Prospective randomized studies investigating STEC infections and HUS are difficult to conduct in humans owing to the sporadic nature of the disease and the unpredictable occurrence of outbreaks. Therefore, there is urgent demand for animal models to study pathophysiological aspects of HUS systematically.

Bacterial Stxs, of which the two major types Stx1 and Stx2 can be discriminated, are acknowledged as key virulence factors of STEC (10). Epidemiological data revealed that Stx2 plays the predominant role in development of hemorrhagic colitis and HUS (11–14). Stxs are typical AB5 toxins. The five B subunits bind to the glycolipid receptor globotriaosylceramide (Gb3) on target cells. The toxin is then internalized (15) and the A subunit, activated by intracellular proteases, exerts N-glycosidase activity hereby deactivating mammalian ribosomes (16) and inhibiting protein synthesis leading to cell death (3). According to current understanding, a pro-thrombotic environment caused by initial endothelial cell injury and subsequent transcription events leading to generation or release of inflammatory cytokines, chemokines, and adhesion molecules, paves the way for development of thrombotic microangiopathy in the kidney with inappropriate deposition of clots in the microvasculature and subsequent tissue ischemia and organ injury [reviewed in Ref. (17, 18)]. Several related mechanisms can lead to the same endothelial injury in different forms of HUS. Thus, comparable to other syndromes associated with excessive endothelial damage, such as sepsis, the pathophysiology of HUS is complex.

Since Karmali linked sporadic cases of HUS with cytotoxin-producing *E. coli* isolated from patient feces in a breakthrough discovery in 1983 (2), numerous *in vivo* models have been developed to study this syndrome, applying such different animals as non-human primates (19, 20), gnotobiotic piglets (21–25), rabbits (26, 27), rats (28–30), and mice (31–34). Reportedly, certain aspects of HUS, such as, thrombotic microangiopathy, glomerular damage, and thrombocytopenia, are difficult to reproduce in murine models (32, 33). Nevertheless, to conduct mechanistic and early interventional studies requiring investigation of relevant signaling pathways by inactivation or overexpression of certain genes, well-defined and reproducible mouse models mimicking key characteristics of HUS are urgently needed.

Identification of novel pathomechanisms and treatable targets in different stages of STEC-HUS carries the potential for development of novel therapeutic strategies. This study was designed to establish refined murine *in vivo* models with an acute and a subacute disease progression to create better tools to further elucidate molecular mechanisms underlying HUS pathogenesis and to prospectively conduct pharmacological studies. The pathology was induced by intravenous (i.v.) application of Stx2 that was purified from the well-characterized O157:H7 patient isolate of enterohemorrhagic *E. coli* (EHEC) 86-24 (35). Here, we established and characterized in-depth two HUS models in C57BL/6J mice that differed conceptually by the endpoint of the experiment and the dose and regimen of Stx2 application. We attenuated severe hypovolemia—for the first time in murine HUS models—by regular intermittent subcutaneous (s.c.) administration of balanced electrolyte solutions, thereby mimicking supportive therapy in common clinical practice, thus increasing the clinical relevance of our models.

MATERIALS AND METHODS

Purification and Characterization of Stx2

Stx2 was purified on different ion exchange columns and finally on a gel filtration column by our own chromatographic procedure from liquid cultures of the Stx2-producing O157:H7 EHEC strain 86-24 (35). Bacteria were grown in 5 l Luria-Bertani medium starting from an overnight culture at 1:1,000 dilution.

After 4 h of incubation, mitomycin C (Sigma-Aldrich Chemie, Munich, Germany) was added to a final concentration of 0.4 mg/l to enhance the Stx release from the bacteria. Incubation was continued for another 20 h. Cultures were then centrifuged for 20 min at 16,000 *g* in an ultracentrifuge using 500 ml polycarbonate beakers in a JA-10 fixed angle rotor (Beckman Coulter, Krefeld, Germany). The supernatant was kept and sterile-filtered (Corning 1,000 ml Vacuum Filter/Storage Bottle System, 0.22 µm Pore; Sigma-Aldrich Chemie). A 70% ammonium sulfate precipitation was carried out at 4°C and the precipitate isolated by centrifugation. The precipitate was dissolved in a low salt buffer at pH 6.2 and dialyzed against 5 mM phosphate/NaCl buffer for 48 h at 4°C (Slide-A-Lyzer Dialysis Cassettes, 10,000 MWCO, 30 ml; Thermo Fisher Scientific, Dreieich, Germany). The crude protein solution was applied on an anion exchange column (HiTrap Q HP XL; GE Healthcare Europe, Freiburg, Germany) using an ÄKTA pure 25 l chromatography system (GE Healthcare Europe) and the protein was eluted with 1 M NaCl buffer at pH 6.2. The appropriate protein fractions were pooled and dialyzed against 5 mM acetate buffer at pH 3.9. The re-buffered protein solution was then applied to a cation exchange column (HiTrap SP HP XL, GE Healthcare Europe). Bound protein was eluted with 1 M NaCl buffer at pH 3.9. Again, the pooled protein fractions were dialyzed in 50 mM Tris/HCl buffer at pH 6.5. In a third chromatographic step, the purified protein solution was applied on a HiLoad 26/600 Superdex 200 prep grade column (GE Healthcare Europe) and eluted with a flow rate of 1 ml/min isocratically. The appropriate fractions were pooled again. To concentrate the toxin, pooled samples were centrifuged using Vivaspin 20 ultrafiltration devices (10,000 MWCO; Sartorius, Göttingen, Germany). Protein concentration was determined by the bicinchoninic acid method following the protocol supplied by the manufacturer (Sigma-Aldrich Chemie). This purified and concentrated Stx2 protein solution of 0.35 mg/ml was then characterized applying SDS polyacrylamide gel electrophoresis and immunoblot analysis, as described previously (36). Two subunits were detected at 32 and 7 kDa and the protein was free of any visible contamination.

Cytotoxicity Testing of Stx2

Cytotoxicity and LD_{50} of purified Stx2 were determined using Vero cells stained with the vital dye neutral red. 1×10^4 Vero cells per well in 200 µl DMEM/10% FBS (Thermo Fisher Scientific) were seeded into a 96-well plate and grown at 37°C/5% CO_2 for 1 day. 10 µl cell culture medium was replaced by 10 µl medium in duplicate, containing 1 ng to 0.01 fg Stx2 in 10-fold dilutions. Cells were incubated further at 37°C/5% CO_2 for 2 days. Then, vital staining was performed with the "*In vitro* Toxicology Assay Kit Neutral Red based" (Sigma-Aldrich Chemie) according to the manufacturer's instructions. Dye release was assessed spectrophotometrically (Tecan Sunrise™ 96-well Absorbance Microplate Reader; Tecan Deutschland, Crailshaim, Germany) by measuring absorbance at a wavelength of 540 nm against the background absorbance of multiwell plates, measured at 690 nm. Values obtained from wells containing only cell culture medium were set at LD_{100}, values from Vero cell monolayers without Stx2 treatment were set at LD_0, and the LD_{50} was calculated from it.

Dose-Response Study for Stx2 *In Vivo*

Male C57BL/6J mice (aged 10–16 weeks, 20–30 g BW) were intravenously subjected to a single dose of either 50, 100, 150, or 300 ng/kg BW Stx2 in 5 ml/kg NaCl 0.9%, subsequently weighed every 24 h and scored every 12 h to monitor disease progression. After 72 h, mice were exsanguinated in deep ketamine (100 mg/kg BW in 5 ml/kg NaCl 0.9% i.p.) and xylazine (10 mg/kg BW in 5 ml/kg NaCl 0.9% i.p.) anesthesia. Blood was obtained by puncturing the *v. cava* to compile hemograms and analyze kidney dysfunction by measuring plasma urea and creatinine.

Animal Experiments

Male wild-type C57BL/6J mice (aged 10–16 weeks, 20–30 g BW) were randomly assigned to one of the two treatment groups (sham, Stx2). Mice were kept under standardized laboratory conditions, and received standard rodent chow and water *ad libitum*. HUS was induced by either a single i.v. injection of Stx2 (300 ng/kg BW in 5 ml/kg NaCl 0.9%; acute model) or three i.v. injections of Stx2 (25 ng/kg BW in 5 ml/kg BW NaCl 0.9% each; subacute model) on days 0, 3, and 6. Sham animals received 5 ml/kg BW NaCl 0.9% only. Mice were weighed every 24 h and scored every 12 h (acute model) or 8 h (subacute model) to monitor disease progression. To prevent the severe dehydration observed in the dose-response study, mice received 500 µl of Ringer's lactate s.c. every 12 h (acute model) or 800 µl Ringer's lactate s.c. every 8 h (subacute model). 72 h (acute model) or 168 h (subacute model) after HUS induction, mice were sacrificed by exsanguination in deep anesthesia (see Dose-Response Study for Stx2 *In Vivo*).

Evaluation of Disease Progression

Disease progression was monitored by both weight loss and scoring. A scoring system based on the activity of mice was used (ranging from 1—normally active, 2—active with slight restrictions, 3—active with clear intermissions, 4—slowed, 5—lethargic, 6—moribund, to 7—dead). In the course of the experiments, a modified HUS score that additionally included neurological symptoms was established and tested in the subacute model (Table S1 in Supplementary Material).

Blood Analysis

Lithium heparin anti-coagulated blood was obtained and hemograms were compiled using the pocH100iV system (Sysmex, Kobe, Japan). According to the manual Sysmex pocH100iV generally distinguishes between small (W-SCC = small cell count, lymphocytes), middle (W-MCC = middle cell count; monocytes, basophils, eosinophils), and large (W-LCC = large cell count; neutrophils) leukocytes. However, our setup for mice only determines small and large cell count; middle-sized cells are included in the small cell count. Afterward, blood was centrifuged at 3,000 *g* for 15 min at room temperature to obtain plasma. Alanine aminotransferase (ALAT), aspartate aminotransferase (ASAT), bilirubin, lactate dehydrogenase (LDH), urea, and creatinine were measured using an Architect c16200/ci8200 automated clinical chemistry system (Abbott Diagnostics, Abbott Park, IL, USA) according to the manufacturer's recommendations.

Plasma neutrophil gelatinase-associated lipocalin (NGAL) was measured using an ELISA kit provided by BioLegend (San Diego, CA, USA) according to the manufacturer's protocol (sham samples were diluted 1:200 and Stx2 samples 1:1,000 due to the assay range).

Hemolysis was quantified (scoring: 0: no hemolysis, absorbance = 0; 1: up to 5% hemolysis, absorbance <0.04; 2: >5–20% hemolysis, absorbance <0.12; 3: >20–50% hemolysis, absorbance <0.16; 4: >50% hemolysis, absorbance >0.16) by measuring hemoglobin absorption spectra (at 500–600 nm) in plasma with a Spark® multimode reader (Tecan, Maennedorf, Swiss) and comparing the intensity to a standard.

Tissue Preparation

At the end of the experiment—after puncture of the *v. cava*—anesthetized mice were perfused with 0.9% NaCl *via* the left ventricle and right atrium for removal of erythrocytes within the tissue. Afterward, kidneys were removed and fixed instantly with 5% buffered formaldehyde solution for at least 72 h at 4°C, processed, and subsequently embedded in paraffin blocks.

Histopathology

Renal sections (1 µm) were deparaffinized and subjected to routine staining: hematoxylin/eosin, periodic acid Schiff (PAS), and acid fuchsin orange G (SFOG). Histomorphological changes were determined on PAS stained kidney sections. Therefore, 10 cortical fields per kidney adjacent to one another were randomly graded mainly for signs of tubular injury (i.e., brush border loss, epithelial cell flattening, or vacuolization) at a magnification of 400× using a scoring system from 0 to 3: 0: no damage, 1: <25% damaged, 2: 25–50% damaged, 3: >50% damaged. Two trained investigators independently evaluated the sections without knowledge of the experimental group.

Immunohistochemical Staining

Renal sections were deparaffinized and hydrated in a descending series of ethanol (3× 5 min xylene, 2× 1 min 100% ethanol, 2× 1 min 96% ethanol, 1× 1 min 70% ethanol, aqua dest.). Endogenous peroxidase activity was blocked by incubating sections in 3% H_2O_2 for 15 min at room temperature. Antigen retrieval was performed in target retrieval solution (pH 6; Dako, Glostrup, Denmark) for 2.5 min at 120°C using a pressure cooker. Nonspecific binding sites were subsequently saturated in serum or blocked with avidin/biotin solution. All tissue sections were incubated with a primary antibody overnight at 4°C in appropriate dilutions (Table S2 in Supplementary Material). Sections were further processed using the VectaStain ABC kit (Vector Laboratories, Burlingame, CA, USA) according to the manufacturer's recommendations and 3,3-diaminobenzidine (DAB) as substrate. Finally, the sections were counterstained in hemalaun, dehydrated, and mounted for observation. Immunohistochemistry images were acquired using an Olympus Bx60 microscope equipped with an XC30 camera at various magnifications. Images were taken after white balance, auto exposure, and introduction of scale bar using cellSens software (Olympus Deutschland, Hamburg, Germany). No further adjustments or signal amplifications were performed.

Quantification of Immunodetection

A grid superimposed on 20 (for F4-80, CD3, cleaved caspase 3 and Ki67) or 30 (for CD31) cortical areas (adjacent to one another) of each section was used for quantification. While for F4-80 and Ki67 the number of intersections overlapping the positive brown staining was counted in each grid, for CD31 the number of positive caskets per grid was counted. For CD3 and cleaved caspase 3, the numbers of positive cells per mm^2 was calculated based on the number of positive cells counted per grid area (grid area = 0.0625 mm^2). To analyze the expression of kidney injury molecule-1 (KIM-1) and C3c, a scoring system from 0 to 3 (0: <25%, 1: 25–50%, 2: 50–75%, 3: >75% strong positive staining per visual field) was used to evaluate 12 visual fields per section in a blinded manner (magnification: 20×).

Ultrastructural Analysis

Ultrastructural analysis using electron microscopy was performed as described previously (37).

Microarray Preparation and Analysis

Total kidney RNA was extracted from approximately 30 mg of kidney tissue using an RNeasy Mini kit (QIAGEN, Santa Clarita, CA, USA) according to the manufacturer's instructions. 200 ng of total RNA was processed with the GeneChip™ Hybridization, Wash, and Stain Kit (Affymetrix, Santa Clara, CA, USA) according to the manufacturer's protocol and hybridized to GeneChip™ mouse 2.0 ST arrays (Affymetrix) that were subsequently scanned with the GeneChip™ Scanner 3000 7G (Affymetrix). CEL files were pre-processed with Robust Multi-Array Average algorithm and background correction using R statistics software and Bioconductor packages. Intra- vs. inter-class differences were assessed *via* one-way ANOVA. Genes with absolute log2-fold change >1 and p-values <0.05 were considered significantly differentially expressed. False discovery rate-based p-value adjustment was performed *via* the Benjamini–Hochberg method. A list of candidate genes was generated by identifying the overlapping differentially expressed genes (DEGs) of both models. This list was further analyzed using the Database for Annotation, Visualization, and Integrated Discovery 6.8 [DAVID 6.8 (38)] with background set to *Mus musculus* and classification stringency set to medium.

Statistics

All values are depicted as mean ± SD of n observations (n representing number of animals studied) unless stated otherwise. Statistical analysis was performed using GraphPad 7.03 (GraphPad Software, San Diego, CA, USA). Outliers were removed using the ROUT test (Q = 5%). Statistics were performed as t-test for parametric data and Mann–Whitney U-test for non-parametric data. A p-value <0.05 was considered significant.

RESULTS

Cytotoxicity of Stx2

Cytotoxicity of Stx2 purified from EHEC 86-24 was measured *in vitro* in Vero cells by neutral red assay. The LD_{50} in this cell line is 9.51 pg/ml (Figure S1 in Supplementary Material).

Dose-Response Relationship of Stx2 *In Vivo*

All parameters observed in the dose-response study followed a clear dose-dependency (**Figure 1**). Clinical signs of HUS reflected by significant rises in HUS score and weight loss were detectable in mice challenged with Stx2 doses higher than 100 ng/kg BW (HUS score) and 50 ng/kg BW (weight loss), respectively (**Figure 1A**). Plasma urea and creatinine as markers of kidney dysfunction (**Figures 1B,C**) also showed dose-dependency with only slight elevations in mice subjected to 50 ng/kg BW Stx2 and highest levels in mice challenged with 300 ng/kg BW. Hematocrit and hemoglobin (**Figures 1D,E**) as indicators of hemoconcentration dose-dependently increased in mice challenged with more than 50 ng/kg BW Stx2. White blood cell count (**Figure 1F**) was decreased in animals challenged with higher doses of Stx2, indicating leukopenia. According to these results, a single dose of 300 ng/kg BW Stx2 was chosen to establish the acute model as it reproducibly induced kidney dysfunction. To develop a subacute model, an application regime of 3× 25 ng/kg BW Stx2 was chosen, as a single dose was not expected to cause significant or lethal symptoms in mice and the accumulated total dose of 75 ng/kg BW Stx2 should be able to induce moderate signs of disease.

Effect of Different Stx2 Regimens on Clinical Presentation

Mice challenged with 300 ng/kg Stx2 did not exhibit a decrease in activity until just before the endpoint 72 h after HUS induction (**Figure 2A**). However, progression of the disease was observable by profound weight loss of mice challenged with Stx2 reaching significance from day 2 after initial Stx2 injection when compared with sham-treated animals (**Figure 2C**). At day 3, mice lost approximately 20% of their body weight and exhibited tremors and ataxia. By contrast, mice challenged with 3× 25 ng/kg of Stx2 were significantly less active starting from 60 h after HUS induction onward compared with the sham group (**Figure 2B**). Of note, one of the animals challenged with 3× 25 ng/kg Stx2 was already moribund 144 h after HUS induction and therefore euthanized and excluded from further analysis. Significant profound weight loss was also observed in mice challenged with 3× 25 ng/kg of Stx2 compared with sham animals from day 3 after initial Stx2 injection (**Figure 2D**). At the endpoint of the subacute model, critically ill mice exhibited tremor, ataxia, and a pronounced hind limb clasping reflex as a sign of neurological involvement. We attempted to further refine our activity-based score in the course of the experiment by including neurological symptoms, weight loss, and fur quality,

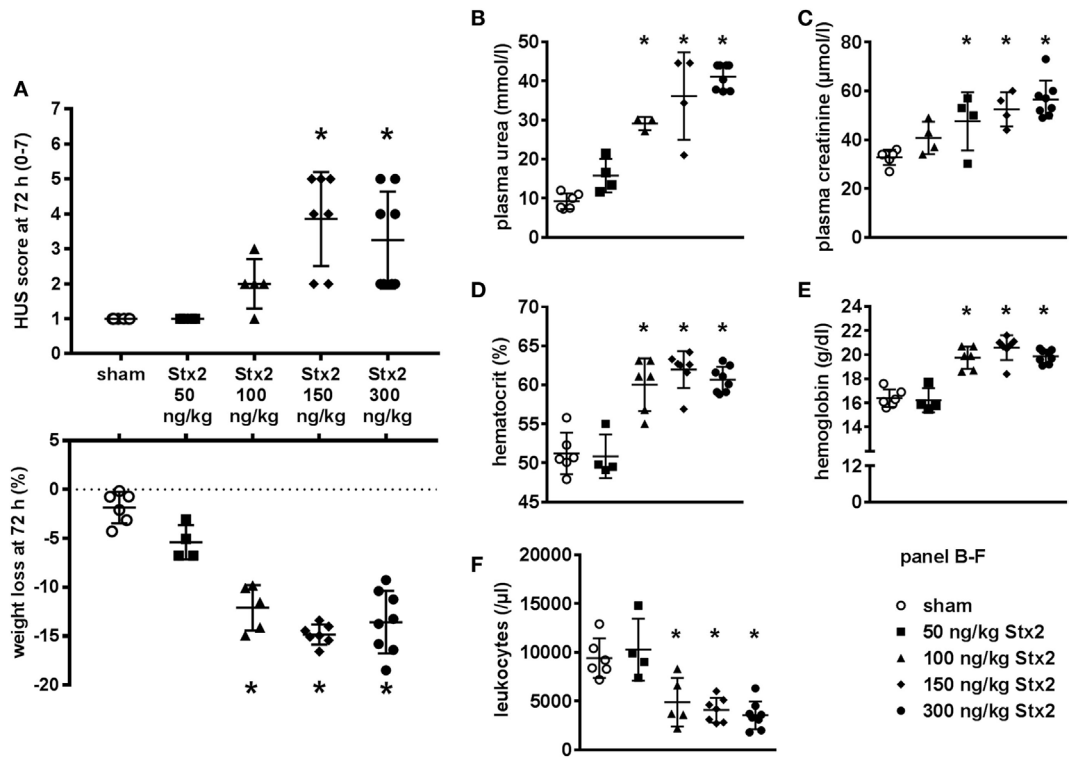

FIGURE 1 | Dose-response study for Stx2 in C57BL/6J mice. **(A–F)** Mice were subjected to different Stx2 concentrations. The effect was assessed after 72 h. Data are expressed as mean ± SD for *n* observations, $^*p < 0.05$ vs. sham. **(A)** Final score and overall weight loss at 72 h (score: Kruskal–Wallis test with Dunn's correction, weight loss: one-way ANOVA with Bonferroni *post hoc* test; sham $n = 6$, 50 ng/kg BW Stx2 $n = 4$, 100 ng/kg BW Stx2 $n = 5$, 150 ng/kg BW Stx2 $n = 7$, 300 ng/kg BW Stx2 $n = 8$). Kidney function was evaluated by **(B)** plasma urea and **(C)** plasma creatinine. **(D)** Hematocrit and **(E)** hemoglobin were measured as indicators of red blood cell count. Immune response was monitored by **(F)** white blood cell count. **(B–F)** Groups: sham $n = 6$, 50 ng/kg Stx2 $n = 4$, 100 ng/kg Stx2 $n = 6$, 150 ng/kg Stx2 $n = 7$, 300 ng/kg Stx2 $n = 8$ (one-way ANOVA with Bonferroni *post hoc* test).

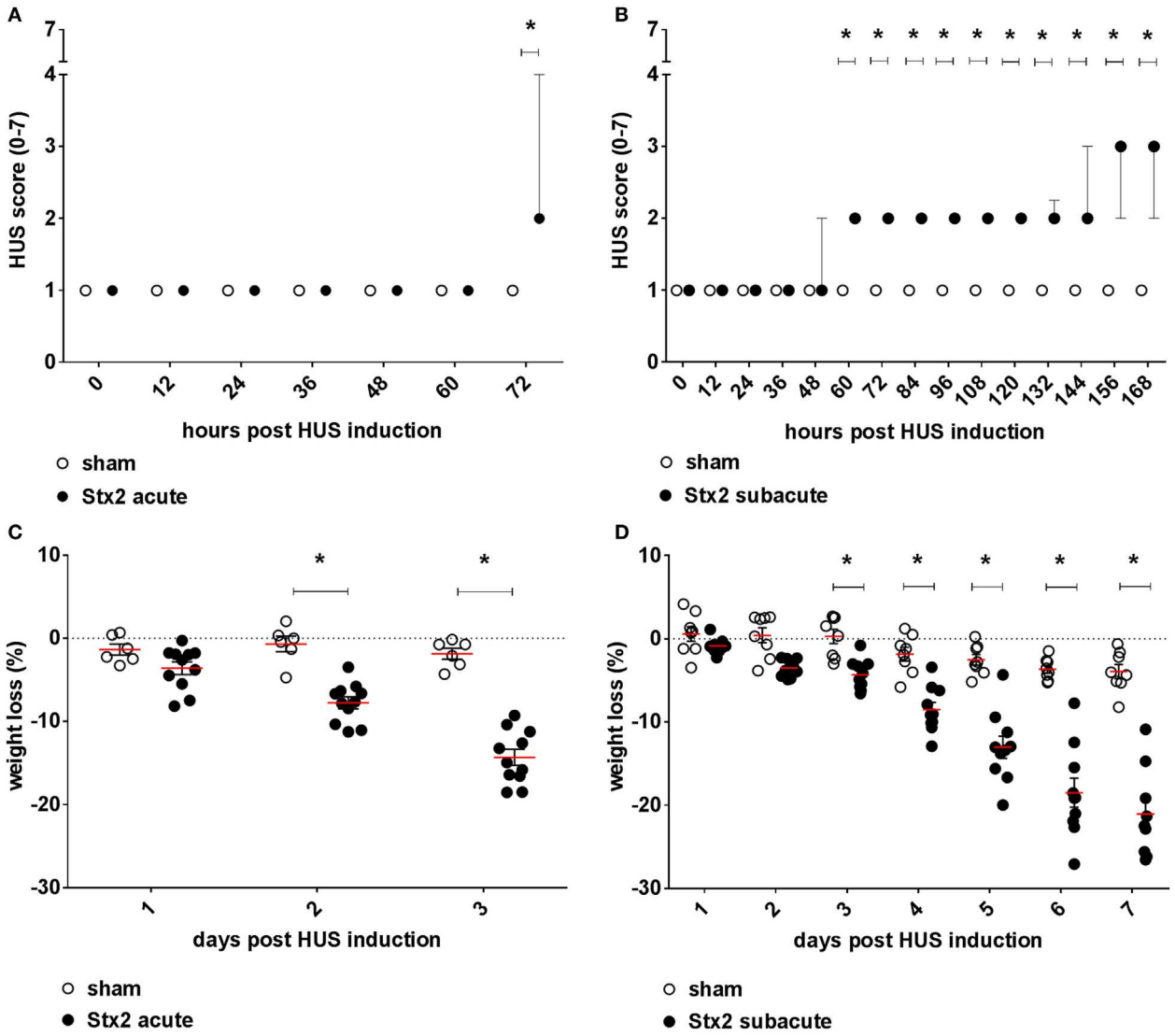

FIGURE 2 | Clinical presentation of C57BL/6J mice subjected to different Stx2 regimens. Clinical presentation was assessed by a score ranging from 1 = very active to 7 = dead for the **(A)** acute model (sham $n = 6$, Stx2 $n = 11$) and **(B)** subacute model (sham $n = 8$, Stx2 $n = 10$). **(A,B)** Data are expressed as median ± interquartile range for n observations. *$p < 0.05$ for sham vs. Stx2 at each respective time point (Mann–Whitney U-test). Weight loss of C57BL/6J wild-type mice was assessed every 24 h for the **(C)** acute model (sham $n = 6$, Stx2 $n = 11$) and the **(D)** subacute model (sham $n = 8$, Stx2 $n = 10$). **(C,D)** Data are expressed as mean ± SD for n observations. *$p < 0.05$ for sham vs. Stx2 at each respective time point (two-way ANOVA with Bonferroni *post hoc* test).

and tested the modified score in the subacute model (Figure S2 in Supplementary Material).

Effect of Different Stx2 Regimens on Hemoconcentration and Thrombocytes

Hemoconcentration occurred in Stx2-challenged mice of both models as indicated by changes in hematocrit as well as hemoglobin. However, these changes were twice as pronounced in the acute model despite the shorter duration of the model (**Figure 3**). At the endpoint of the acute model, the hematocrit significantly increased by 8.6% ± 2.7% ($p < 0.0001$) compared with sham controls. The increase of hematocrit was half as pronounced in mice challenged with 3× 25 ng/kg Stx2 (3.9% ± 2.5%; $p = 0.0135$; **Figure 3A**). Consequently, we observed significantly increased blood hemoglobin levels in the acute (19.2% ± 5.9%; $p < 0.0001$) and subacute model (10.9% ± 5.2%; $p = 0.0023$) compared with sham-treated mice (**Figure 3B**). In line with the hemoconcentration, a rise in the thrombocyte count was observed in Stx2-challenged mice that was again much more pronounced in the acute model (45.6% ± 3.1%; $p = 0.0004$) compared with the subacute model (21.1% ± 5.6%; $p = 0.0131$; **Figure 3C**). Thus, we cannot show thrombocytopenia in our models. However, slight occurrence of thrombocytopenia might be masked by hypovolemia and consecutive hemoconcentration.

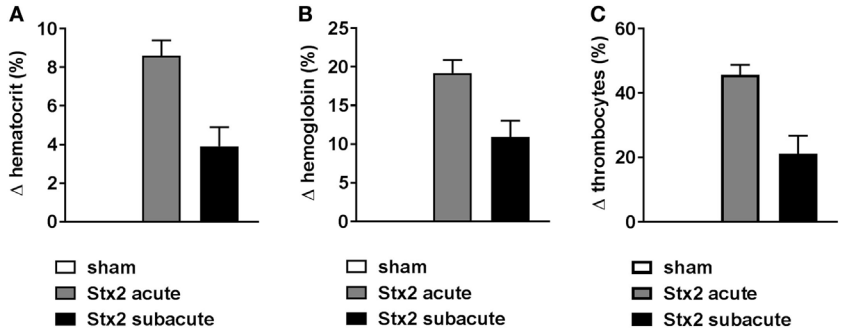

FIGURE 3 | Hemoconcentration and thrombocytes in C57BL/6J mice subjected to different Stx2 regimens. Percentage change of **(A)** hematocrit, **(B)** hemoglobin, and **(C)** thrombocytes for the acute (sham $n = 6$, Stx2 $n = 11$) and subacute model (sham $n = 5$, Stx2 $n = 6$) compared with the respective sham group. **(A–C)** Data are expressed as mean ± SEM for n observations.

Effect of Different Stx2 Regimens on Hemolysis

Both plasma LDH and bilirubin were measured as indirect hemolysis markers. While plasma LDH was significantly higher ($p = 0.0058$) in the Stx2 group of the acute model (**Figures 4C,D**), plasma bilirubin was significantly increased ($p = 0.0018$) only in the Stx2 group of the subacute model compared with the respective sham group (**Figures 4A,B**). Photometric determination of free plasma hemoglobin revealed hemolysis in Stx2-challenged animals of both models, however, to a significant extent only in the subacute model ($p = 0.017$) (**Figures 4E,F**).

Effect of Different Stx2 Regimens on Immune Response

A significant drop in leukocyte count was found in Stx2-challenged mice in both the acute ($p = 0.0003$) and the subacute ($p = 0.0069$) model compared with the respective sham group (**Figure 5A**). This general leukopenia (−62.7% ± 13.0% and −56.7% ± 24.6%) was accompanied by a shift in the ratio of neutrophils to lymphocytes (including medium-sized white blood cells; acute model: 0.19 ± 0.04 in sham group vs. 0.55 ± 0.32 in Stx2 group; subacute model: 0.14 ± 0.02 in sham group vs. 0.42 ± 0.04 in Stx2 group) indicating neutrophilia and lymphocytopenia (**Figures 5B,C**). Immune cell invasion in the kidney was investigated by staining renal sections for F4-80 (surface marker for macrophages) and CD3 (surface marker for T lymphocytes) using immunohistochemistry. Subsequent quantification revealed no renal increase of both macrophages and T lymphocytes in the acute HUS model (**Figures 5D,E**, upper panels). By contrast, in the subacute model on day 7 renal infiltrations with F4-80-positive cells ($p = 0.0079$) as well as CD3-positive cells ($p = 0.0159$) were significantly increased (**Figures 5D,E**, lower panels).

Effect of Different Stx2 Regimens on Kidney Dysfunction and Injury

We assessed kidney dysfunction and injury by laboratory markers, histomorphological, and immunohistochemical analysis. In the acute and subacute HUS model, we observed severe kidney dysfunction, indicated by a significant rise in plasma urea (**Figures 6A,D**), creatinine (**Figures 6B,E**), and NGAL (**Figures 6C,F**). As expected, we found no signs of liver injury evaluated by plasma ASAT and ALAT measurement (Section "Supplementary Results" and Figure S3 in Supplementary Material). Examinations of PAS stained renal sections revealed significant histomorphological changes in the acute HUS model as indicated by tubule dilatation and atrophy and occasional loss of the tubular brush border in proximal tubules (**Figure 6G**, upper panels). In the subacute model, these changes were more pronounced: tubular protein casts and tubular necrosis could be additionally detected (**Figure 6G**, lower panels). Interestingly, expression of KIM-1 was lacking in the acute HUS model but significantly increased in the subacute HUS model, markedly showing KIM-1 expression in injured tubular cells (**Figure 6H**). Concurrently, renal apoptosis of tubular epithelial cells, as monitored by staining for cleaved caspase 3, was only significantly increased in the subacute but not in the acute HUS model (**Figure 7A**). An increase in renal tubular repair, as reflected by an increased proliferative activity, was similarly exclusively observed in the Stx2 group of the subacute model ($p = 0.0159$), as assessed by evaluation of the proliferation marker Ki67 (**Figure 7B**). However, significantly reduced numbers of renal endothelial cells could be demonstrated by CD31 immunostaining in the acute ($p = 0.0112$) and subacute HUS model ($p = 0.0159$) (**Figure 7C**), indicating loss of endothelial cells by Stx2 challenge.

Effect of Different Stx2 Regimens on Thrombus Formation and Complement Activation

One hallmark of renal HUS pathology is the formation of microthrombi. Fibrin depositions (bright red/pink) were detected by SFOG staining and found in Stx2-challenged mice of both the acute and the subacute model but not in sham-treated mice (**Figure 8A**). To investigate a contribution of the complement system in HUS progression, renal sections were stained with an antibody against C3c that not only detects the soluble cleavage product C3c but also C3 and C3b. Compared

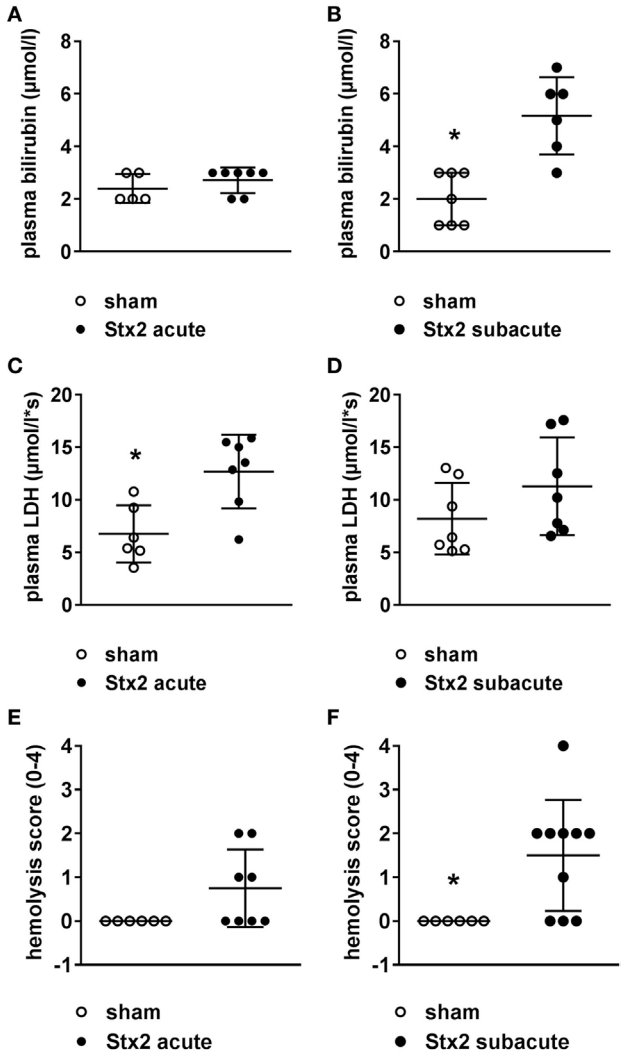

FIGURE 4 | Indicators of hemolysis in C57BL/6J mice subjected to different Stx2 regimens. Plasma bilirubin levels were measured for the **(A)** acute model (sham $n = 5$, Stx2 $n = 7$) and **(B)** subacute model (sham $n = 7$, Stx2 $n = 6$). Plasma lactate dehydrogenase (LDH) levels were measured for the **(C)** acute model (sham $n = 6$, Stx2 $n = 7$) and **(D)** subacute model (sham $n = 7$, Stx2 $n = 7$). **(A–D)** Data are expressed as mean ± SD for n observations. *$p < 0.05$ sham vs. Stx2 (t-test). Hemolysis was photometrically quantified in plasma samples of the **(E)** acute model (sham $n = 6$, Stx2 $n = 8$) and **(F)** subacute model (sham $n = 6$, Stx2 $n = 10$). **(E,F)** Data are expressed as mean ± SD for n observations. *$p < 0.05$ for sham vs. Stx2 (Mann–Whitney U-test).

with sham controls, Stx2-challenged mice showed a significant (acute $p = 0.0303$, subacute $p = 0.0159$) peritubular complement deposition, which was much higher in the subacute model (**Figure 8B**).

Effect of Different Stx2 Regimens on Ultrastructural Changes

Electron microscopy of kidneys from mice that received Stx2 demonstrated tubular damage in both models. Ultrastructural images from Stx2-challenged mice of the acute model showed extensive vacuolization and less mitochondria compared with sham-treated mice (**Figure 9B**). Kidneys from Stx2-challenged mice of the subacute model show smaller vacuoles, loss of the brush border, epithelial cell flattening, and more detached necrotic cells indicating higher tubular injury (**Figure 9C**). No pathological findings were observed in kidneys of sham mice (**Figure 9A**). Changes of total kidney volume, the total glomeruli count, and tuft volume in the subacute model were further assessed by light sheet fluorescence microscopy (LSFM; Section "Supplementary Results" and Figure S4 in Supplementary Material).

Effect of Different Stx2 Regimens on Renal Gene Expression

A heatmap based on the ANOVA-results of gene expression data and comprising the z-scores of the most significant features of the array revealed that all four groups of the experiment are clearly distinguishable by their expression patterns. Hierarchical clustering demonstrated that both sham groups are highly related and the Stx2 acute group also clusters closely with them. The Stx2 subacute group was most distinct (**Figure 10A**). This was also reflected in the proportional Venn diagram of DEGs for the acute and subacute model (**Figure 10B**). 152 genes in total were altered in the acute model and 1,888 genes in the subacute model. Of that, 91 genes were altered both in the acute and subacute model. These overlapping DEGs were assigned to different biological processes and molecular functions according to their functional annotation *via* DAVID 6.8 as depicted in **Table 1**. Both Stx2 regimens led to upregulation of genes associated with immune response, differentiation, proliferation, apoptosis, coagulation, blood pressure, responses to several types of stress, and DNA binding in the whole kidney. Several genes from different metabolic pathways were altered, however, upregulation and downregulation is balanced. Interestingly, a high number of genes for proteins with transporter activity required for normal kidney function and water homeostasis was downregulated in both models of murine HUS. Of note, almost all 91 DEGs common to both models were regulated in the same manner. The only exceptions were *C3ar1* (encoding complement C3a receptor 1) that was downregulated in the acute but upregulated in the subacute model and Gm15889 (predicted gene and protein coding) that was upregulated in the acute and downregulated in the subacute model. Gene expression data were analyzed for further candidate genes from the complement pathway. Apart from *C3ar1*, *C3* (encoding complement factor C3), *C1qb* (encoding complement C1q B chain), and *F3* (encoding Tissue Factor) were also significantly upregulated in the subacute, but not in the acute model (**Figures 10C–F**).

Functional annotation clustering of the 91 DEGs was performed *via* DAVID 6.8 to identify the most overrepresented biological terms and thereby clarify the biological processes altered by Stx2. 26 annotation clusters were identified. Of these, 12 annotation clusters were significantly enriched (enrichment score ≥ 1.3). These clusters were mainly associated with inflammatory and immune response (4 of 12), transporter activities

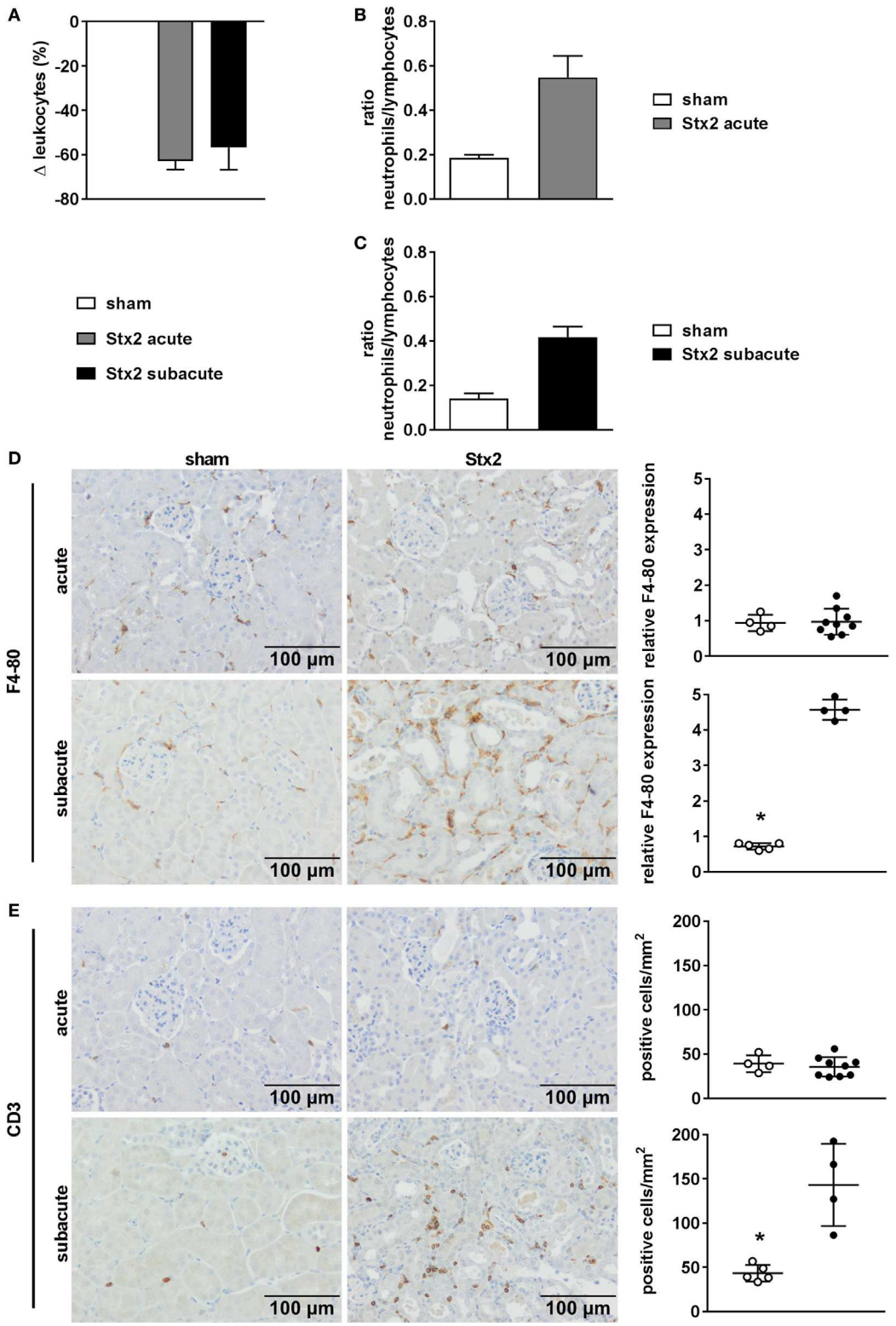

FIGURE 5 | Immune response in C57BL/6J mice subjected to different Stx2 regimens. **(A)** Percentage change of leukocyte counts and **(B,C)** ratio of neutrophils to lymphocytes for the acute and subacute model compared with the respective sham group. **(A–C)** Data are expressed as mean ± SEM for *n* observations (acute: sham $n = 6$, Stx2 $n = 11$; subacute: sham $n = 5$, Stx2 $n = 6$). Representative images (scale bar 100 µm) of immunohistochemical detection and quantitative data of **(D)** F4-80 (surface antigen of macrophages) and **(E)** CD3 (surface antigen of T cells) in renal sections of C57BL/6J wild-type mice are depicted (acute: sham $n = 4$, Stx2 $n = 9$; subacute: sham $n = 5$, Stx2 $n = 4$). $^*p < 0.05$ for sham (white dots) vs. Stx2 (black dots; *t*-test).

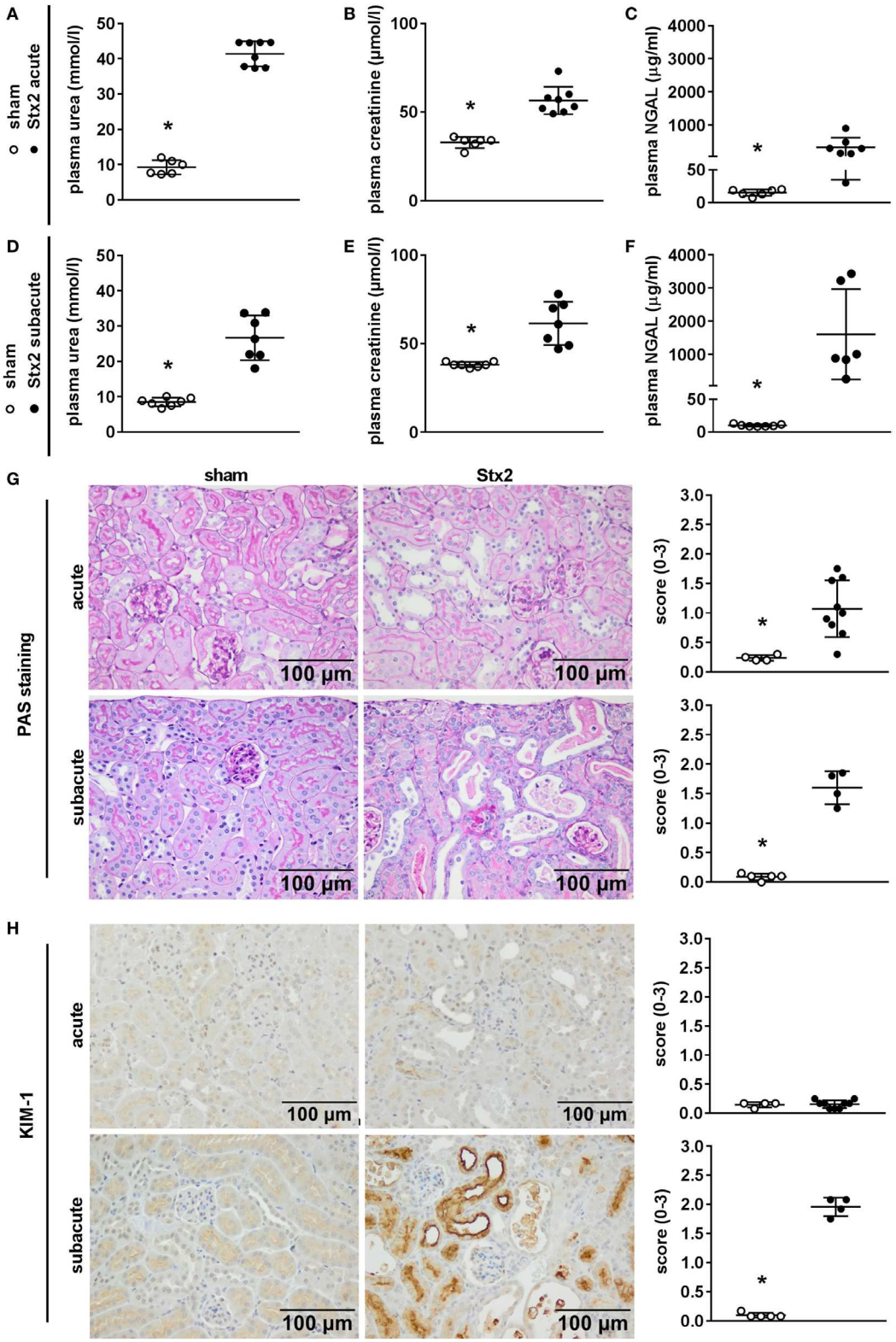

FIGURE 6 | Indicators of kidney injury in mice subjected to different Stx2 regimens. **(A,D)** Plasma urea, **(B,E)** plasma creatinine, and **(C,F)** plasma neutrophil gelatinase-associated lipocalin (NGAL) levels were measured for the acute model (sham $n = 6$, Stx2 $n = 8$) and subacute model (sham $n = 7$, Stx2 $n = 7$, NGAL Stx2 $n = 6$). Data are expressed as mean ± SD for n observations. *$p < 0.05$ for sham vs. Stx2 (t-test). Representative images (scale bar 100 µm) and quantitative data of **(G)** periodic acid Schiff (PAS) staining and **(H)** immunohistochemical detection of kidney injury molecule-1 (KIM-1) in renal sections of C57BL/6J wild-type mice are depicted (acute: sham $n = 4$, Stx2 $n = 9$; subacute: sham $n = 5$, Stx2 $n = 4$). *$p < 0.05$ for sham (white dots) vs. Stx2 (black dots; Mann–Whitney U-test).

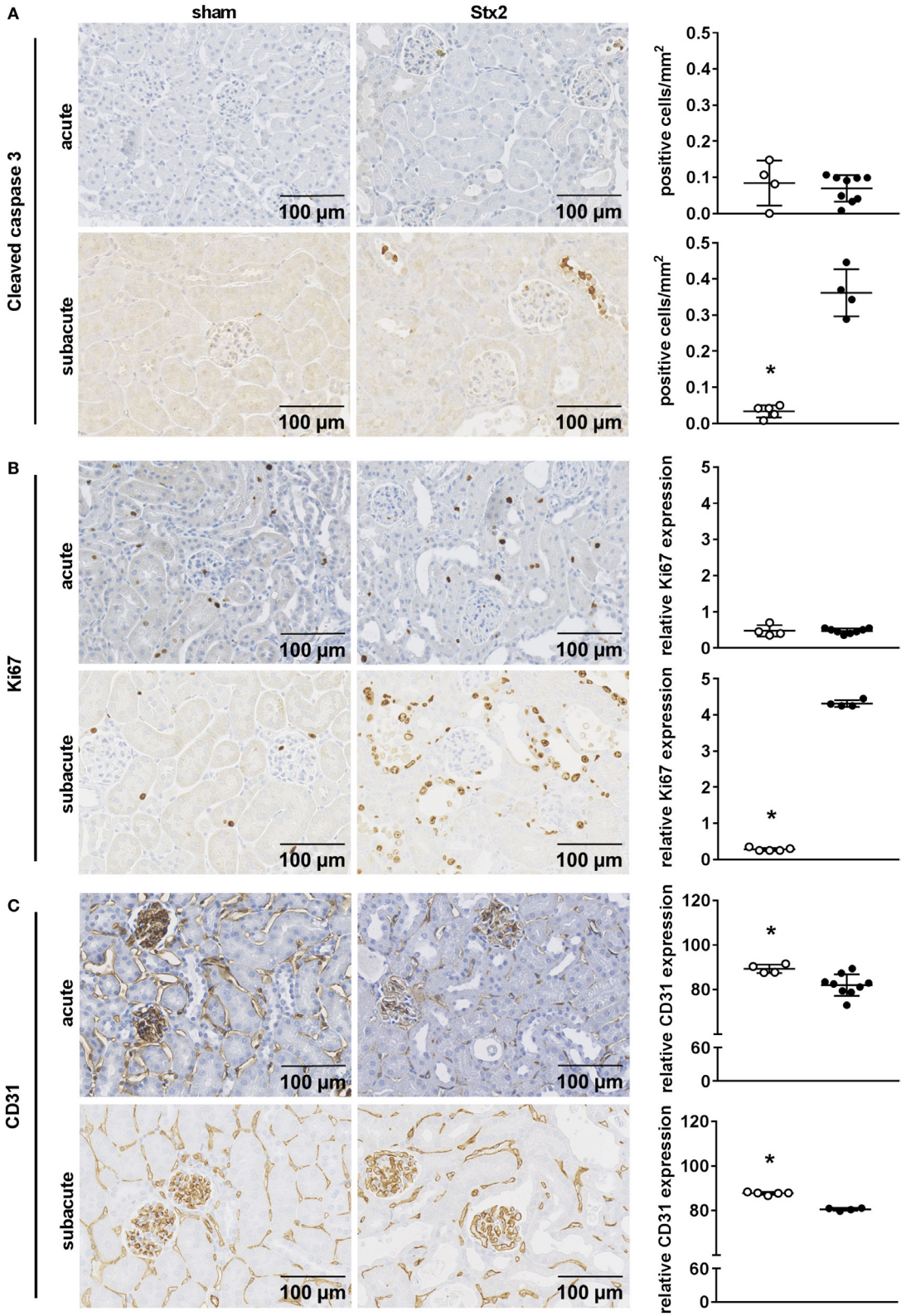

FIGURE 7 | Indicators of cell death, reactive proliferation, and endothelial damage in kidney tissue of C57BL/6J mice subjected to different Stx2 regimens. Representative images of immunohistochemical detection and quantitative data of **(A)** cleaved caspase 3 (acute: sham $n = 4$, Stx2 $n = 9$; subacute: sham $n = 5$, Stx2 $n = 3$), **(B)** Ki67, and **(C)** CD31 (acute: sham $n = 4$, Stx2 $n = 9$; subacute: sham $n = 5$, Stx2 $n = 4$) in renal sections of C57BL/6J wild-type mice are depicted. *$p < 0.05$ for sham (white dots) vs. Stx2 (black dots; *t*-test).

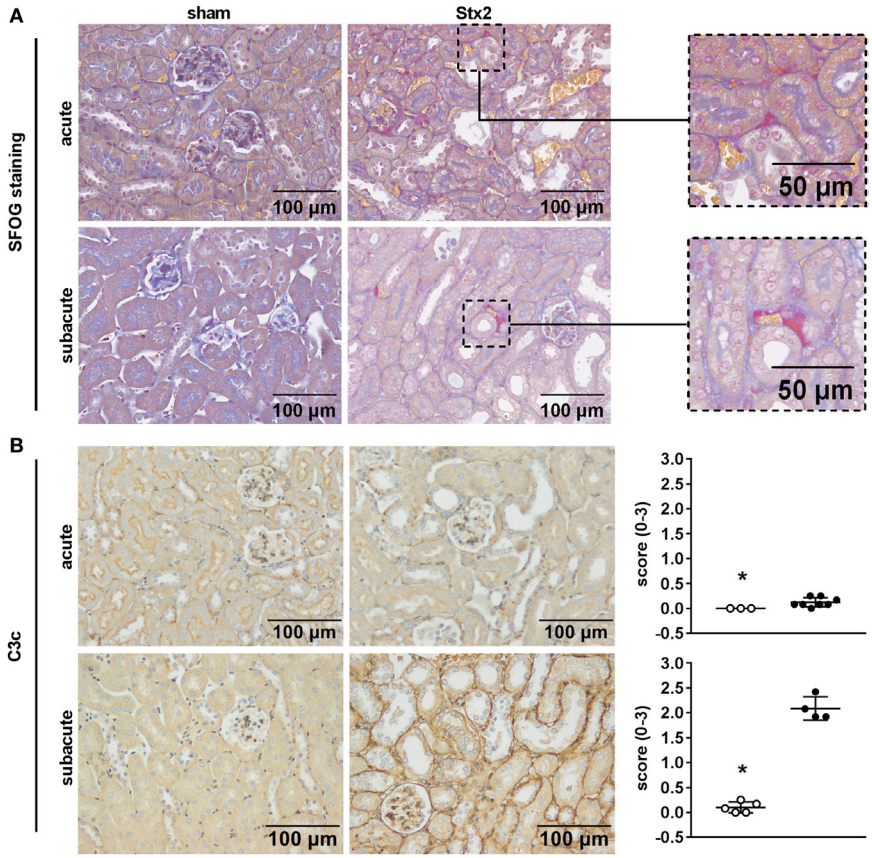

FIGURE 8 | Indicators of thrombus formation and complement activation in C57BL/6J mice subjected to different Stx2 regimens. **(A)** Representative images (scale bar 100 µm) of SFOG staining in renal sections. Thrombus formation was observed in Stx2 groups of both models (see zoomed areas on the right, scale bar 50 µm). **(B)** Representative images (scale bar 100 µm) of immunohistochemical detection and quantification of C3 and C3b complement deposition by C3c staining in renal sections of C57BL/6J wild-type mice are depicted (acute: sham $n = 3$, Stx2 $n = 8$; subacute: sham $n = 5$, Stx2 $n = 4$). *$p < 0.05$ for sham (white dots) vs. Stx2 (black dots; Mann–Whitney U-test).

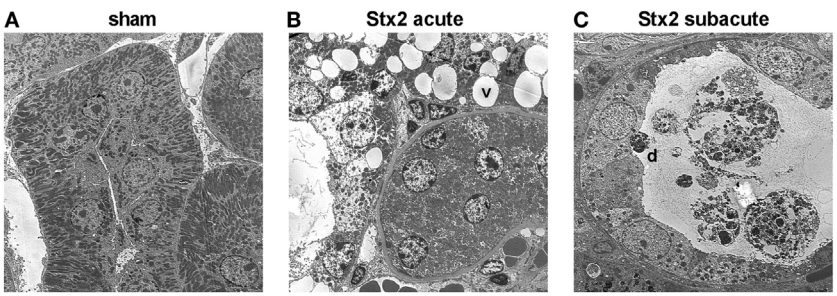

FIGURE 9 | Electron microscopic analysis of kidney tissue from C57BL/6J mice subjected to different Stx2 regimens. Representative ultrastructural images of renal tubules show **(A)** no pathological changes in sham animals, **(B)** prominent vacuoles (v) in the acute and **(C)** pronounced tubular atrophy (d = detached tubular cell) in the subacute model. Magnification: 2,000×; ultrathin sections, $n = 2$ animals were studied per group.

(3 of 12), and cytokine activity (3 of 12). The remaining two clusters were associated with apoptosis and positive regulation of transcription (**Table 2**).

The microarray dataset was published in Gene Expression Online and is available under "GSE99229—Alterations in gene expression in response to different regimes of Shiga toxin 2."

DISCUSSION

Reproducible Induction of HUS-Like Disease by i.v. Administration of Stx2

Several groups have attempted, more or less successful, to generate murine models of HUS. Mice were challenged either by

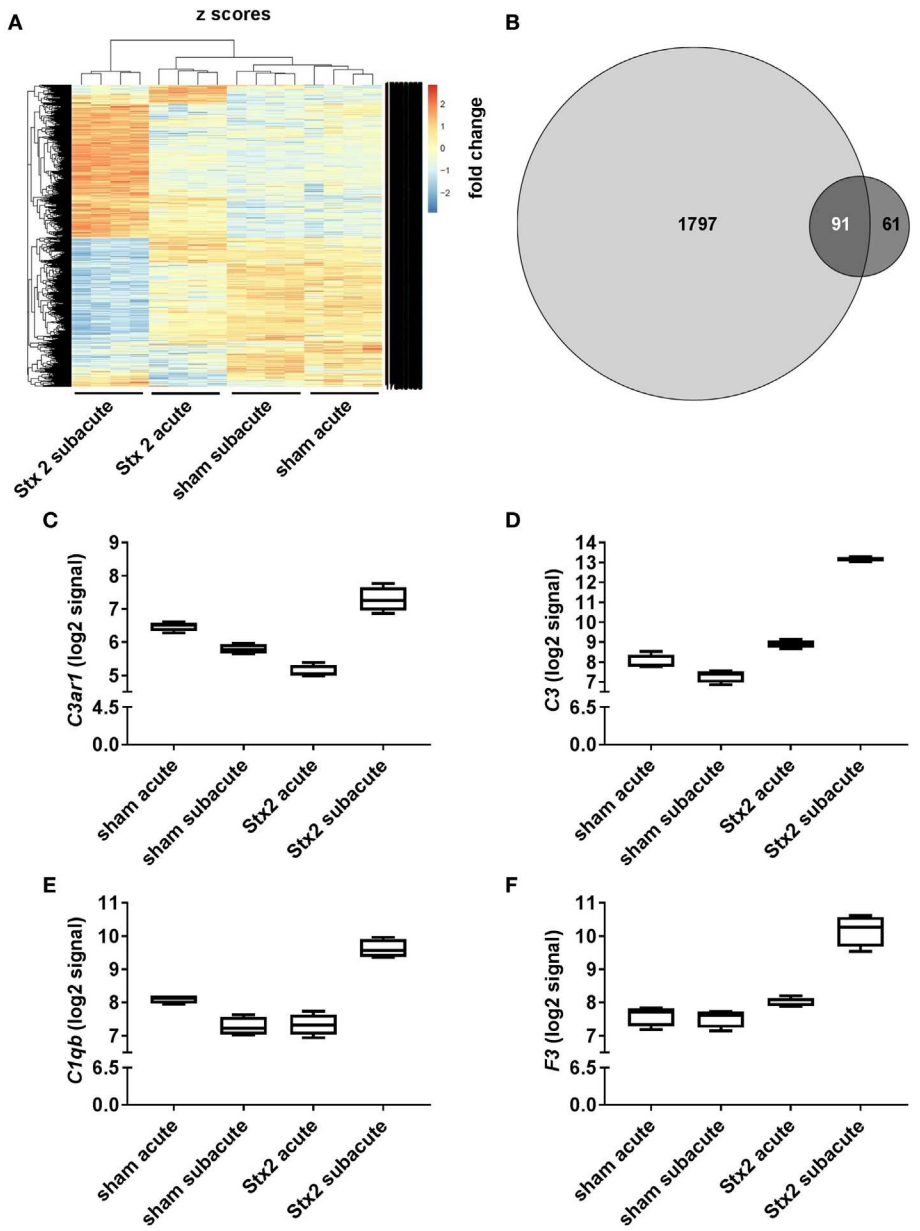

FIGURE 10 | Changes in renal gene expression in response to different Stx2 regimens. **(A)** Heat map of features obtained from ANOVA filtering adjusted $p < 0.05$ comprising *z*-score scaled values. In each group, $n = 4$ animals were studied. **(B)** Proportional Venn diagram of differentially expressed genes according to the limit fold change for acute (dark gray) vs. subacute model (light gray). Number of overlapping genes is highlighted in white. Gene expression data were filtered for candidate genes from complement pathway. Log2 signals for **(C)** complement C3a receptor 1 (*C3ar1*), **(D)** complement factor C3 (*C3*), **(E)** complement C1q B chain (*C1qb*), and **(F)** tissue factor (*F3*) are illustrated by box plots.

gavage of viable STEC [reviewed by Mohawk and O'Brien (34)], by i.p. co-application of a single high dose of lipopolysaccharide (LPS) and Stx2 (31, 32), by i.p. application of a single high dose of Stx2 alone (32), or by multiple i.p. applications of sub-lethal doses of Stx2 (33, 39, 40). In most studies, injection of Stx alone appeared to be insufficient to induce HUS-like disease in mice (31, 32, 41). However, in 2008, Sauter et al. introduced a model where repeated i.p. injections of sub-lethal doses of Stx2 led to the manifestation of HUS-typical symptoms in C57BL/6J mice (33). In our study, acute or subacute progression of HUS-like disease in mice was induced by application of different doses of Stx2, purified from the well-characterized EHEC O157:H7 patient isolate 86-24 originating from a HUS outbreak in the USA (35). Apart from being the causative agent for HUS in humans, this strain reproducibly induced a HUS-like disease in gnotobiotic piglets (22, 24, 25). In contrast to other studies, we injected Stx2 i.v. aiming for rapid delivery and highest bioavailability (42). We used mice aged 10–16 weeks as they resemble

TABLE 1 | The 91 overlapping differentially expressed genes of the acute and subacute model were assigned to biological process or molecular function and itemized to upregulation and downregulation for each model.

Biological process/molecular function	Stx2 acute		Stx2 subacute	
	Up	Down	Up	Down
Biological process				
Angiogenesis	2	2	2	2
Apoptosis	9	2	9	2
Blood pressure	2	–	2	–
Circadian rhythm	1	–	1	–
Coagulation	3	–	3	–
Cytokine signaling	5	2	5	2
Development		2		2
Differentiation	8	2	8	2
Immune response	9	1	9	1
– Of that: chemotaxis	5	1	6	
Inflammatory response	11	3	12	2
Keratinization	1	–	1	–
Metabolism	6	11	6	11
– Of that: cholesterol metabolism	1	2	1	2
– Of that: lipid metabolism	3	4	3	4
– Of that: metabolism of vitamin D	1	2	1	2
– Of that: urea cycle	1	–	1	–
– Of that: steroid metabolism	–	3	–	3
Proliferation	8	1	8	1
– Of that: cell cycle regulation	6	1	6	1
Regulation of pH	1	1	1	1
Response to DNA damage	1	–	1	–
Response to hypoxia	1	4	1	4
Response to molecules of bacterial origin	2	–	2	–
Response to oxidative stress	3	1	3	1
Response to stress	3	–	3	–
Molecular function				
Coding unknown proteins	2	1	1	2
Complement activity	–	1	1	–
DNA binding	15	1	15	1
Glycosylation	–	1	–	1
Ion binding	–	1	–	1
Integral membrane component	–	1	–	1
ncRNA	4	1	4	1
Transporter activity	–	17		17
– Of that: ion transport	–	10	–	10
– Of that: urea transport	–	1	–	1
– Of that: toxin transport	–	1	–	1
– Of that: water transport	–	3	–	3
tRNA processing	1	–	1	–

Almost all genes were regulated in the same manner in both models, exceptions are highlighted by red boxes.

TABLE 2 | The 12 significantly enriched annotation clusters identified with DAVID 6.8 in the 91 differentially expressed genes of the acute and subacute model.

Annotation cluster	Key words	Enrichment score	Number of genes
1	Inflammatory response ($p = 0.00003$), cytokine activity ($p = 0.0012$), immune response ($p = 0.028$)	3.5	22
2	Apoptosis ($p = 0.0096$)	2.96	11
3	Basolateral plasma membrane ($p = 0.00097$), major intrinsic protein ($p = 0.038$), water channel activity ($p = 0.048$)	2.87	10
4	Cellular response to interferon-gamma ($p = 0.028$), interleukin-1 ($p = 0.034$), or tumor necrosis factor ($p = 0.77$)	2.69	6
5	Cytokine ($p = 0.0012$), growth factor ($p = 0.37$)	2.35	8
6	Cytokine activity ($p = 0.0012$), cytokine ($p = 0.0012$), secreted ($p = 0$ 0.017)	2.34	26
7	Response to hypoxia ($p = 0.075$), regulation of blood pressure ($p = 0.093$)	2.16	7
8	Integral component of plasma membrane ($p = 0.00019$), ion transport ($p = 0.0029$), glycoprotein ($p = 0.014$)	1.94	45
9	Domain: leucine zipper ($p = 0.000074$), DNA-binding region: basic motif ($p = 0.00044$), transcriptional factor activity ($p = 0.049$)	1.8	28
10	Epstein–Barr virus infection ($p = 0.053$), NFκB signaling pathway ($p = 0.091$)	1.49	23
11	Response to endoplasmic reticulum stress ($p = 0.56$)	1.34	4
12	Sodium transport ($p = 0.37$)	1.32	3

Clusters were arranged according to the enrichment score. The most important key words (Benjamini-adjusted p-values in brackets) and number of genes in each cluster are given for each cluster.

human adolescents or young adults (43) which are an important patient subgroup based on the estimation of global STEC-HUS incidence performed by Majowicz et al. (44).

LPS Does Not Appear to Be a Prerequisite for the Development of HUS in Humans and Mice

The role of LPS in infection-associated HUS is not entirely clear. LPS has been reported to augment Stx-mediated cytotoxicity by cytokine release in mice (45, 46), but does not appear to be prerequisite for HUS development in humans. In STEC-HUS, high serum levels of anti-LPS antibodies (47) and elevated LPS binding protein levels (48) were detectable, but most notably, endotoxemia has not yet been reported. Only in very rare cases of non-STEC-HUS, e.g., caused by infections with *Shigella ssp.* (49), LPS was detectable in the plasma of patients by *Limulus* assay. It was reported previously that Stx2 alone could induce pro-inflammatory transcription events that might contribute to HUS pathogenesis (50, 51). In this study, we avoided the use of additional pro-inflammatory stimuli and focused on patho-mechanisms exclusively mediated by Stx2.

Standardized Surveillance of Stx2-Challenged Mice by a Scoring System Is Necessary

Especially in the early stage, we noticed that disease aggravation occurs with unapparent clinical signs and loss of weight appears as the first symptom. We observed a profound weight loss over time in both models comparable to what has been reported by other groups (32, 33). Interestingly, in the subacute model mice frequently developed a pronounced hind limb clasping reflex in addition to neurological symptoms like tremors and ataxia that have already been described by Sauter

et al. (33). To monitor disease progression, we developed and introduced—for the first time—a scoring system based on the activity of mice. It detects critically ill mice that need to be euthanized and, thus, became very important not only for accurate experimentation but also in terms of animal welfare.

Volume Resuscitation Is a Crucial Measure to Attenuate Hemoconcentration in Mice

As a consequence of the profound hemoconcentration and weight loss observed in pilot experiments, we, for the first time, established a volume resuscitation regimen to prevent severe hypovolemia. While characterizing the acute model, we realized that s.c. administration of 0.5 ml balanced crystalloids twice daily was not sufficient to alleviate hemoconcentration. Therefore, we expanded volume resuscitation in the subacute model to three doses of 0.8 ml daily. Upon hospital admission, STEC-HUS patients frequently show slightly elevated levels of hemoglobin or hematocrit as a consequence of diarrhea-induced dehydration (52, 53). Thus, we assume prerenal pathomechanisms contribute to HUS pathology and might aggravate disease progression. This hypothesis is supported by studies that identified hemoconcentration as an independent risk factor for increased mortality (54) and severity of HUS (53). However, in our study, we aimed to prevent, by volume replacement therapy, the prerenal mechanisms from outweighing the Stx2-related mechanisms. Even though profound hemoconcentration was observed previously in murine HUS models (32), volume resuscitation strategies have thus far not been included in experimental designs.

The Development of a Photometrical Assay Allows a More Accurate Quantification of Hemolysis

Hemolysis is a defining feature of HUS. Recently, the central role of extracellular "free" heme as a perpetuating factor in life-threatening infections, even with only a very moderate degree of hemolysis, has been acknowledged (55). Here, we determined the degree of hemolysis not only by measuring indirect markers, such as plasma bilirubin and LDH, but also by developing a photometrical assay to quantify free plasma hemoglobin. We detected hemolysis in both models, however, it was more pronounced in the subacute model. Our results are in line with other studies, which observed hemolysis in murine HUS either by simple visual inspection (32) or photometrically (33).

Persistent Neutrophilia Might Contribute to Disease Progression

In accordance with our recent observations in EHEC-infected gnotobiotic piglets (25) and with the finding by Sauter et al. in Stx2-challenged mice (33), we found low leukocyte counts in both models that were accompanied by persistent neutrophilia. There is some evidence that neutrophilia directly contributes to Stx2 toxicity as mortality and kidney damage are reduced in a murine model of HUS using polymorphonuclear-cell-(PMN)-depleted mice (56). Neutrophil extracellular traps were shown to aggravate intravascular coagulation during sepsis in mice (57) and their degradation appears to be impaired in HUS patients (58), which further underlines the role of neutrophilia in HUS pathogenesis. Furthermore, we demonstrated macrophages and T lymphocyte invasion in the kidneys of mice that underwent the subacute, but not the acute protocol, indicating an activation of the innate and adaptive immune response. The role of mitochondria in immune response was intensively studied during the past years [as reviewed in Ref. (59)]. Distinct changes in the metabolic profile of human endothelial cells in response to Stx2 were shown *in vitro* (60) but not yet assessed *in vivo*. In this context, further analysis on the interrelation between immune response and metabolism might elucidate novel aspects of HUS progression.

Stx2 Challenge Induced Kidney Dysfunction, Renal Endothelial Damage, and Thrombotic Microangiopathy as Key Features of HUS

Consistent with the literature (31–33), we observed kidney dysfunction following Stx2 challenge, indicated by significant rises of plasma urea and creatinine. Furthermore, we detected—for the first time—significantly higher levels of plasma NGAL in the acute and subacute model, which have also been shown in HUS patients with renal dysfunction (61), but to our knowledge have not been examined in murine models of HUS. Occurrence of renal endothelial damage is crucial for the development of HUS (62, 63). So far, evidence for endothelial damage in mouse models of HUS was mainly provided on an ultrastructural level (31–33). Here, we additionally demonstrated by immunohistochemical assessment and quantification a significant decrease of CD31-positive endothelial cells in both disease models, indicating severe endothelial cell injury. Thrombotic microangiopathy in the kidneys is a hallmark of HUS that was so far only detectable in murine HUS models induced by co-application of Stx2 and LPS (31, 32). It could not be demonstrated in the repetitive Stx2 injection model presented by Sauter et al. (33). However, we were able to demonstrate microthrombi formation in our acute and subacute model.

In Contrast to Human HUS Tubular Rather Than Glomerular Lesions Predominate in Stx2-Induced Murine HUS

Tubular (64) and glomerular injury (65, 66) contribute to HUS pathology in patients. In rodent models of HUS, tubular rather than glomerular injury is a common finding (41, 67–69) possibly owing to the higher expression of the Gb3 receptor on glomerular cells in humans as opposed to on tubular cells in rodents (70). Nevertheless, some studies found glomerular injury in an ultrastructural analysis (31–33). In both models, we could not detect glomerular injury on the ultrastructural level and we found no significant changes in the kidney volume and total count of glomeruli of mice by LSFM (only assessed in the subacute model). In many former preclinical HUS studies, tubular injury in mice could either not be detected [Stx2/LPS co-administration (70)] or has not been examined [Stx2/LPS co-administration (31, 32),

Stx2 model (33)]. However, we observed severe tubular injury in both Stx2 models. The results of ultrastructural and immunohistochemical analyses indicate that tubular damage is more pronounced in the subacute model.

Apoptosis and Proliferation Only Occur in the Subacute Course of HUS-Like Disease in Mice

We detected elevated apoptosis rates of tubular epithelial cells indicated by significant increase in cleaved caspase 3 staining in the subacute, but not in the acute model. Apoptosis was shown to be profound in tubular epithelial cells in human STEC-HUS, independent from the grade of thrombotic microangiopathy, indicating that it separately contributes to the pathogenesis of tubular injury observed in these patients (64). Although potentially involved in HUS pathogenesis, apoptosis was not yet examined in most murine models of HUS (31–33). Most notably, we demonstrate for the first time that proliferation of tubular epithelial cells is increased in response to Stx2 as indicated by a significantly higher expression of Ki67 in the subacute model. We hypothesize that this effect might be a reactive mechanism to the re-occurring harmful stimuli of multiple Stx2 injections.

Complement Activation Plays a Major Role in HUS Pathogenesis

Complement activation is a hallmark of HUS pathogenesis in STEC-HUS (71, 72) as well as in atypical HUS (73). Complement activation was found in mouse models of Stx2/LPS co-injection (74) and EHEC infection (75). Here, we demonstrate that a single high dose of Stx2 is not sufficient to provoke complement activation in mice, whereas multiple doses of Stx2 induce profound activation of the complement system as indicated by significant renal C3c deposition. The differences in complement activation in the acute and subacute course of disease were further supported by gene expression data of kidneys.

Further Characterization of Regulated Pathways Can Potentially Lead to New Insights Into Pathophysiological Mechanisms of HUS

Our observations that 1,888 genes were differentially regulated in the subacute disease model and only 152 in the acute one support our hypothesis of different underlying pathomechanisms. However, differential gene expression analysis of kidneys revealed 91 overlapping genes in significantly enriched categories (e.g., cytokine signaling, apoptosis, immune, and inflammatory response, transporter activity). While changes in renal gene expression following Stx2 or Stx2/LPS co-challenge have already been characterized by Keepers et al. (32), we are the first to demonstrate that also three repetitive sub-lethal doses of Stx2 lead to considerable changes in transcriptional events in a murine model of HUS. The gene clusters we found to be differentially regulated in both models also match the ones proposed by Keepers et al. in a model of LPS/Stx2-co-challenge (32). As we isolated total kidney mRNA, it remains unclear if these changes might be cell-type specific. Furthermore, the more prominent changes in the subacute model might be partially explained by the high amount of invading immune cells that might contribute to changed expression patterns.

CONCLUSION

We have established two murine models that allow studying the action of Stx2 in an acute and subacute phase of HUS-like disease. Acute kidney dysfunction and injury, hemolysis, renal endothelial cell damage and microthrombi, as well as neurological symptoms were reproducibly observed in both models as pathognomonic signs of HUS in humans. Most notably, intrarenal changes, such as complement activation, accumulation of macrophages and T lymphocytes, as well as apoptosis and proliferation could only be observed in the subacute model, whereas hypovolemia, as a prerenal pathomechanism, appears to play a major role for the development of kidney dysfunction in the acute model. With this study, we provide murine models of HUS that will serve as suitable and valuable tools to further characterize the pathophysiology of HUS and perform pharmacological trials in HUS and related conditions associated with impaired microcirculation in the kidney.

ETHICS STATEMENT

This study was carried out in accordance with the German legislation and approved guidelines ("Tierschutzgesetz" and "Tierschutz-Versuchstierverordnung"). The animal protocols were approved by the regional animal welfare committee and the Thuringian State Office for Consumer Protection and Food Safety, Bad Langensalza, Germany (registration number 02-058/14).

AUTHOR CONTRIBUTIONS

Conception and design of the study: SC; conception and performance of animal experiments: SD, BW, WP, and SC; sample analysis and statistical analysis: SD, WP, BW, CD, MK, and SC; contribution of important intellectual content to histologically analysis: CD and KA; purification and supply of Stx2: FG and WR; LSFM: WP and MG; automated LSFM image analysis: AM and MF; microarray analysis: SD, SL, and SC; drafting the manuscript for important intellectual content: SC, SD, WP, FG, and CD; revising the manuscript prior to submission: SC, SD, CD, FG, PZ, WP, BW, SL, MF, and MG; all authors carefully reviewed and approved the manuscript.

ACKNOWLEDGMENTS

We acknowledge Markus Bläß and the German Cancer Research Center (DKFZ) for expert support in microarray preparation and measurements as well as Alexandra Brenzel and the Imaging Center Essen (IMCES) for expert support in LSFM imaging. We would like to thank Jacqueline Fischer, Ulrike Vetterling, Manuela Brandt, Florian Guggenbichler, and Cora Richert for technical assistance.

FUNDING

The research leading to these results has received funding from the German Research Foundation (DFG; Research Unit FOR1738, project P9, award no. CO912/2-1 to SC and SFB 1192, project B06 to PZ) and the Federal Ministry of Education and Research (BMBF; ZIK Septomics Research Centre, Translational Septomics, award no. 03Z22JN12 to SC and Center for Sepsis Control and Care, project TaSep, award no. 01EO1502 to SC) and from the European Community's Seventh Framework Programme "European Consortium for High-Throughput Research in Rare Kidney Diseases (EURenOmics, award no. 2012-305608 to PZ)." The funders had no role in study design, data collection and analysis, decision to publish, or preparation of the manuscript.

SUPPLEMENTARY MATERIAL

The Supplementary Material for this article can be found online at https://www.frontiersin.org/articles/10.3389/fimmu.2018.01459/full#supplementary-material.

REFERENCES

1. Fakhouri F, Zuber J, Fremeaux-Bacchi V, Loirat C. Haemolytic uraemic syndrome. *Lancet* (2017) 390:681–96. doi:10.1016/S0140-6736(17)30062-4
2. Karmali MA, Steele BT, Petric M, Lim C. Sporadic cases of haemolytic-uraemic syndrome associated with faecal cytotoxin and cytotoxin-producing *Escherichia coli* in stools. *Lancet* (1983) 1:619–20. doi:10.1016/S0140-6736(83)91795-6
3. Karmali MA. Infection by Shiga toxin-producing *Escherichia coli*: an overview. *Mol Biotechnol* (2004) 26:117–22. doi:10.1385/MB:26:2:117
4. Meinel C, Sparta G, Dahse HM, Hörhold F, König R, Westermann M, et al. *Streptococcus pneumoniae* from patients with hemolytic uremic syndrome binds human plasminogen via the surface protein PspC and uses plasmin to damage human endothelial cells. *J Infect Dis* (2018) 217(3):358–70. doi:10.1093/infdis/jix305
5. Rodriguez De Cordoba S, Hidalgo MS, Pinto S, Tortajada A. Genetics of atypical hemolytic uremic syndrome (aHUS). *Semin Thromb Hemost* (2014) 40:422–30. doi:10.1055/s-0034-1375296
6. Gerber A, Karch H, Allerberger F, Verweyen HM, Zimmerhackl LB. Clinical course and the role of Shiga toxin-producing *Escherichia coli* infection in the hemolytic-uremic syndrome in pediatric patients, 1997–2000, in Germany and Austria: a prospective study. *J Infect Dis* (2002) 186:493–500. doi:10.1086/341940
7. Constantinescu AR, Bitzan M, Weiss LS, Christen E, Kaplan BS, Cnaan A, et al. Non-enteropathic hemolytic uremic syndrome: causes and short-term course. *Am J Kidney Dis* (2004) 43:976–82. doi:10.1053/j.ajkd.2004.02.010
8. Legendre CM, Licht C, Muus P, Greenbaum LA, Babu S, Bedrosian C, et al. Terminal complement inhibitor eculizumab in atypical hemolytic-uremic syndrome. *N Engl J Med* (2013) 368:2169–81. doi:10.1056/NEJMoa1208981
9. Frank C, Werber D, Cramer JP, Askar M, Faber M, An Der Heiden M, et al. Epidemic profile of Shiga-toxin-producing *Escherichia coli* O104:H4 outbreak in Germany. *N Engl J Med* (2011) 365:1771–80. doi:10.1056/NEJMoa1106483
10. Mayer CL, Leibowitz CS, Kurosawa S, Stearns-Kurosawa DJ. Shiga toxins and the pathophysiology of hemolytic uremic syndrome in humans and animals. *Toxins (Basel)* (2012) 4:1261–87. doi:10.3390/toxins4111261
11. Boerlin P, Mcewen SA, Boerlin-Petzold F, Wilson JB, Johnson RP, Gyles CL. Associations between virulence factors of Shiga toxin-producing *Escherichia coli* and disease in humans. *J Clin Microbiol* (1999) 37:497–503.
12. Jenkins C, Willshaw GA, Evans J, Cheasty T, Chart H, Shaw DJ, et al. Subtyping of virulence genes in verocytotoxin-producing *Escherichia coli* (VTEC) other than serogroup O157 associated with disease in the United Kingdom. *J Med Microbiol* (2003) 52:941–7. doi:10.1099/jmm.0.05160-0
13. Persson S, Olsen KE, Ethelberg S, Scheutz F. Subtyping method for *Escherichia coli* Shiga toxin (verocytotoxin) 2 variants and correlations to clinical manifestations. *J Clin Microbiol* (2007) 45:2020–4. doi:10.1128/JCM.02591-06
14. Brandal LT, Wester AL, Lange H, Lobersli I, Lindstedt BA, Vold L, et al. Shiga toxin-producing *Escherichia coli* infections in Norway, 1992–2012: characterization of isolates and identification of risk factors for haemolytic uremic syndrome. *BMC Infect Dis* (2015) 15:324. doi:10.1186/s12879-015-1017-6
15. Sandvig K, Grimmer S, Lauvrak SU, Torgersen ML, Skretting G, Van Deurs B, et al. Pathways followed by ricin and Shiga toxin into cells. *Histochem Cell Biol* (2002) 117:131–41. doi:10.1007/s00418-001-0346-2
16. Endo Y, Mitsui K, Motizuki M, Tsurugi K. The mechanism of action of ricin and related toxic lectins on eukaryotic ribosomes. The site and the characteristics of the modification in 28 S ribosomal RNA caused by the toxins. *J Biol Chem* (1987) 262:5908–12.
17. Proulx F, Seidman EG, Karpman D. Pathogenesis of Shiga toxin-associated hemolytic uremic syndrome. *Pediatr Res* (2001) 50:163–71. doi:10.1203/00006450-200108000-00002
18. Bielaszewska M, Karch H. Consequences of enterohaemorrhagic *Escherichia coli* infection for the vascular endothelium. *Thromb Haemost* (2005) 94:312–8. doi:10.1160/TH05-04-0265
19. Taylor FB Jr, Tesh VL, Debault L, Li A, Chang AC, Kosanke SD, et al. Characterization of the baboon responses to Shiga-like toxin: descriptive study of a new primate model of toxic responses to Stx-1. *Am J Pathol* (1999) 154:1285–99. doi:10.1016/S0002-9440(10)65380-1
20. Stearns-Kurosawa DJ, Oh SY, Cherla RP, Lee MS, Tesh VL, Papin J, et al. Distinct renal pathology and a chemotactic phenotype after enterohemorrhagic *Escherichia coli* Shiga toxins in non-human primate models of hemolytic uremic syndrome. *Am J Pathol* (2013) 182:1227–38. doi:10.1016/j.ajpath.2012.12.026
21. Dykstra SA, Moxley RA, Janke BH, Nelson EA, Francis DH. Clinical signs and lesions in gnotobiotic pigs inoculated with Shiga-like toxin I from *Escherichia coli*. *Vet Pathol* (1993) 30:410–7. doi:10.1177/030098589303000502
22. Tzipori S, Gunzer F, Donnenberg MS, De Montigny L, Kaper JB, Donohue-Rolfe A. The role of the eaeA gene in diarrhea and neurological complications in a gnotobiotic piglet model of enterohemorrhagic *Escherichia coli* infection. *Infect Immun* (1995) 63:3621–7.
23. Baker DR, Moxley RA, Francis DH. Variation in virulence in the gnotobiotic pig model of O157:H7 *Escherichia coli* strains of bovine and human origin. *Adv Exp Med Biol* (1997) 412:53–8. doi:10.1007/978-1-4899-1828-4_6
24. Gunzer F, Hennig-Pauka I, Waldmann KH, Sandhoff R, Gröne HJ, Kreipe HH, et al. Gnotobiotic piglets develop thrombotic microangiopathy after oral infection with enterohemorrhagic *Escherichia coli*. *Am J Clin Pathol* (2002) 118:364–75. doi:10.1309/UMW9-D06Q-M94Q-JGH2
25. Wöchtl B, Gunzer F, Gerner W, Gasse H, Koch M, Bago Z, et al. Comparison of clinical and immunological findings in gnotobiotic piglets infected with *Escherichia coli* O104:H4 outbreak strain and EHEC O157:H7. *Gut Pathog* (2017) 9:30. doi:10.1186/s13099-017-0179-8
26. Garcia A, Bosques CJ, Wishnok JS, Feng Y, Karalius BJ, Butterton JR, et al. Renal injury is a consistent finding in Dutch Belted rabbits experimentally infected with enterohemorrhagic *Escherichia coli*. *J Infect Dis* (2006) 193:1125–34. doi:10.1086/501364
27. Garcia A, Marini RP, Catalfamo JL, Knox KA, Schauer DB, Rogers AB, et al. Intravenous Shiga toxin 2 promotes enteritis and renal injury characterized by polymorphonuclear leukocyte infiltration and thrombosis in Dutch Belted rabbits. *Microbes Infect* (2008) 10:650–6. doi:10.1016/j.micinf.2008.03.004
28. Shibolet O, Shina A, Rosen S, Cleary TG, Brezis M, Ashkenazi S. Shiga toxin induces medullary tubular injury in isolated perfused rat kidneys. *FEMS Immunol Med Microbiol* (1997) 18:55–60. doi:10.1111/j.1574-695X.1997.tb01027.x

29. Yamamoto ET, Mizuno M, Nishikawa K, Miyazawa S, Zhang L, Matsuo S, et al. Shiga toxin 1 causes direct renal injury in rats. *Infect Immun* (2005) 73:7099–106. doi:10.1128/IAI.73.11.7099-7106.2005
30. Ochoa F, Lago NR, Gerhardt E, Ibarra C, Zotta E. Characterization of stx2 tubular response in a rat experimental model of hemolytic uremic syndrome. *Am J Nephrol* (2010) 32:340–6. doi:10.1159/000319444
31. Ikeda M, Ito S, Honda M. Hemolytic uremic syndrome induced by lipopolysaccharide and Shiga-like toxin. *Pediatr Nephrol* (2004) 19:485–9. doi:10.1007/s00467-003-1395-7
32. Keepers TR, Psotka MA, Gross LK, Obrig TG. A murine model of HUS: Shiga toxin with lipopolysaccharide mimics the renal damage and physiologic response of human disease. *J Am Soc Nephrol* (2006) 17:3404–14. doi:10.1681/ASN.2006050419
33. Sauter KA, Melton-Celsa AR, Larkin K, Troxell ML, O'brien AD, Magun BE. Mouse model of hemolytic-uremic syndrome caused by endotoxin-free Shiga toxin 2 (Stx2) and protection from lethal outcome by anti-Stx2 antibody. *Infect Immun* (2008) 76:4469–78. doi:10.1128/IAI.00592-08
34. Mohawk KL, O'Brien AD. Mouse models of *Escherichia coli* O157:H7 infection and Shiga toxin injection. *J Biomed Biotechnol* (2011) 2011:258185. doi:10.1155/2011/258185
35. Griffin PM, Ostroff SM, Tauxe RV, Greene KD, Wells JG, Lewis JH, et al. Illnesses associated with *Escherichia coli* O157:H7 infections. A broad clinical spectrum. *Ann Intern Med* (1988) 109:705–12. doi:10.7326/0003-4819-109-9-705
36. Matussek A, Lauber J, Bergau A, Hansen W, Rohde M, Dittmar KE, et al. Molecular and functional analysis of Shiga toxin-induced response patterns in human vascular endothelial cells. *Blood* (2003) 102:1323–32. doi:10.1182/blood-2002-10-3301
37. Mulay SR, Eberhard JN, Pfann V, Marschner JA, Darisipudi MN, Daniel C, et al. Oxalate-induced chronic kidney disease with its uremic and cardiovascular complications in C57BL/6 mice. *Am J Physiol Renal Physiol* (2016) 310:F785–95. doi:10.1152/ajprenal.00488.2015
38. Huang Da W, Sherman BT, Lempicki RA. Systematic and integrative analysis of large gene lists using DAVID bioinformatics resources. *Nat Protoc* (2009) 4:44–57. doi:10.1038/nprot.2008.211
39. Parello CS, Mayer CL, Lee BC, Motomochi A, Kurosawa S, Stearns-Kurosawa DJ. Shiga toxin 2-induced endoplasmic reticulum stress is minimized by activated protein C but does not correlate with lethal kidney injury. *Toxins (Basel)* (2015) 7:170–86. doi:10.3390/toxins7010170
40. Mejias MP, Fernandez-Brando RJ, Ramos MV, Abrey-Recalde MJ, Zotta E, Meiss R, et al. Development of a mouse model of Shiga Toxin 2 (Stx2) intoxication for testing therapeutic agents against hemolytic uremic syndrome (HUS). *Curr Pharm Des* (2016) 22:5294–9. doi:10.2174/1381612822666160628080350
41. Palermo M, Alves-Rosa F, Rubel C, Fernandez GC, Fernandez-Alonso G, Alberto F, et al. Pretreatment of mice with lipopolysaccharide (LPS) or IL-1beta exerts dose-dependent opposite effects on Shiga toxin-2 lethality. *Clin Exp Immunol* (2000) 119:77–83. doi:10.1046/j.1365-2249.2000.01103.x
42. Viel T, Dransart E, Nemati F, Henry E, Theze B, Decaudin D, et al. In vivo tumor targeting by the B-subunit of Shiga toxin. *Mol Imaging* (2008) 7:239–47. doi:10.2310/7290.2008.00022
43. Dutta S, Sengupta P. Men and mice: relating their ages. *Life Sci* (2016) 152:244–8. doi:10.1016/j.lfs.2015.10.025
44. Majowicz SE, Scallan E, Jones-Bitton A, Sargeant JM, Stapleton J, Angulo FJ, et al. Global incidence of human Shiga toxin-producing *Escherichia coli* infections and deaths: a systematic review and knowledge synthesis. *Foodborne Pathog Dis* (2014) 11:447–55. doi:10.1089/fpd.2013.1704
45. Keepers TR, Gross LK, Obrig TG. Monocyte chemoattractant protein 1, macrophage inflammatory protein 1 alpha, and RANTES recruit macrophages to the kidney in a mouse model of hemolytic-uremic syndrome. *Infect Immun* (2007) 75:1229–36. doi:10.1128/IAI.01663-06
46. Roche JK, Keepers TR, Gross LK, Seaner RM, Obrig TG. CXCL1/KC and CXCL2/MIP-2 are critical effectors and potential targets for therapy of *Escherichia coli* O157:H7-associated renal inflammation. *Am J Pathol* (2007) 170:526–37. doi:10.2353/ajpath.2007.060366
47. Bitzan M, Moebius E, Ludwig K, Müller-Wiefel DE, Heesemann J, Karch H. High incidence of serum antibodies to *Escherichia coli* O157 lipopolysaccharide in children with hemolytic-uremic syndrome. *J Pediatr* (1991) 119:380–5. doi:10.1016/S0022-3476(05)82049-9
48. Proulx F, Seidman E, Mariscalco MM, Lee K, Caroll S. Increased circulating levels of lipopolysaccharide binding protein in children with *Escherichia coli* O157:H7 hemorrhagic colitis and hemolytic uremic syndrome. *Clin Diagn Lab Immunol* (1999) 6:773.
49. Koster F, Levin J, Walker L, Tung KS, Gilman RH, Rahaman MM, et al. Hemolytic-uremic syndrome after shigellosis. Relation to endotoxemia and circulating immune complexes. *N Engl J Med* (1978) 298:927–33. doi:10.1056/NEJM197804272981702
50. Stearns-Kurosawa DJ, Collins V, Freeman S, Tesh VL, Kurosawa S. Distinct physiologic and inflammatory responses elicited in baboons after challenge with Shiga toxin type 1 or 2 from enterohemorrhagic *Escherichia coli*. *Infect Immun* (2010) 78:2497–504. doi:10.1128/IAI.01435-09
51. Petruzziello-Pellegrini TN, Yuen DA, Page AV, Patel S, Soltyk AM, Matouk CC, et al. The CXCR4/CXCR7/SDF-1 pathway contributes to the pathogenesis of Shiga toxin-associated hemolytic uremic syndrome in humans and mice. *J Clin Invest* (2012) 122:759–76. doi:10.1172/JCI57313
52. Ojeda JM, Kohout I, Cuestas E. Dehydration upon admission is a risk factor for incomplete recovery of renal function in children with haemolytic uremic syndrome. *Nefrologia* (2013) 33:372–6. doi:10.3265/Nefrologia.pre2012.Nov.11648
53. Ardissino G, Dacco V, Testa S, Civitillo CF, Tel F, Possenti I, et al. Hemoconcentration: a major risk factor for neurological involvement in hemolytic uremic syndrome. *Pediatr Nephrol* (2015) 30:345–52. doi:10.1007/s00467-014-2918-0
54. Oakes RS, Siegler RL, Mcreynolds MA, Pysher T, Pavia AT. Predictors of fatality in postdiarrheal hemolytic uremic syndrome. *Pediatrics* (2006) 117:1656–62. doi:10.1542/peds.2005-0785
55. Larsen R, Gozzelino R, Jeney V, Tokaji L, Bozza FA, Japiassu AM, et al. A central role for free heme in the pathogenesis of severe sepsis. *Sci Transl Med* (2010) 2:51ra71. doi:10.1126/scitranslmed.3001118
56. Fernandez GC, Lopez MF, Gomez SA, Ramos MV, Bentancor LV, Fernandez-Brando RJ, et al. Relevance of neutrophils in the murine model of haemolytic uraemic syndrome: mechanisms involved in Shiga toxin type 2-induced neutrophilia. *Clin Exp Immunol* (2006) 146:76–84. doi:10.1111/j.1365-2249.2006.03155.x
57. McDonald B, Davis RP, Kim SJ, Tse M, Esmon CT, Kolaczkowska E, et al. Platelets and neutrophil extracellular traps collaborate to promote intravascular coagulation during sepsis in mice. *Blood* (2017) 129:1357–67. doi:10.1182/blood-2016-09-741298
58. Leffler J, Prohaszka Z, Mikes B, Sinkovits G, Ciacma K, Farkas P, et al. Decreased neutrophil extracellular trap degradation in Shiga toxin-associated haemolytic uraemic syndrome. *J Innate Immun* (2017) 9:12–21. doi:10.1159/000450609
59. Weinberg SE, Sena LA, Chandel NS. Mitochondria in the regulation of innate and adaptive immunity. *Immunity* (2015) 42:406–17. doi:10.1016/j.immuni.2015.02.002
60. Betzen C, Plotnicki K, Fathalizadeh F, Pappan K, Fleming T, Bielaszewska M, et al. Shiga toxin 2a-induced endothelial injury in hemolytic uremic syndrome: a metabolomic analysis. *J Infect Dis* (2016) 213:1031–40. doi:10.1093/infdis/jiv540
61. Lukasz A, Beneke J, Menne J, Vetter F, Schmidt BM, Schiffer M, et al. Serum neutrophil gelatinase-associated lipocalin (NGAL) in patients with Shiga toxin mediated haemolytic uraemic syndrome (STEC-HUS). *Thromb Haemost* (2014) 111:365–72. doi:10.1160/TH13-05-0387
62. Obrig TG, Louise CB, Lingwood CA, Boyd B, Barleymaloney L, Daniel TO. Endothelial heterogeneity in Shiga toxin receptors and responses. *J Biol Chem* (1993) 268:15484–8.
63. Mayer CL, Parello CS, Lee BC, Itagaki K, Kurosawa S, Stearns-Kurosawa DJ. Pro-coagulant endothelial dysfunction results from EHEC Shiga toxins and host damage-associated molecular patterns. *Front Immunol* (2015) 6:155. doi:10.3389/fimmu.2015.00155
64. Porubsky S, Federico G, Müthing J, Jennemann R, Gretz N, Büttner S, et al. Direct acute tubular damage contributes to Shigatoxin-mediated kidney failure. *J Pathol* (2014) 234:120–33. doi:10.1002/path.4388
65. Argyle JC, Hogg RJ, Pysher TJ, Silva FG, Siegler RL. A clinicopathological study of 24 children with hemolytic uremic syndrome. A report of the Southwest Pediatric Nephrology Study Group. *Pediatr Nephrol* (1990) 4:52–8. doi:10.1007/BF00858440

66. Inward CD, Howie AJ, Fitzpatrick MM, Rafaat F, Milford DV, Taylor CM. Renal histopathology in fatal cases of diarrhoea-associated haemolytic uraemic syndrome. British Association for Paediatric Nephrology. *Pediatr Nephrol* (1997) 11:556–9. doi:10.1007/s004670050337
67. Rutjes NW, Binnington BA, Smith CR, Maloney MD, Lingwood CA. Differential tissue targeting and pathogenesis of verotoxins 1 and 2 in the mouse animal model. *Kidney Int* (2002) 62:832–45. doi:10.1046/j.1523-1755.2002.00502.x
68. Rasooly R, Do PM, Griffey SM, Vilches-Moure JG, Friedman M. Ingested Shiga toxin 2 (Stx2) causes histopathological changes in kidney, spleen, and thymus tissues and mortality in mice. *J Agric Food Chem* (2010) 58:9281–6. doi:10.1021/jf101744z
69. Russo LM, Melton-Celsa AR, Smith MA, Smith MJ, O'brien AD. Oral intoxication of mice with Shiga toxin type 2a (Stx2a) and protection by anti-Stx2a monoclonal antibody 11E10. *Infect Immun* (2014) 82:1213–21. doi:10.1128/IAI.01264-13
70. Psotka MA, Obata F, Kolling GL, Gross LK, Saleem MA, Satchell SC, et al. Shiga toxin 2 targets the murine renal collecting duct epithelium. *Infect Immun* (2009) 77:959–69. doi:10.1128/IAI.00679-08
71. Thurman JM, Marians R, Emlen W, Wood S, Smith C, Akana H, et al. Alternative pathway of complement in children with diarrhea-associated hemolytic uremic syndrome. *Clin J Am Soc Nephrol* (2009) 4:1920–4. doi:10.2215/CJN.02730409
72. Morigi M, Galbusera M, Gastoldi S, Locatelli M, Buelli S, Pezzotta A, et al. Alternative pathway activation of complement by Shiga toxin promotes exuberant C3a formation that triggers microvascular thrombosis. *J Immunol* (2011) 187:172–80. doi:10.4049/jimmunol.1100491
73. Sanchez-Corral P, Perez-Caballero D, Huarte O, Simckes AM, Goicoechea E, Lopez-Trascasa M, et al. Structural and functional characterization of factor H mutations associated with atypical hemolytic uremic syndrome. *Am J Hum Genet* (2002) 71:1285–95. doi:10.1086/344515
74. Locatelli M, Buelli S, Pezzotta A, Corna D, Perico L, Tomasoni S, et al. Shiga toxin promotes podocyte injury in experimental hemolytic uremic syndrome via activation of the alternative pathway of complement. *J Am Soc Nephrol* (2014) 25:1786–98. doi:10.1681/ASN.2013050450
75. Arvidsson I, Rebetz J, Loos S, Herthelius M, Kristoffersson AC, Englund E, et al. Early terminal complement blockade and C6 deficiency are protective in enterohemorrhagic *Escherichia coli*-infected mice. *J Immunol* (2016) 197:1276–86. doi:10.4049/jimmunol.1502377

Conflict of Interest Statement: The authors declare that the research was conducted in the absence of any commercial or financial relationships that could be construed as a potential conflict of interest.

3.2 Manuscript II

Manuskript Nr. II

Titel des Manuskriptes: Targeting the innate repair receptor axis *via* erythropoietin or pyroglutamate helix B surface peptide attenuates hemolytic-uremic syndrome in mice

Autoren: S. Dennhardt, W. Pirschel, B. Wissuwa, D. Imhof, C. Daniel, J. T. Kielstein, I. Hennig-Pauka, K. Amann, F. Gunzer, S. M. Coldewey

Bibliographische Informationen: Dennhardt S, Pirschel W, Wissuwa B, Imhof D, Daniel C, Kielstein JT, Hennig-Pauka I, Amann K, Gunzer F, Coldewey SM. Targeting the innate repair receptor axis *via* erythropoietin or pyroglutamate helix B surface peptide attenuates hemolytic-uremic syndrome in mice. Front Immunol. 2022 Sep 23;13:1010882. doi: 10.3389/fimmu.2022.1010882. PMID: 36211426; PMCID: PMC9537456.

Der Kandidat / Die Kandidatin ist (bitte ankreuzen)

☒ Erstautor/-in, □ Ko-Erstautor/-in, □ Korresp. Autor/-in, □ Koautor/-in.

Status: publiziert

Anteile (in %) der Autoren / der Autorinnen an der Publikation (anzugeben ab 20%)

Autor/-in	**Konzeptionell**	**Datenanalyse**	**Experimentell**	**Verfassen des Manuskriptes**	**Bereitstellung von Material**
S. Dennhardt	30	60	60	60	
W. Pirschel		20	20		
B. Wissuwa					
D. Imhof					
C. Daniel					
J. T. Kielstein					
I. Hennig-Pauka					
K. Amann					
F. Gunzer					
S. M. Coldewey	70			30	80

frontiers | Frontiers in Immunology

TYPE Original Research
PUBLISHED 23 September 2022
DOI 10.3389/fimmu.2022.1010882

OPEN ACCESS

EDITED BY
Manuela Mengozzi,
Brighton and Sussex Medical School, United Kingdom

REVIEWED BY
Adrien Joseph,
Assistance Publique Hopitaux De Paris, France
Massimo Collino,
University of Turin, Italy

*CORRESPONDENCE
Sina M. Coldewey
sina.coldewey@med.uni-jena.de

SPECIALTY SECTION
This article was submitted to Inflammation, a section of the journal Frontiers in Immunology

RECEIVED 03 August 2022
ACCEPTED 30 August 2022
PUBLISHED 23 September 2022

CITATION
Dennhardt S, Pirschel W, Wissuwa B, Imhof D, Daniel C, Kielstein JT, Hennig-Pauka I, Amann K, Gunzer F and Coldewey SM (2022) Targeting the innate repair receptor axis *via* erythropoietin or pyroglutamate helix B surface peptide attenuates hemolytic-uremic syndrome in mice. *Front. Immunol.* 13:1010882. doi: 10.3389/fimmu.2022.1010882

Targeting the innate repair receptor axis *via* erythropoietin or pyroglutamate helix B surface peptide attenuates hemolytic-uremic syndrome in mice

Sophie Dennhardt[1,2,3], Wiebke Pirschel[1,2], Bianka Wissuwa[1,2], Diana Imhof[4], Christoph Daniel[5], Jan T. Kielstein[6], Isabel Hennig-Pauka[7], Kerstin Amann[5], Florian Gunzer[8] and Sina M. Coldewey[1,2,3]*

[1]Department of Anesthesiology and Intensive Care Medicine, Jena University Hospital, Jena, Germany, [2]Septomics Research Center, Jena University Hospital, Jena, Germany, [3]Center for Sepsis Control and Care, Jena University Hospital, Jena, Germany, [4]Pharmaceutical Biochemistry and Bioanalytics, Pharmaceutical Institute, University of Bonn, Bonn, Germany, [5]Department of Nephropathology, Friedrich-Alexander University (FAU) Erlangen-Nürnberg, Erlangen, Germany, [6]Medical Clinic V, Nephrology | Rheumatology | Blood Purification, Academic Teaching Hospital Braunschweig, Braunschweig, Germany, [7]Field Station for Epidemiology, University of Veterinary Medicine Hannover, Bakum, Germany, [8]Department of Hospital Infection Control, University Hospital Carl Gustav Carus, TU Dresden, Dresden, Germany

Hemolytic-uremic syndrome (HUS) can occur as a systemic complication of infections with Shiga toxin (Stx)-producing *Escherichia coli* and is characterized by microangiopathic hemolytic anemia and acute kidney injury. Hitherto, therapy has been limited to organ-supportive strategies. Erythropoietin (EPO) stimulates erythropoiesis and is approved for the treatment of certain forms of anemia, but not for HUS-associated hemolytic anemia. EPO and its non-hematopoietic analog pyroglutamate helix B surface peptide (pHBSP) have been shown to mediate tissue protection *via* an innate repair receptor (IRR) that is pharmacologically distinct from the erythropoiesis-mediating receptor (EPO-R). Here, we investigated the changes in endogenous EPO levels in patients with HUS and in piglets and mice subjected to preclinical HUS models. We found that endogenous EPO was elevated in plasma of humans, piglets, and mice with HUS, regardless of species and degree of anemia, suggesting that EPO signaling plays a role in HUS pathology. Therefore, we aimed to examine the therapeutic potential of EPO and pHBSP in mice with Stx-induced HUS. Administration of EPO or pHBSP improved 7-day survival and attenuated renal oxidative stress but did not significantly reduce renal dysfunction and injury in the employed model. pHBSP, but not EPO, attenuated renal nitrosative stress and reduced tubular dedifferentiation. In conclusion, targeting the EPO-R/IRR axis reduced mortality and renal oxidative stress in murine HUS without occurrence of thromboembolic complications or other adverse side effects. We therefore suggest that repurposing EPO for the

10.3389/fimmu.2022.1010882

treatment of patients with hemolytic anemia in HUS should be systematically investigated in future clinical trials.

KEYWORDS

erythropoietin, hemolytic-uremic syndrome, shiga toxin, mice, pyroglutamate helix B surface peptide, microangiopathic hemolytic anemia, thrombotic microangiopathy

Introduction

Hemolytic-uremic syndrome (HUS) belongs to the group of thrombotic microangiopathies and includes atypical and typical HUS. The latter accounts for approximately 90% of HUS cases and is a life-threatening systemic complication of infections with certain bacterial pathogens, most commonly Shiga toxin (Stx)-producing *Escherichia coli* (STEC) (1).

STEC-infections can cause diarrhea or hemorrhagic colitis with bloody diarrhea. STEC-HUS typically presents with microangiopathic hemolytic anemia, thrombocytopenia, acute kidney injury (AKI) and other organ dysfunctions (1). One-third of patients with STEC-HUS also develop long-term renal and up to 4%, long-term neurological sequelae (2). Renal oxidative stress was shown to be an important factor in HUS pathogenesis in pediatric HUS (3, 4). Its pathophysiological relevance was also demonstrated in a murine model of Stx2-induced HUS (5).

To date, organ supportive therapy in the intensive care unit (ICU), including hemodialysis, fluid resuscitation as well erythrocyte transfusion if indicated, has been the standard of care in patients with STEC-HUS (6). In the absence of targeted therapeutic options, there is a medical need to further investigate molecular therapeutic approaches for the treatment of this life-threatening systemic syndrome.

Due to the low incidence – of e. g. 0.07 per 100,000 persons/year for Germany (7) up to 0.67 per 100,000 persons/year for Argentina (8) – conducting prospective randomized clinical trials has proven difficult. To provide tools for preclinical studies, we have recently introduced and characterized several animal models for STEC-HUS, including an infection model employing the Northern German outbreak strain O104:H4 of 2011 and the well-characterized outbreak strain O157:H7 86-24 in gnotobiotic piglets (9), as well as a clinically relevant mouse model (10–12) reflecting most aspects of human pathology by repeatedly exposing animals to low doses of Stx isolated from an EHEC O157:H7 86-24. All previously described small animal models of STEC-HUS mimic well the critical illness, renal failure and microangiopathy seen in humans, while being limited in their modeling of hemolytic anemia, which is oftentimes masked by hemoconcentration secondary to fluid deficiency (10, 13, 14).

Erythropoietin (EPO), a pleiotropic hormone that has been shown to exert tissue-protective effects *via* the innate repair receptor (IRR) independent of its hematopoietic properties *via* the EPO receptor (EPO-R) homodimer (15, 16), appears to be a promising candidate to be further evaluated in HUS. Preclinical trials usually use one magnitude higher doses of EPO compared with clinical trials (1000-5000 IU/kg versus 300 IU/kg) (17). This could explain why preclinical tissue protection following EPO administration could often not be translated into the clinical setting. Furthermore, beside its potential beneficial effects, the thrombogenic effect of this erythropoiesis-stimulating hormone was critically discussed in the context of clinical studies (18, 19), as tissue-protective effects require high levels of EPO and administration of high EPO doses can increase the risk of thrombosis (16) and hypertension (17). For this reason, EPO-derived non-hematopoietic small peptide activators of the IRR, such as the pyroglutamate helix B surface peptide (pHBSP), have been developed (15). Preclinically, pHBSP has been shown to convey tissue protection in numerous disease models (20), such as nephroprotection in ischemia-reperfusion models of AKI (21, 22). Furthermore, pHBSP has been successfully employed in phase II studies in patients with diabetes or sarcoidosis and neuropathic pain (23, 24).

HUS can be considered as a specific phenotype of sepsis, as it represents a combination of infection and organ dysfunction. We previously reported that EPO attenuated AKI (25) and cardiac dysfunction (26) in mouse models of endotoxemia and cecal ligation and puncture-induced sepsis. There is no clinical evidence on the beneficial or harmful effects of EPO in patients with sepsis and there is only little evidence regarding the beneficial or harmful effects of EPO in ICU patients in general (27, 28). To our knowledge, the tissue-protective effects of EPO or pHBSP in HUS have not been investigated, yet. One trial that aimed to investigate the effects of EPO on the microcirculation of patients with severe sepsis was discontinued due to lack of recruitment (NCT01087450). We did not find the results of a study that examined the immunomodulatory effects of activated protein C and/or EPO in sepsis (NCT00229034). A third study

examining the effects of EPO on renal function in critically ill patients with and without multiorgan failure appears to be not completed (EudraCT number: 2008-003733-24). Altogether, there is no evidence from randomized controlled trials regarding the effects of EPO administration in sepsis and HUS. Despite this lack of evidence, it is however conceivable, that in the presence of severe hemolytic anemia in patients with HUS, the stimulation of hematopoiesis by EPO could be beneficial by reducing the need for allogenic erythrocyte transfusion, which carry non-negligible risks (29, 30).

Anemia is usually accompanied by a regulatory increase in endogenous EPO production due to hypoxia-mediated feedback mechanisms. In patients with iron deficiency or hemolytic anemia, serum EPO levels exceeding 2000 mU/ml (two orders of magnitude above normal range) have been reported (31). In contrast, renal anemia is often accompanied by insufficient EPO production due to direct damage to EPO-producing cells in the kidney (32) or inhibition of EPO production by various cytokines (33). Already in the early 1990's, it was hypothesized that anemias associated with low serum EPO levels might respond to treatment with recombinant EPO (34).

Currently, EPO can be considered in the treatment of anemia associated with chemotherapy (35) and chronic kidney disease (36). The current national guideline for the treatment of HUS in pediatric patients states that EPO can be considered in the treatment of HUS-associated hemolytic anemia as expert consensus without citing evidence (37). So far, no adverse effects have been observed in children receiving EPO for the treatment of hemolytic anemias (38–41). However, a reduction of red blood cell transfusion could not be shown in two small studies (38, 39). Hitherto, there are no sufficiently powered clinical studies in this context. Even a neutral effect of EPO in terms of nephroprotection in the absence of side effects might positively impact the therapy of HUS-associated hemolytic anemia and save the need for red blood cell transfusions.

In view of the above, we consider it necessary and promising to assess the role of EPO in this orphan disease which comprises a specific form of septic organ failure. The first objective of this study is to further elucidate the role of endogenous EPO and its potential clinical relevance in HUS by measuring endogenous EPO levels in different species: human patients (infection with EHEC O104:H4, 2011 German outbreak), gnotobiotic piglets (subjected to EHEC O104:H4 or EHEC O157:H7 86-24) and mice (subjected to Stx2 derived from EHEC O157:H7 86-24). The second objective of this study is to examine the effect of EPO and the non-hematopoietic peptide pHBSP in a murine model of HUS by measuring surrogate parameters of kidney injury and dysfunction, intrarenal barrier integrity, microangiopathy, oxidative and nitrosative stress and metabolome. Hereby, we aim to provide preclinical evidence to assess whether treatment of HUS with EPO or pHBSP should be considered and further investigated, particularly for HUS-associated hemolytic anemia.

Material and methods

Study design

Plasma samples of patients with STEC-HUS (n = 27, median age 47, 24 female) were provided by the German STEC-HUS Registry (42). These samples were taken within 10 d after admission to the hospital (HUS acute stage) and at the day of the last plasmapheresis (HUS pre-discharge). We analyzed the subcohort of 7 patients of which samples were available from day 1 to day 3 after hospital admission and within 3 d before hospital discharge. Age- and sex-matched samples of healthy controls (n = 21, median age 63.5, 15 female) were provided by Jena University Hospital [ICROS study (43)]. Ethic approval was obtained by the primary investigators from the Ethics Committee of Hannover Medical School (1123-2011) and of the Friedrich Schiller University Jena (5276-09/17). Participants provided written informed consent prior to inclusion in the respective studies.

Samples from gnotobiotic piglets (9) were collected 4 to 6 days after STEC-infection or mock infection (sham). Experimental procedures in gnotobiotic piglets were approved by the local permitting authorities in the Lower Saxony State Office for Consumer Protection and Food Safety and in accordance with the requirements of the national animal welfare law (Approval Number: 33.9-42502-04-13/1149) in accordance with the German legislation following the guidelines of FELASA and ARRIVE (9).

All procedures performed in mice were approved by the regional animal welfare committee and the Thuringian State Office for Consumer Protection (registration number 02-058/14) and performed in accordance with the German legislation. HUS-like disease in mice was induced by repetitive doses of Stx2 as described previously (10). Briefly, wild-type C57BL/6J mice aged 10-16 weeks weighing 20-30 g were randomly assigned to one of four groups (sham n = 16, Stx+vehicle n = 26, Stx+EPO n = 22, or Stx+pHBSP n = 21) and received 3x25 ng/kg body weight (BW) Stx or 0.9% NaCl i.v. on days 0, 3, and 6. EPO (1000 IU/kg BW) was applied s.c. 1 h after initial Stx injection. Due to its short plasma half-life, pHBSP (30 µg/kg BW) was applied s.c. every 24 h starting 1 h after initial Stx injection. Vehicle (Ringer's solution) was applied s.c. starting 1 h after initial Stx injection. Mice received 3x800 µl Ringer's solution each day for volume replacement. In compliance with ethical regulations, survival was monitored for 7 days using humane endpoints (mice were euthanized when reaching a high-grade disease state, Figure 3). Disease progression was monitored by weight loss and activity-based HUS score (ranging from 1-normally active, 2-active with slight restrictions, 3-active with clear intermissions, 4-slowed, 5-lethargic, 6-moribund, to 7-dead) as described previously (10). Animals were exsanguinated in deep ketamine/xylazine anesthesia (10). Renal tissue, blood and plasma samples were collected on day 7. An additional experiment with a

comparable survival rate including sham and Stx+vehicle mice was performed to compensate for the lower survival rate in the Stx+vehicle group and to increase the statistical power in the analysis of day-7-samples for plasma urea and creatinine and all histological [Schiff's periodic acid (PAS), acid fuchsin orange G (SFOG)] and immunohistochemistry (IHC) stainings (kidney-injury molecule 1 (KIM-1), cluster of differentiation 31 (CD31), E-cadherin, glycoprotein 1b (GP1b), nitrotyrosine and NADPH oxygenase 1 (NOX-1), Figures 4–7). Plasma EPO levels (Figure 2B) and plasma metabolome (Figure 8) were measured in an independent experimental setup with comparable survival rates since availability of plasma per animal was limited.

Compounds

Stx purification was performed as described previously (10). Human recombinant EPO (Epoeitin beta, Hoffmann-La Roche) was diluted to 1000 U/kg BW in Ringer's solution (vehicle). A standard N-(9-fluorenyl)methoxycarbonyl protocol for automated solid-phase peptide synthesis was implemented for pHBSP synthesis (Supplementary Methods). pHBSP was diluted to 30 µg/kg BW in Ringer's solution (vehicle).

Blood and plasma sample analysis

Human (42), piglet (9) and murine (10) blood samples were taken as described elsewhere. Hematology and analysis of laboratory chemistry parameters in murine samples were performed as recently described (10). Briefly, blood counts were analyzed using impedance technology implemented in the pocH100iv system (Sysmex, Kobe, Japan). Laboratory parameters were analyzed by an Architect™ c16200/ci8200 automated clinical chemistry system (Abbott Diagnostics, Abbott. Park, USA). This system uses the Jaffè method for plasma creatinine measurements and the urease/nicotinamide adenine dinucleotide hydrogen method for plasma urea measurements. The following parameters were measured using commercially available ELISA kits: serum or plasma EPO and murine plasma neutrophil-gelatinase-associated lipocalin (NGAL, Supplementary Table S1).

Tissue preparation, histopathology and IHC staining

Processing of kidney samples, histopathological analysis and IHC stainings were performed as described previously (10). SFOG and thrombocyte (GP1b) staining was performed as described recently (11). Until antigen demasking, sections for E-cadherin, NOX-1 and nitrotyrosine staining were treated similarly. The Vector M.O.M. Immunodetection kit (Vector Laboratories) was used for E-cadherin staining. Blocking of nitrotyrosine staining was performed in normal goat serum. IHC sections were washed with Tris(hydroxymethyl) aminomethan (TRIS) buffer during staining [50 mM TRIS, 300 mM NaCl, pH was adjusted to 7.6 with HCl (all Carl Roth); 0.04% Tween®20 (Sigma Aldrich)], incubated with primary antibodies overnight at 4°C in appropriate dilutions (Supplementary Table S2) and subsequently incubated for 30 min with secondary antibodies (Supplementary Table S3). NOX-1 sections were incubated in primary antibody directly after antigen retrieval. Nitrotyrosine sections were stained using the CSA kit and rabbit Link (Dako).

Histology and IHC quantification

Quantification and scoring of histopathological and IHC stainings were performed as described previously (10). For quantification of renal E-cadherin expression, all cut and completely positively stained tubules (with entirely visible lumen, excluding those with spotty staining) were counted in 12 adjacent cortical fields [one cortical field = region of interest (ROI)] per section in 400x magnification. Nitrotyrosine staining was quantified by superimposing a 10x10 grid (area of 0.0977 mm^2) over each field and counting positively stained fields in 20 adjacent cortical fields per section in 400x magnification (blinded). NOX-1 staining was analyzed using a scoring system (0 to 3; 0: < 25%, 1: 25-50%, 2: 50-75%, 3: > 75% positive staining per field, 12 fields/section, magnification 200x, blinded). Quantification of SFOG and thrombocyte staining was performed as described recently (11).

Targeted metabolomics and statistical analysis

Targeted metabolomics from heparinized plasma was performed at Biocrates Life Sciences by mass spectrometry using an MxP® Quant 500 kit. Data analysis was performed using R version 3.4.4 (R Core Team) as follows: Readings below detection level were set to half of detection level for each analyte separately. Metabolome data was then log 2 transformed without any further normalization. Z scores were calculated using mean and standard deviation of all samples. Trends along the four sample groups were tested using linear regression models where sample group assignment was used as the independent variable and each analyte as the dependent variable in a separate model. Prior to linear regression, the independent variable sample group assignment was transformed to a pseudo-continuous variable where all samples of group "sham" were set to 0, samples of group "Stx+pHBSP" were set to 1/3, samples of group "Stx+EPO" were set to 2/3 and samples of group "Stx+vehicle" were set to 1. Applying this transformation, the linear regression models test

whether there is an increasing or decreasing trend along the four groups in the assigned order. P-values for all models were Benjamini-Hochberg adjusted (44). Analytes with adjusted P-values below 0.05 and an absolute effect of one or bigger were considered significantly changing along the four sample groups.

Statistics

Data are depicted as mean ± SD for n observations. GraphPad Prism 7.05 (GraphPad Software) was used for data analysis applying Student's t-test and Wilcoxon signed rank test for comparisons between 2 groups. One-way ANOVA with Holm-Sidak *post hoc* test (parametric data) or Kruskal-Wallis test with Dunn's *post hoc* test (nonparametric data) were used for comparisons between more than 2 groups. Survival was depicted as Kaplan-Meier curve and analyzed by Mantel-Cox test. Association between EPO levels in patients with STEC-HUS and hematological and laboratory parameters and piglet samples was performed with GraphPad Prism 7.05 implementing non-parametric Spearman's rank correlation coefficients. A P-value < 0.05 was considered significant. Mean ± SD and P-values for all analyses are given in Supplementary Table S4.

Results

Elevated EPO levels in humans suffering from HUS

In patients with STEC-HUS, EPO serum levels were elevated in the acute stage of disease compared with healthy controls (Figure 1A, upper panel, Supplementary Tables S5, S6 for individual values). Pre-discharge, EPO levels decreased compared to the acute phase, yet continued to be higher than in healthy controls. In a subgroup, in which blood samples were consequently taken within 3 days after admission and 3 days before discharge from the hospital, a reduction of serum EPO levels was observed in 6 out of 7 HUS patients (Figure 1A, lower panel). Several hematological, laboratory and clinical parameters at hospital admission are listed in Table 1 and EPO values were correlated with these parameters. Anemia was present in 6 out of 7 patients (Figures 1B, C) and there was a trend towards a negative correlation between endogenous EPO levels and hemoglobin (Hb; r = -0.5357, P = 0.2357) or hematocrit (r = -0.6071, P = 0.1667) at hospital admission. No correlation was observed between endogenous EPO levels and lactate dehydrogenase (LDH) or creatinine at hospital admission (Figures 1D, E), although intriguingly, the lowest endogenous EPO levels were observed in patients with pronounced kidney dysfunction (Figure 1E).

While anemia appears to be a major driver of increased EPO secretion in patients with STEC-HUS, we wondered whether other mechanisms might also play a role. Considering that – at least in our limited subcohort-endogenous EPO was lowest in those patients with pronounced kidney dysfunction and injury, we hypothesize that these patients might profit from therapeutic EPO administration.

Elevated EPO levels in animal models of HUS

To further assess the role of EPO in HUS, we measured endogenous EPO levels in two well-characterized animal models of this condition. In gnotobiotic piglets with STEC-HUS, EPO levels were elevated in EHEC O104:H4- and EHEC O157:H7-infected piglets compared with sham piglets (Figure 2A). STEC-infected gnotobiotic piglets did not display clear signs of anemia or kidney injury compared with mock-infected sham animals (Table 2). No correlations were observed between EPO-levels and hematological parameters (Supplementary Table S7). In O157:H7-infected piglets, although LDH was comparably low, there was a trend towards negative correlation with EPO levels (Supplementary Table S7). In C57BL/6 mice subjected to Stx, slight hemoconcentration was observed (Supplementary Table 3, significant increase in Hb in Stx+vehicle compared with sham mice). Despite the absence of anemia in Stx+vehicle mice, EPO plasma levels were elevated compared with sham mice (Figure 2B). There was no correlation between plasma EPO levels and plasma NGAL as surrogate parameter for kidney damage in mice (Supplementary Figure S1).

As anemia appears not to be the sole driver of increased EPO levels during HUS and patients with pronounced kidney damage showed the lowest EPO levels, we next wanted to analyze the therapeutic potential of EPO and the non-hematopoietic EPO derivative pHBSP in a murine model of HUS.

Effect of EPO and pHBSP treatment on survival and clinical presentation of mice with HUS

7-day survival was significantly increased in Stx+EPO (68.2%) and Stx+pHBSP mice (76.2%) compared with Stx+vehicle mice (42.3%; Figure 3A). Consistently, disease progression was reduced on days 6 and 7 in these treatment groups (Figure 3B). All surviving Stx-challenged animals lost up to 20% weight until the end of the experiment. Statistical comparison of weight loss was performed until the first animals had to be euthanized at day 5 (Figure 3C). Weight loss in Stx+EPO mice was less pronounced compared with Stx+vehicle mice on days 4 and 5 (Figure 3C). While neurological involvement assessed by hind limb clasping reflex frequently occurred in Stx+vehicle mice (approx. 39%, P = 0.0067 vs. sham, Table 3), it was less common in Stx+EPO (approx. 27%; Table 3) and Stx+pHBSP mice (approx. 24%; Table 3). No differences were observed in plasma alanine aminotransferase (ALAT) and aspartate aminotransferase (ASAT), while Hb and/or hematocrit as

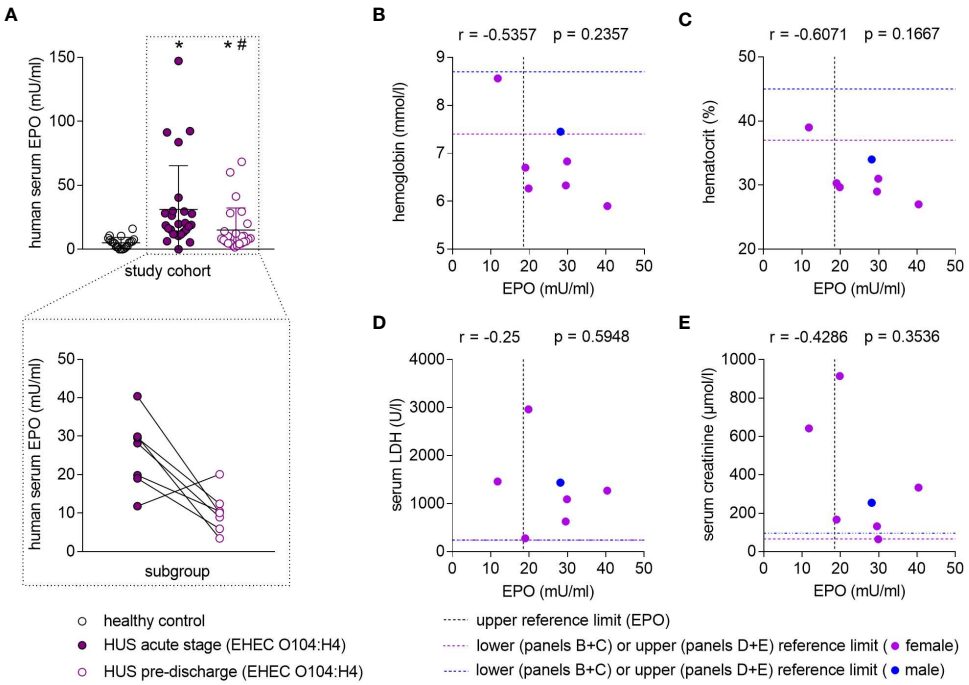

FIGURE 1
Endogenous EPO levels in patients with STEC-HUS and their correlation with anemia and kidney damage. **(A)** Upper panel: EPO serum levels in healthy controls (n = 20) and HUS patients (n = 26) within 10 d after admission to the hospital (HUS acute stage) and the last plasmapheresis (HUS pre-discharge) determined by ELISA. Data are expressed as scatter dot plot with mean ± SD. *P < 0.05 vs. healthy control (Mann-Whitney U-test), #P < 0.05 vs. HUS acute stage (Wilcoxon signed-rank test). Lower panel: Pairwise comparison of EPO serum levels of a subcohort of patients (n = 7) in which blood samples were available from day 1 to 3 after hospital admission and within 3 days before hospital discharge. Data are expressed as scatter dot plot with connecting line between respective measurements. **(B-E)** Correlation analysis implementing Spearman's correlation coefficient (r) for correlations of endogenous EPO levels with **(B)** hemoglobin (n = 7), **(C)** hematocrit (n = 7), **(D)** lactate dehydrogenase (LDH, n = 7) and **(E)** creatinine (n = 7) in the subcohort. The upper reference limit for EPO in health are indicated by dashed vertical lines. Gender-specific lower or upper reference limits for the respective parameters of anemia and kidney damage are indicated by dashed horizontal lines.

indicators of hemoconcentration were increased in all Stx-challenged mice (Table 3). Compared with sham mice, Hb was elevated in Stx+EPO mice, while it was not in Stx+pHBSP mice. However, there was no significant difference between Stx+EPO mice and Stx-vehicle mice. The effects of EPO-treatment on Hb might be masked by the slight hemoconcentration observed in all Stx-challenged groups.

Effect of EPO and pHBSP treatment on kidney injury and dysfunction in mice with HUS

After observing significantly increased survival rates in EPO- and pHBSP-treated animals, we analyzed the impact of both treatments on kidney injury and dysfunction. Stx+vehicle,

TABLE 1 Hematological, laboratory and renal function parameters in the subgroup of patients with STEC-HUS assessed at hospital admission.

Patient no.	Sex	Age	EPO (T1, mU/ml)	Hb (g/dl)	Hct (%)	LDH (U/l)	Crea (mg/dl)	Dialysis	Plasmapheresis (number)	RBC
5	m	26	28.194	12.0	34.0	1437	2.88	no	yes (6)	no
9	f	74	19.856	10.1	29.7	2966	10.35	yes	yes (4)	n/a
11	f	29	40.382	9.5	27.0	1273	3.78	yes	yes (6)	yes
12	f	39	29.546	10.2	29.0	627	1.49	no	no	no
13	f	44	19.034	10.8	30.3	279	1.89	no	yes (4)	yes
15	f	50	29.914	11.0	31.0	1091	0.73	yes	yes (7)	yes
25	f	73	11.820	13.8	39.0	1460	7.26	yes	yes (5)	yes

Hb, hemoglobin; Hct, hematocrit; LDH, lactate dehydrogenase; Crea, creatinine; RBC, red blood cell transfusion.

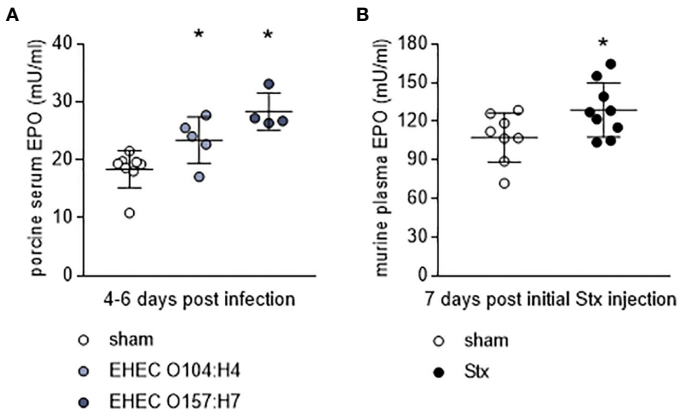

FIGURE 2
Endogenous EPO levels in animal models of HUS. **(A)** EPO serum levels in gnotobiotic piglets that were either mock-infected (sham) or infected with EHEC O157:H7 or EHEC O104:H4 determined by ELISA. Samples were taken 4-6 d after infection (sham n = 8, EHEC O104:H4 n = 5, EHEC O157:H7 n = 4). Data are expressed as scatter dot plot with mean ± SD. *P < 0.05 vs. sham (one-way ANOVA, Holm-Sidak's multiple comparison test). **(B)** EPO plasma levels in mice with HUS on day 7 of experiment (sham n = 8, Stx n = 10) determined by ELISA. Data are expressed as scatter dot plot with mean ± SD, *P < 0.05 vs. sham (unpaired t-test).

Stx+EPO and Stx+pHBSP mice presented with increased plasma urea, creatinine and NGAL compared with sham mice (Figures 4A–C). PAS staining revealed renal tissue damage in all Stx-challenged groups irrespective of treatment (Figure 4D). KIM-1 expression was elevated in Stx+vehicle, Stx+EPO and Stx+pHBSP mice compared with sham mice (Figure 4E). In Stx+pHBSP compared with Stx+vehicle mice, KIM-1 expression was reduced (Figure 4E).

Effects of EPO and pHBSP treatment on intrarenal barriers in mice with HUS

The integrity of endothelial and epithelial barriers in the kidney is crucial for its function. It was demonstrated before that Stx can damage both endothelial as well as epithelial cells in the kidney and thereby influence the integrity of these barriers (1). We stained kidney sections for endothelial and epithelial cell

TABLE 2 Hematological, laboratory and renal function parameters in STEC-infected piglets and mock-infected controls (sham) assessed 4-6 days after infection.

-	ID	EPO (U/l)	Hb (g/l)	Hct (L/l)	LDH (U/l)	Crea (µmol/l)
sham	16	17.983	94.9	0.25	702	59
	32	19.211	95.86	0.27	1105	63
	33	10.827	79.3	0.24	901	57
	44	19.726	124.02	0.19	1445	67
	46	19.331	60.35	0.19	884	74
	47	21.491	69.92	0.21	924	73
	48	18.587	54.46	0.17	1145	60
	49	19.578	60.72	0.18	808	70
O104: H4	18	17.048	69.6	0.21	909	54
	19	25.473	97.5	0.27	997	59
	36	27.684	78.2	0.22	1767	73
	42	24.029	116.66	0.24	977	53
	43	22.659	96.42	0.29	1761	63
O157: H7	20	33.098	78.8	0.23	538	61
	21	26.325	97.9	0.26	804	52
	34	26.667	65.14	0.33	740	65
	35	27.173	*n.d.*	*n.d.*	680	72

Hb and Hct could not be assessed in one piglet of the O157:H7 group (n.d.). Hb, hemoglobin; Hct, hematocrit; LDH, lactate dehydrogenase; Crea, creatinine.

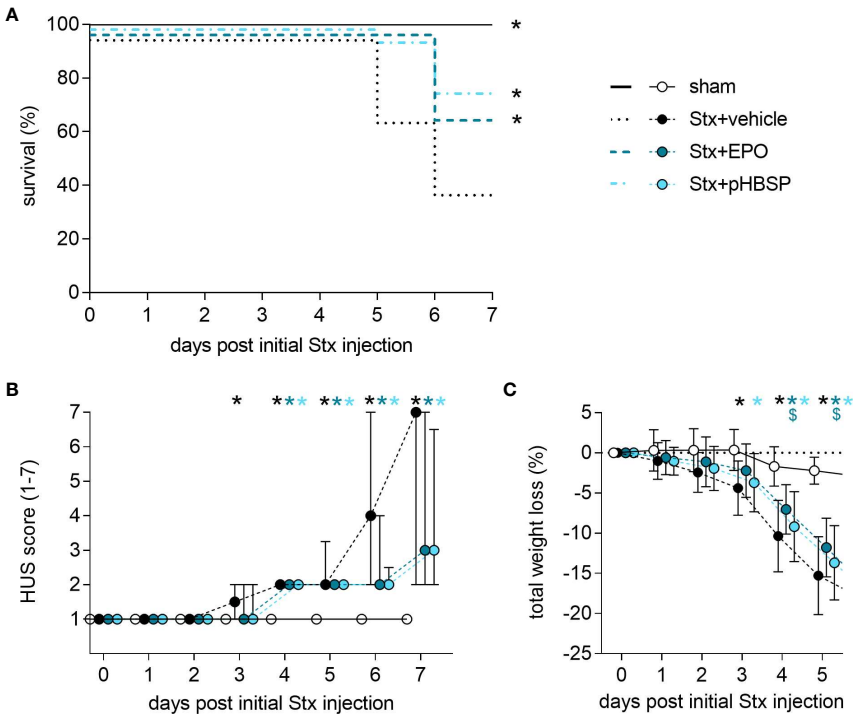

FIGURE 3
Effect of EPO and pHBSP treatment on survival and clinical presentation of mice with HUS. **(A-C)** Mice received either Stx or vehicle intravenously to induce experimental HUS. Mice with HUS were treated with vehicle (Ringer's solution 1 h post HUS induction s.c.), EPO (1 h post HUS induction s.c., 1000 IU/kg BW once) or pHBSP (1 h post HUS induction s.c., 30 µg/kg BW every 24 h; sham n = 15, Stx+vehicle n = 26, Stx+EPO n = 22, Stx+pHBSP n = 21). **(A)** Kaplan-Meier 7-day survival curves of sham mice, Stx-challenged mice treated with vehicle, Stx-challenged mice treated with EPO and Stx-challenged mice treated with pHBSP with humane endpoints. *P < 0.05 vs. Stx+vehicle (log-rank Mantel-Cox test). **(B)** Activity-based HUS score (ranging from 1-normally active, 2-active with slight restrictions, 3-active with clear intermissions, 4-slowed, 5-lethargic, 6-moribund, to 7-dead) was assessed three times daily and is depicted every 24 h until day 7 starting with first Stx injection. Data are expressed as median ± interquartile range. *P < 0.05 vs. sham (Kruskal-Wallis test, Dunn's multiple comparison test at every single time point). **(C)** Total weight loss referred to day 0 was assessed every 24 h and is depicted until day 5. Data are expressed as mean ± SD. *P < 0.05 sham vs. the respective color-coded group, $^{\$}$P < 0.05 vs. Stx+vehicle (two-way ANOVA, Holm-Sidak's multiple comparison test).

markers to assess the influence of EPO and pHBSP treatment on intrarenal barriers. Loss of renal CD31-positive endothelial cells (Figure 5A) and reduced E-cadherin expression was detected in kidneys of all Stx-challenged groups compared with sham mice (Figure 5B). However, E-cadherin expression was less decreased in Stx+pHBSP compared with Stx+vehicle and Stx+EPO mice (Figure 5B).

Effect of EPO and pHBSP treatment on microangiopathy in mice with HUS

GP1b was stained to highlight thrombocytes in the kidneys as indicators of microangiopathy (Figure 6A). An insignificant elevation of thrombocytes was observed in all Stx-challenged animals regardless of treatment, although it was weakest in the Stx+pHBSP group (Figure 6A). SFOG staining was performed to visualize fibrin deposits as indicators of microthrombi in renal sections (Figure 6B). Fibrin deposits were observed in all Stx-challenged groups compared with sham animals. There was an insignificant trend towards lower mean values of fibrin deposition in Stx+EPO and Stx+pHBSP mice compared with Stx+vehicle mice (Figure 6B).

Effects of EPO and pHBSP treatment on nitrosative and oxidative stress in mice with HUS

To further characterize the potential protective mechanism of EPO and pHBSP in HUS, surrogate parameters of nitrosative (nitrotyrosin formation) and oxidative (NOX-1 expression) stress were analyzed. Renal nitrotyrosine formation was elevated in all Stx-challenged groups compared with sham mice (Figure 7A). Compared with Stx+vehicle mice, formation of nitrotyrosine was decreased in the kidneys of Stx+EPO and Stx+pHBSP mice (Figure 7A). Compared with Stx+EPO mice, nitrotyrosine staining was even further decreased in Stx+pHBSP

10.3389/fimmu.2022.1010882

TABLE 3 Hematological and laboratory parameters of mice with HUS and effects of EPO and pHBSP treatment.

		sham	Stx+vehicle	Stx+EPO	Stx+pHBSP	P-values
clinical appearance	neurological symptoms	0/15 (0%)	10/26 (39%)	6/22 (27%)	5/21 (24%)	sham vs. Stx+vehicle: P = 0.0067
hematology	Hct (%)	34.8 ± 1.6	38.7 ± 2.5	39.1 ± 3.3	37.8 ± 2.3	sham vs. Stx+EPO: P = 0.005
	erythrocytes (cells/µl)	8162000 ± 337817	9196667 ± 477521	9200000 ± 811640	8926000 ± 546150	sham vs. Stx+vehicle: P = 0.0261
	Hb (g/dl)	11.3 ± 0.4	12.5 ± 0.6	12.6 ± 1	12.1 ± 0.8	sham vs. Stx+vehicle: P = 0.0374 sham vs. Stx+EPO: P = 0.0374
	thrombocytes (cells/µl)	890600 ± 71853	1078833 ± 123106	858167 ± 144950	1026400 ± 113372	Stx+vehicle vs. Stx+EPO: P = 0.0279
	leukocytes (cells/µl)	2500 ± 686	833.3 ± 151	1617 ± 799	1700 ± 957	sham vs. Stx+vehicle: P = 0.0059
	hemolysis score	0 ± 0	1.6 ± 1.4	1.3 ± 1.3	0.8 ± 1.1	sham vs. Stx+vehicle: P = 0.0023 sham vs. Stx+EPO: P = 0.013
laboratory markers	plasma ALAT (µmol/l*s)	0.6 ± 0.1	0.7 ± 0.2	0.6 ± 0.2	0.6 ± 0.2	ns
	plasma ASAT (µmol/l*s)	1.8 ± 1.1	2.6 ± 1.6	1.9 ± 1.1	1.3 ± 0.3	ns
	plasma LDH (µmol/l*s)	7.4 ± 2.9	16.4 ± 8.3	10.4 ± 4.6	8.1 ± 2.5	sham vs. Stx+vehicle: P = 0.0412
	plasma bilirubin (µmol/l)	2.0 ± 1.1	4.5 ± 1.5	5.0 ± 0.0	4.2 ± 1.1	sham vs. Stx+vehicle: P = 0.0153 sham vs. Stx+EPO: P = 0.0222
	plasma albumin (mg/dl)	13.5 ± 0.6	14.4 ± 1.0	15.0 ± 1.2	15.0 ± 0.7	sham vs. Stx+pHBSP: P = 0.0386

Hct, hematocrit; Hb, hemoglobin; ALAT, alanine aminotransferase; ASAT, aspartate aminotransferase; LDH, lactate dehydrogenase.

mice (Figure 7A). Of note, the predominantly glomerular staining of nitrotyrosine in Stx+vehicle mice was mitigated in Stx+EPO mice and attenuated in Stx+pHBSP mice (Figure 7A, arrowheads). NOX-1 expression was increased only in Stx+vehicle compared with sham mice, whereas Stx+pHBSP mice displayed lower NOX-1 expression compared with Stx +vehicle and Stx+EPO mice (Figure 7B).

Effect of EPO and pHBSP treatment on metabolome in mice with HUS

Oxidative stress and metabolism are closely interrelated and studies on the metabolome have not yet been reported in animal models of HUS. Therefore, we performed targeted metabolomics in the plasma of all four groups. Of the 630 metabolites analyzed in plasma, 426 were within the limit of detection. These 426 metabolites were analyzed using a linear regression model to test whether their abundance increases or decreases in the assigned order: sham–Stx+pHBSP–Stx+EPO–Stx+vehicle. 32 metabolites fitted this hypothesis, they are highlighted in heatmaps (Figures 8A, B) and assigned to the following substance classes: amino acids and derivatives (7/32), alkaloids (1/32), aminoxides (1/32, heatmap A) and lipids (23/32, triacylglycerides in heatmap B).

Discussion

To date, the role of EPO in HUS, a systemic orphan disease with occurrence of microangiopathic hemolytic anemia and AKI, has not been systematically investigated. We hypothesized that EPO treatment may be beneficial in patients with HUS-mediated hemolytic anemia and, targeting the IRR axis with EPO or non-hematopoietic EPO analogs, such as pHBSP, may convey nephroprotection in HUS.

The role of endogenous EPO levels in patients, piglets and mice with STEC-HUS

In response to cellular hypoxia (46), a regulatory increase in renal EPO secretion in patients with anemia would be expected. To our knowledge, there are no systematic studies on changes in endogenous EPO levels in adult patients with STEC-HUS and

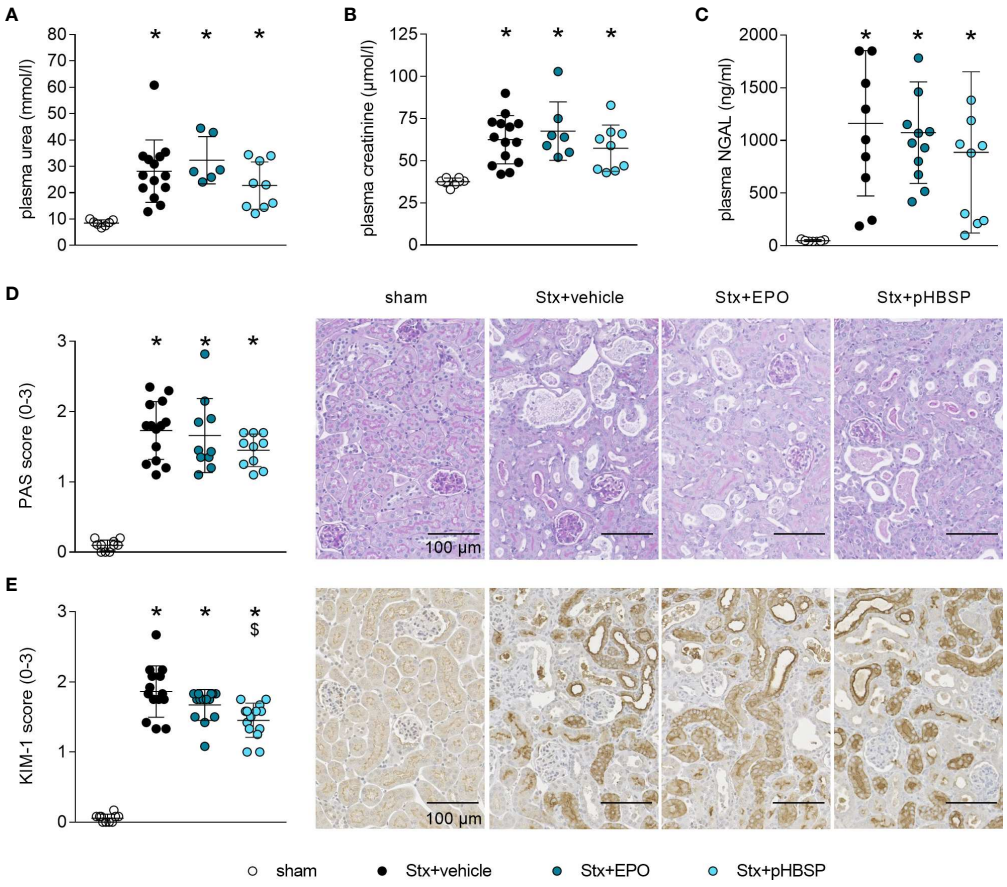

FIGURE 4
Effect of EPO and pHBSP treatment on kidney dysfunction and tubular injury in mice with HUS. Kidney injury and dysfunction was assessed on day 7 of HUS experiment. Plasma samples of mice with HUS and sham mice were analyzed for the kidney dysfunction parameters **(A)** urea and **(B)** creatinine (sham n = 7, Stx+vehicle n = 14, Stx+EPO n = 6, Stx+pHBSP n = 9) by an Architect^{TM} ci16200 System (Abbott), as well as the kidney injury marker **(C)** NGAL (sham n = 7, Stx+vehicle n = 10, Stx+EPO n = 12, Stx+pHBSP n = 10) by ELISA. **(A–C)** Data are expressed as scatter dot plot with mean ± SD. *P < 0.05 vs. sham (one-way ANOVA, Holm-Sidak's multiple comparison test). Quantification data as well as representative images (scale bar 100 µm) of **(D)** PAS staining (sham n = 10, Stx+vehicle n = 14, Stx+EPO n = 10, Stx+pHBSP n = 10, 10 fields per slide, score 0: no damage, 1: < 25% damaged, 2: 25–50% damaged, 3: > 50% damaged) and **(E)** immunohistochemical KIM-1 staining (score 0: < 25%, 1: 25–50%, 2: 50–75%, 3: > 75% strong positive staining per visual field, sham n = 10, Stx+vehicle n = 14, Stx+EPO n = 14, Stx+pHBSP n = 14, 12 fields per slide) in renal sections of sham and Stx-challenged mice. **(D, E)** Data are expressed as scatter dot plot with mean ± SD. *P < 0.05 vs. sham, $^{\$}$P < 0.05 vs. Stx+vehicle, (Kruskal-Wallis test, Dunn's multiple comparison test).

only one brief report in pediatric patients (32). We observed increased EPO serum levels in a small cohort of adult patients with STEC-HUS compared to healthy controls already at a reduced Hb level of about 11 g/dl. Our data showed no correlation between the degree of anemia and EPO levels. This observation is consistent with the above-mentioned report in children with STEC-HUS (32) and in critically ill patients with AKI of other origins (47–50). However, we cannot exclude a gender bias, as our patient cohort was mainly female as women were more frequently affected in the 2011 EHEC outbreak (51). Therefore, our observations should be validated in a larger, gender balanced cohort.

In the kidneys, EPO is produced by fibroblast-like type I interstitial cells located between peritubular capillaries and the proximal convoluted tubule (52). Thus, EPO expression is likely to be impaired when EPO-producing cells are damaged. Consistent with these considerations, patients with very high LDH or creatinine levels as surrogate parameters for tissue damage and renal dysfunction had the lowest EPO levels in our study. However, we found no correlation between LDH or creatinine levels and EPO levels in patients with HUS. We attribute this to the small number of patients studied. Nevertheless, clinical data suggests that EPO response appears to be impaired in STEC-HUS and EPO regulation may play an important role in the pathogenesis and disease resolution. Analyzing serum EPO levels in a larger cohort of patients with HUS and acute kidney injury of other origins may help to further elucidate whether the degree of renal dysfunction and/or injury

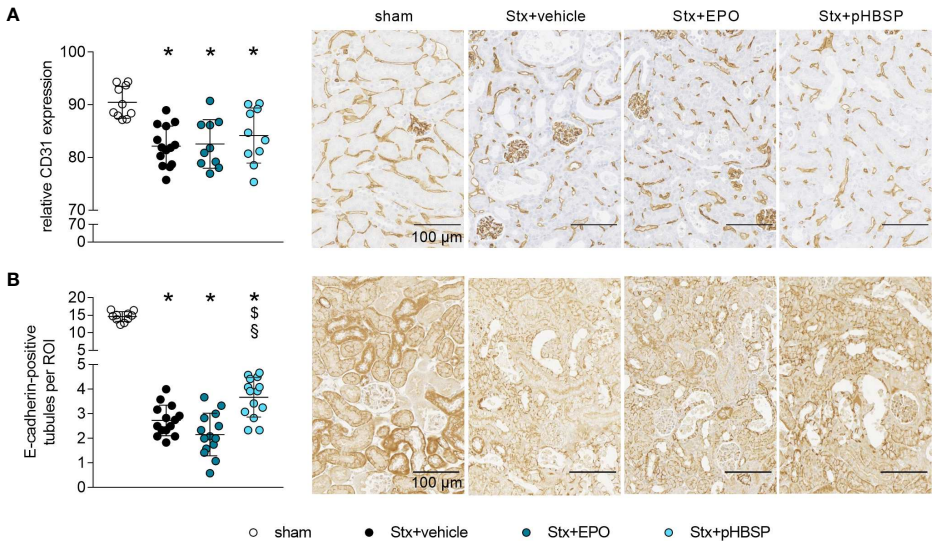

FIGURE 5
Effect of EPO and pHBSP treatment on intrarenal barriers in mice with HUS. Intrarenal barriers were assessed on day 7 of HUS experiment. Quantification data as well as representative images (scale bar 100 µm) of immunohistochemical **(A)** CD31 staining (sham n = 10, Stx+vehicle n = 14, Stx+EPO n = 10, Stx+pHBSP n = 10) and **(B)** E-cadherin (sham n = 10, Stx+vehicle n = 14, Stx+EPO n = 14, Stx+pHBSP n = 14), in renal sections of sham mice and mice subjected to Stx. **(A, B)** Data are expressed as scatter dot plot with mean ± SD. *P < 0.05 vs. sham, $P < 0.05 vs. Stx+vehicle, §P < 0.05 vs. Stx+EPO (one-way ANOVA, Holm-Sidak's multiple comparison test).

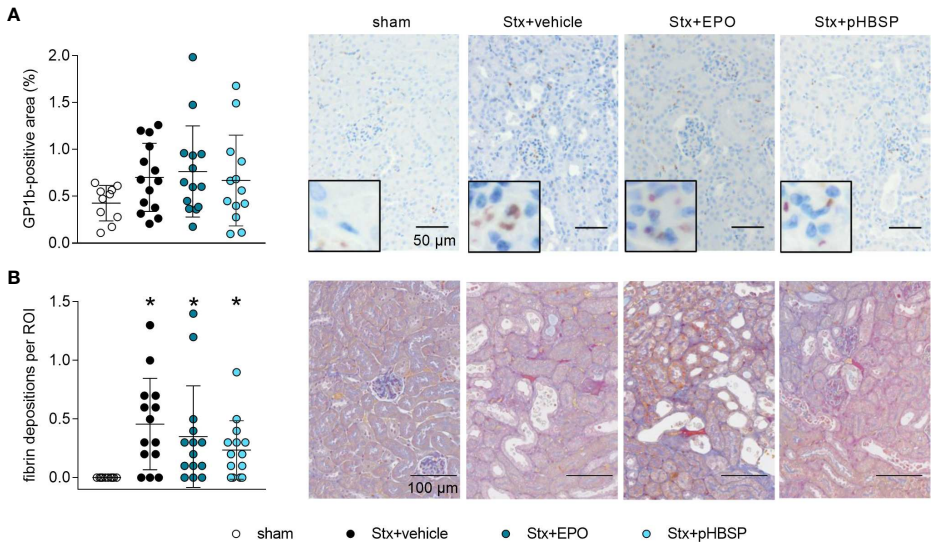

FIGURE 6
Effects of EPO and pHBSP treatment on microangiopathy in mice with HUS. Thrombocytes (indicated by glycoprotein 1b (GP1b) staining) and renal fibrin depositions (indicated by acid fuchsin orange G (SFOG) staining) were assessed on day 7 of HUS experiment. Quantification data and representative images of **(A)** immunohistochemical staining of thrombocytes (sham n = 10, Stx+vehicle n = 14, Stx+EPO n = 14, Stx+pHBSP n = 13) and **(B)** fibrin depositions (sham n = 10, Stx+vehicle n = 14, Stx+EPO n = 14, Stx+pHBSP n = 14) in kidney sections of sham mice and Stx-challenged mice. Quantitative data are expressed as scatter dot plot with mean ± SD. *P < 0.05 vs. sham (Kruskal-Wallis test, Dunn's multiple comparison test), scale bar 100 µm.

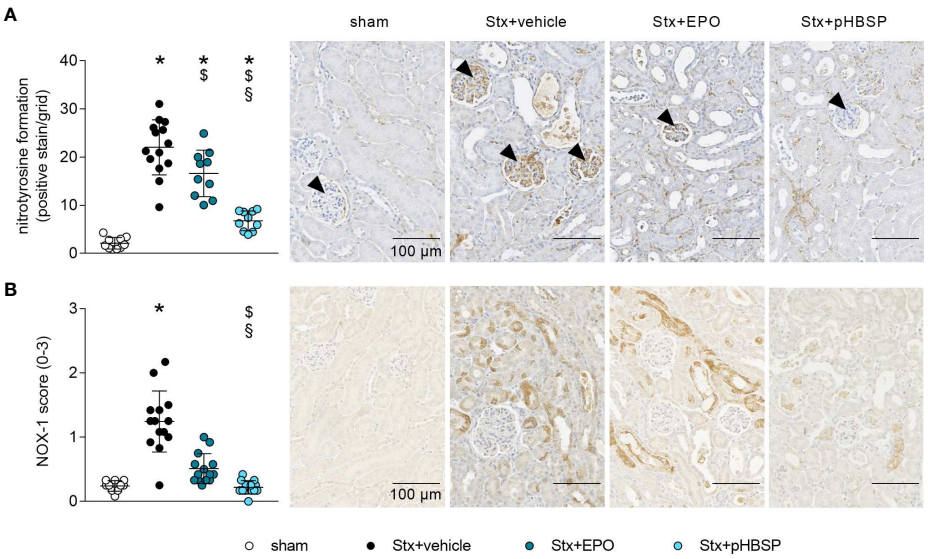

FIGURE 7
Effects of EPO and pHBSP treatment on nitrosative and oxidative stress in mice with HUS. Nitrosative and oxidative stress were assessed on day 7 of HUS experiment. Quantification data and representative images of immunohistochemical staining of **(A)** nitrotyrosine (sham n = 10, Stx+vehicle n = 14, Stx+EPO n = 10, Stx+pHBSP n = 10, arrowheads indicating glomeruli) and **(B)** NOX-1 (sham n = 10, Stx+vehicle n = 14, Stx+EPO n = 14, Stx+pHBSP n = 14) in kidney sections of sham mice and Stx-challenged mice. Quantitative data are expressed as scatter dot plot with mean ± SD. *P < 0.05 vs. sham, $P < 0.05 vs. Stx+vehicle, §P < 0.05 vs. Stx+EPO (A: one-way ANOVA, Holm-Sidak's multiple comparison test, B: Kruskal-Wallis test, Dunn's multiple comparison test), scale bar 100 µm.

correlates with the endogenous EPO production. Here, we pursued our line of thought by further conducting studies in animals with experimental HUS.

In gnotobiotic piglets with EHEC infection (9) and in mice after Stx challenge, we found an increase in EPO expression despite an absence of anemia in these animal models. We and others reported earlier that the extent of systemic hemolysis and subsequent anemia in experimental HUS is not as pronounced as in patients with HUS (9, 10, 14, 53, 54).

Based on pathophysiological considerations and evidence, these findings could imply that EPO expression in HUS does not increase proportionally to the extent of anemia but rather depends on the degree of renal hypoxia as first mechanistically described by Semenza et al. (55, 56). Microthrombotic occlusion in the kidneys can result in

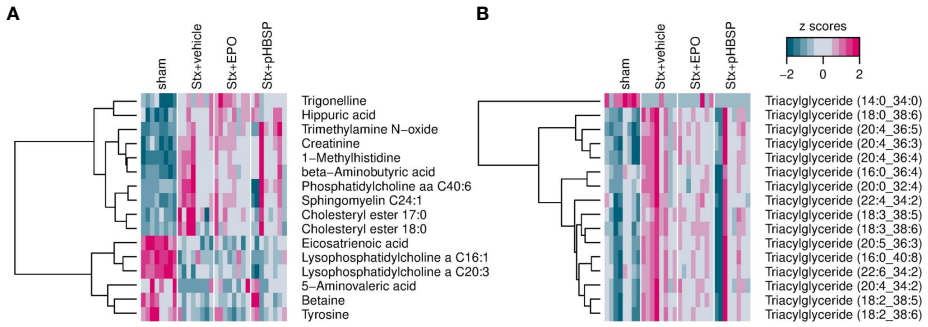

FIGURE 8
Effect of EPO and pHBSP treatment on plasma metabolome in mice with HUS. Metabolites in plasma of sham mice and Stx-challenged mice were assessed on day 7 of HUS experiment. Statistic modelling was performed to test the hypothesis that their abundance either increases or decreases in the following order: sham–Stx+pHBSP–Stx+EPO–Stx+vehicle **(A)** Small metabolites in murine plasma showing a significant trend for the four groups under investigation. **(B)** Triacylglyceroles in murine plasma showing a significant trend for the four groups under investigation. Data are shown as heatmaps depicting z-scores for all samples. The analytes were hierarchically clustered using Ward's minimum variance method (45) and an euclidian distance between z scores. Dendograms provide information about distances between clusters.

local hypoxia increasing the expression of the master regulator hypoxia-induced factor 1α (HIF-1α) and thereby EPO (57). However, direct damage to the EPO-expressing cells in the kidneys of HUS patients with hemolytic anemia may, especially in cases with severe renal injury, also result in insufficient EPO production to adequately stimulate hematopoiesis. Thus, patients with severe renal injury could benefit from treatment with exogenous EPO (58, 59).

EPO and pHBSP in the context of anemia correction and tissue protection

In our experimental setting, we observed a survival benefit in mice with HUS treated with either EPO or pHBSP. Tissue-protective effects of EPO and non-hematopoietic analogs have been the subject of discussion in the literature for nearly two decades (15, 16). Despite the observed beneficial effects of EPO in preclinical models of endotoxemia, sepsis, hemorrhagic shock and ischemia-reperfusion induced AKI (60–63), EPO failed to convey nephroprotection in several clinical trials that included patients following cardiac surgery (64, 65), cardiac arrest (66), kidney-transplantation (67) as well as ICU patients at risk for the development of AKI (EARLYARF trial) (68). However, in a small pilot trial with patients suffering from AKI after coronary artery bypass grafting surgery, treatment with EPO had a beneficial effect on all-cause mortality (69). Corwin et al. reported that administration of high-dose EPO (40,000 IU) to intensive care patients reduced the number of red blood cell transfusions without affecting mortality or clinical outcome (27). In a follow-up study of ICU patients, a subcohort of trauma patients treated with high-dose EPO showed no reduced need for red blood cell transfusions, however mortality was significantly reduced (18). Notably, an increase in thrombotic vascular events was noted in ICU patients who had not received thromboprophylaxis at baseline (18).

In the subset of mice surviving up to day 7 of the HUS experiments, we further investigated surrogate parameters for renal dysfunction and injury as well as barrier integrity, microangiopathy, oxidative and nitrosative stress and metabolome in plasma and/or renal tissue samples. As we have observed previously that AKI is accompanied by electrolyte imbalances, we propose that, in this model, mice die due to a severe AKI-induced hyperkalemia with subsequent cardiac arrhythmias and cardiac arrest (unpublished data). As fewer animals survived up to day 7 in the Stx+vehicle group (11/26, 42.3% survival) compared with the Stx+EPO (15/22, 68.2% survival) and Stx+pHBSP (16/21, 76.2% survival) group, the results need to be carefully interpreted in the light of a reverse survivorship bias, that might explain why we did not observe an effect of treatment with EPO or pHBSP on plasma creatinine, urea and NGAL, as surrogate parameters for AKI and renal dysfunction. However, we observed significant effects of EPO and/or pHBSP treatment on barrier integrity, oxidative and nitrosative stress and on selected metabolites in the samples studied.

Intact renal endothelial and epithelial barriers are important for the physiological function of the kidneys. We observed a pronounced Stx-induced damage of renal endothelial cells independent of treatment. Treatment with pHBSP, but not EPO led to a decrease in KIM-1 and an increase in E-cadherin expression in Stx-challenged mice in our setting. This could indicate less renal damage and enhanced epithelial barrier integrity, as tubular dedifferentiation – an important step in AKI progression – is characterised by a downregulation of E-cadherin (70). Although not resulting in amelioration of AKI in our model, this could have contributed to the increased survival observed after pHBSP treatment in Stx-challenged mice. In line with our results, the pharmaceutical upregulation of E-cadherin expression also proved nephroprotective in preclinical studies of cis-platin-induced AKI (71, 72).

In our recent study, we observed survival benefits in animals with reduced microangiopathy (11). Microangiopathy is a pathophysiological hallmark of HUS. As EPO can exert pro-thrombogenic effects, we consequently assessed the effects of EPO or pHBSP treatment on fibrin deposition and thrombocytes as surrogate parameters of microangiopathy to evaluate the potential of adverse treatment effects in HUS. Notably, we did not observe an aggravation of microthrombi formation or fibrin deposition in mice with HUS treated with either EPO or pHBSP.

Oxidative stress is involved in the pathogenesis of STEC-HUS (3–5). Nitrosative stress resembles a subtype of oxidative stress that has been shown to contribute to cell death (73). We observed an intense glomerular staining of nitrotyrosine in Stx+vehicle mice. Nitrotyrosine results from the reaction of the peroxynitrite radical – created when excess nitric oxide (NO) and superoxide radicals combine (74) – with accessible tyrosine residues (75). While basal NO plays a critical role in the regulation of the perfusion and vascular tone in glomeruli (74), it has been shown previously that inducible NO synthase (iNOS) induction and overproduction of NO had deleterious effects in ischemic AKI (76). In mice, iNOS is – among others – expressed in macrophages and glomerular mesangial cells and inducible by various pro-inflammatory stimuli (77). EPO and pHBSP have been demonstrated to reduce the expression of iNOS either on protein level in AKI of different etiologies (63, 78) or on mRNA level in lung and brain injury (79, 80). Thus, the reduction in renal nitrotyrosine staining in Stx+EPO and Stx+pHBSP mice could result from an inhibition of iNOS in the glomeruli of these mice.

Due to its critical role in the reabsorption of nutrients and maintenance of homeostasis, energy demand and metabolic activity are high in the kidneys (81). By analyzing the plasma metabolome, we observed an increase in triglycerides and cholesteryl esters in Stx-challenged mice that was consistently reported in HUS patients (82). Notably, we observed that alterations in some metabolites associated with kidney injury, e. g. trimethylamine N-oxide (83, 84) and trigonelline (85, 86) as well as lipid compounds were less distinct in mice with HUS after EPO or pHBSP treatment. In line with our results, a recent study demonstrated that EPO reduces lipidemia by stimulating lipid catabolism in peripheral adipose tissue (87). Further studies are required to examine the complex metabolic changes in animals and patients with HUS.

Taken together, we found that treatment with EPO or pHBSP positively affects several pathomechanisms of STEC-HUS which might explain the observed improvement in clinical outcome of mice with HUS. Further systematic studies in this context in animal models and even more importantly larger patient cohorts are needed to provide sufficient evidence to adjust clinical management.

Conclusion

We report here for the first time, that I) EPO levels in patients with STEC-HUS, STEC-infected piglets and Stx-challenged mice are elevated in a uniform manner, II) EPO or pHBSP treatment of mice with HUS improves survival and disease outcome, III) protective effects of pHBSP and EPO are associated with reduced renal oxidative stress, and IV) treatment with pHBSP in Stx-challenged mice is additionally associated with ameliorated nitrosative stress, less KIM-1 expression and tubular dedifferentiation. In the light of our results demonstrating favourable tissue-protective effects of EPO in a preclinical model, treatment of HUS-induced hemolytic anemia with EPO should be considered in patients. Further studies are needed to evaluate the effect of EPO and pHBSP treatment in clinical studies in patients with STEC-HUS.

Data availability statement

The metabolomics dataset presented in this study can be found in online repositories. The names of the repository/repositories and accession number(s) can be found below: https://www.ebi.ac.uk/biostudies/BioStudies accession number S-BSST657. Original data can be requested from sina.coldewey@med.uni-jena.de.

Ethics statement

The studies involving human participants were reviewed and approved by Ethics Committee of Hannover Medical School (1123-2011) and Ethics Committee of Friedrich Schiller University Jena (5276-09/17). The patients/participants provided their written informed consent to participate in this study. The animal studies were reviewed and approved by the Lower Saxony State Office for Consumer Protection and Food Safety (Approval Number: 33.9-42502-04-13/1149) and the regional animal welfare committee and the Thuringian State Office for Consumer Protection (registration number 02-058/14).

Author contributions

SC designed and planned the study; planned, performed and analyzed experiments and wrote the manuscript. SD planned, performed and analyzed experiments and wrote the manuscript. WP planned and performed histology and immunohistochemistry and analyzed data. BW planned and performed animal experiments. FG provided purified Stx and gnotobiotic piglet samples and contributed important intellectual content. DI synthesized and purified pHBSP and contributed important intellectual content. CD and KA performed histology and immunohistochemistry and contributed important intellectual content to histology and immunohistochemistry. JK provided HUS patient samples. IH-P provided gnotobiotic piglet samples. All authors provided important intellectual content and revised the manuscript prior to submission.

Funding

The research leading to these results has received funding from the German Research Foundation (DFG; Research Unit FOR1738, grant no. CO912/2-1 to SC and IM97/7-2 to DI) and the Federal Ministry of Education and Research (BMBF; ZIK Septomics Research Center, Translational Septomics, grant no. 03Z22JN12 to SC and Center for Sepsis Control and Care, project TaSep, grant no. 01EO1502 to SC).

Acknowledgments

We would like to thank J. Fischer (Septomics Research Center, Jena) and Dr. H. H. Brewitz (University of Bonn) for technical assistance, Prof. Dr. J. Menne (KRH Klinikum Siloah, Hannover) for provision of HUS patient samples and D. Driesch (BioControl) for support in metabolomics data analysis.

Conflict of interest

The authors declare that the research was conducted in the absence of any commercial or financial relationships that could be construed as a potential conflict of interest.

Publisher's note

Supplementary material

The Supplementary Material for this article can be found online at: https://www.frontiersin.org/articles/10.3389/fimmu.2022.1010882/full#supplementary-material

References

1. Joseph A, Cointe A, Mariani Kurkdjian P, Rafat C, Hertig A. Shiga toxin-associated hemolytic uremic syndrome: A narrative review. *Toxins (Basel)* (2020) 12(2):32. doi: 10.3390/toxins12020067

2. Spinale JM, Ruebner RL, Copelovitch L, Kaplan BS. Long-term outcomes of shiga toxin hemolytic uremic syndrome. *Pediatr Nephrol* (2013) 28:2097–105. doi: 10.1007/s00467-012-2383-6

3. Ferraris V, Acquier A, Ferraris JR, Vallejo G, Paz C, Mendez CF. Oxidative stress status during the acute phase of haemolytic uraemic syndrome. *Nephrol Dial Transplant* (2011) 26:858–64. doi: 10.1093/ndt/gfq511

4. Kanzelmeyer NK, Pape L, Chobanyan-Jurgens K, Tsikas D, Hartmann H, Fuchs AJ, et al. L-arginine/NO pathway is altered in children with haemolytic-uraemic syndrome (HUS). *Oxid Med Cell Longev* (2014) 2014:203512. doi: 10.1155/2014/203512

5. Gomez SA, Abrey-Recalde MJ, Panek CA, Ferrarotti NF, Repetto MG, Mejias MP, et al. The oxidative stress induced *in vivo* by shiga toxin-2 contributes to the pathogenicity of haemolytic uraemic syndrome. *Clin Exp Immunol* (2013) 173:463–72. doi: 10.1111/cei.12124

6. Adamski J. Thrombotic microangiopathy and indications for therapeutic plasma exchange. *Hematol Am Soc Hematol Educ Program* (2014) 2014:444–9. doi: 10.1182/asheducation-2014.1.444

7. RKI. *Infektionsepidemiologisches jahrbuch meldepflichtiger krankheiten für 2020*. Robert Koch Institut (2020). Available at: https://www.rki.de/DE/Content/Infekt/Jahrbuch/Jahrbuch_2020.html.

8. Ministerio de Salud. *Boletín integrado de vigilancia N560 SE30 2021* (2021). Available at: https://bancos.salud.gob.ar/recurso/boletin-integrado-de-vigilancia-n560-se30-2021.

9. Wöchtl B, Gunzer F, Gerner W, Gasse H, Koch M, Bago Z, et al. Comparison of clinical and immunological findings in gnotobiotic piglets infected with escherichia coli O104:H4 outbreak strain and EHEC O157:H7. *Gut Pathog* (2017) 9:30. doi: 10.1186/s13099-017-0179-8

10. Dennhardt S, Pirschel W, Wissuwa B, Daniel C, Gunzer F, Lindig S, et al. Modeling hemolytic-uremic syndrome: In-depth characterization of distinct murine models reflecting different features of human disease. *Front Immunol* (2018) 9:1459. doi: 10.3389/fimmu.2018.01459

11. Pirschel W, Mestekemper AN, Wissuwa B, Krieg N, Kroller S, Daniel C, et al. Divergent roles of haptoglobin and hemopexin deficiency for disease progression of shiga-toxin-induced hemolytic-uremic syndrome in mice. *Kidney Int* (2022) 101(6):1171–85. doi: 10.1016/j.kint.2021.12.024

12. Sobbe IV, Krieg N, Dennhardt S, Coldewey SM. Involvement of NF-kappaB1 and the non-canonical NF-kappaB signaling pathway in the pathogenesis of acute kidney injury in shiga-toxin-2-induced hemolytic-uremic syndrome in mice. *Shock* (2021) 56:573–81. doi: 10.1097/SHK.0000000000001558

13. Keepers TR, Psotka MA, Gross LK, Obrig TG. A murine model of HUS: Shiga toxin with lipopolysaccharide mimics the renal damage and physiologic response of human disease. *J Am Soc Nephrol* (2006) 17:3404–14. doi: 10.1681/ASN.2006050419

14. Sauter KA, Melton-Celsa AR, Larkin K, Troxell ML, O'Brien AD, Magun BE. Mouse model of hemolytic-uremic syndrome caused by endotoxin-free shiga toxin 2 (Stx2) and protection from lethal outcome by anti-Stx2 antibody. *Infect Immun* (2008) 76:4469–78. doi: 10.1128/IAI.00592-08

15. Brines M, Patel NS, Villa P, Brines C, Mennini T, De Paola M, et al. Nonerythropoietic, tissue-protective peptides derived from the tertiary structure of erythropoietin. *Proc Natl Acad Sci United States America* (2008) 105:10925–30. doi: 10.1073/pnas.0805594105

16. Brines M, Grasso G, Fiordaliso F, Sfacteria A, Ghezzi P, Fratelli M, et al. Erythropoietin mediates tissue protection through an erythropoietin and common beta-subunit heteroreceptor. *Proc Natl Acad Sci United States America* (2004) 101:14907–12. doi: 10.1073/pnas.0406491101

17. Pearl RG. Erythropoietin and organ protection: lessons from negative clinical trials. *Crit Care* (2014) 18:526. doi: 10.1186/s13054-014-0526-9

18. Corwin HL, Gettinger A, Fabian TC, May A, Pearl RG, Heard S, et al. Efficacy and safety of epoetin alfa in critically ill patients. *N Engl J Med* (2007) 357:965–76. doi: 10.1056/NEJMoa071533

19. Ehrenreich H, Weissenborn K, Prange H, Schneider D, Weimar C, Wartenberg K, et al. Recombinant human erythropoietin in the treatment of acute ischemic stroke. *Stroke* (2009) 40:e647–56. doi: 10.1161/STROKEAHA.109.564872

20. Collino M, Thiemermann C, Cerami A, Brines M. Flipping the molecular switch for innate protection and repair of tissues: Long-lasting effects of a non-erythropoietic small peptide engineered from erythropoietin. *Pharmacol Ther* (2015) 151:32–40. doi: 10.1016/j.pharmthera.2015.02.005

21. Netrebenko AS, Gureev VV, Pokrovskii MV, Gureeva AV, Tsuverkalova YM, Rozhkov IS. Assessment of the nephroprotective properties of the erythropoietin mimetic peptide and infliximab in kidney ischemia-reperfusion injury in rats. *Arch Razi Inst* (2021) 76:995–1004. doi: 10.22092/ari.2021.355849.1728

22. Patel NS, Kerr-Peterson HL, Brines M, Collino M, Rogazzo M, Fantozzi R, et al. Delayed administration of pyroglutamate helix b surface peptide (pHBSP), a novel nonerythropoietic analog of erythropoietin, attenuates acute kidney injury. *Mol Med* (2012) 18:719–27. doi: 10.2119/molmed.2012.00093

23. Brines M, Dunne AN, van Velzen M, Proto PL, Ostenson CG, Kirk RI, et al. ARA 290, a nonerythropoietic peptide engineered from erythropoietin, improves metabolic control and neuropathic symptoms in patients with type 2 diabetes. *Mol Med* (2015) 20:658–66. doi: 10.2119/molmed.2014.00215

24. Dahan A, Dunne A, Swartjes M, Proto PL, Heij L, Vogels O, et al. ARA 290 improves symptoms in patients with sarcoidosis-associated small nerve fiber loss and increases corneal nerve fiber density. *Mol Med* (2013) 19:334–45. doi: 10.2119/molmed.2013.00122

25. Coldewey SM, Khan AI, Kapoor A, Collino M, Rogazzo M, Brines M, et al. Erythropoietin attenuates acute kidney dysfunction in murine experimental sepsis by activation of the beta-common receptor. *Kidney Int* (2013) 84:482–90. doi: 10.1038/ki.2013.118

26. Khan AI, Coldewey SM, Patel NS, Rogazzo M, Collino M, Yaqoob MM, et al. Erythropoietin attenuates cardiac dysfunction in experimental sepsis in mice *via* activation of the beta-common receptor. *Dis Model Mech* (2013) 6:1021–30. doi: 10.1242/dmm.011908

27. Corwin HL, Gettinger A, Pearl RG, Fink MP, Levy MM, Shapiro MJ, et al. Efficacy of recombinant human erythropoietin in critically ill patients: A randomized controlled trial. *JAMA* (2002) 288:2827–35. doi: 10.1001/jama.288.22.2827

28. MacLaren R, Gasper J, Jung R, Vandivier RW. Use of exogenous erythropoietin in critically ill patients. *J Clin Pharm Ther* (2004) 29:195–208. doi: 10.1111/j.1365-2710.2004.00552.x

29. Pasricha SR, Frazer DM, Bowden DK, Anderson GJ. Transfusion suppresses erythropoiesis and increases hepcidin in adult patients with beta-thalassemia major: A longitudinal study. *Blood* (2013) 122:124–33. doi: 10.1182/blood-2012-12-471441

30. Rasmussen SR, Kandler K, Nielsen RV, Jakobsen PC, Ranucci M, Ravn HB. Association between transfusion of blood products and acute kidney injury following cardiac surgery. *Acta Anaesthesiol Scand* (2020) 64:1397–404. doi: 10.1111/aas.13664

31. Schrezenmeier H, Noe G, Raghavachar A, Rich IN, Heimpel H, Kubanek B. Serum erythropoietin and serum transferrin receptor levels in aplastic anaemia. *Br J Haematol* (1994) 88:286–94. doi: 10.1111/j.1365-2141.1994.tb05020.x

32. Exeni R, Donato H, Rendo P, Antonuccio M, Rapetti MC, Grimoldi I, et al. Low levels of serum erythropoietin in children with endemic hemolytic uremic syndrome. *Pediatr Nephrol* (1998) 12:226–30. doi: 10.1007/s004670050443

33. Faquin WC, Schneider TJ, Goldberg MA. Effect of inflammatory cytokines on hypoxia-induced erythropoietin production. *Blood* (1992) 79:1987–94. doi: 10.1182/blood.V79.8.1987.1987

34. Erslev AJ. Erythropoietin. *N Engl J Med* (1991) 324:1339–44. doi: 10.1056/NEJM199105093241907

35. Deutsche Krebsgesellschaft, AWMF. *Supportive therapie bei onkologischen PatientInnen - langversion 1.0* (2016). Available at: http://leitlinienprogramm-onkologie.de/Supportive-Therapie.95.0.html.

36. K.D.I.O.K.A.W. Group. KDIGO clinical practice guideline for anemia in chronic kidney disease. *Kidney Inter Supplement* (2012) pp:279–335. doi: 10.1038/kisup.2012.35

37. Gesellschaft für Pädiatrische Nephrologie e.V. (GPN), AWMF. *Hämolytisch-urämisches syndrom im kindesalter* (2022). Available at: https://www.awmf.org/leitlinien/detail/ll/166-002.html.

38. Balestracci A, Capone MA, Meni Battaglia L, Toledo I, Martin SM, Beaudoin L, et al. Erythropoietin in children with hemolytic uremic syndrome: A pilot randomized controlled trial. *Pediatr Nephrol* (2022) 37(10):2383–92. doi: 10.1007/s00467-022-05474-9

39. Balestracci A, Martin SM, Toledo I, Alvarado C, Wainsztein RE. Early erythropoietin in post-diarrheal hemolytic uremic syndrome: A case-control study. *Pediatr Nephrol* (2015) 30:339–44. doi: 10.1007/s00467-014-2911-7

40. Pape L, Ahlenstiel T, Kreuzer M, Drube J, Froede K, Franke D, et al. Early erythropoietin reduced the need for red blood cell transfusion in childhood hemolytic uremic syndrome: a randomized prospective pilot trial. *Pediatr Nephrol* (2009) 24:1061–4. doi: 10.1007/s00467-008-1087-4

41. Woo da E, Lee JM, Kim YK, Park YH. Recombinant human erythropoietin therapy for a jehovah's witness child with severe anemia due to hemolytic-uremic syndrome. *Korean J Pediatr* (2016) 59:100–3. doi: 10.3345/kjp.2016.59.2.100

42. Kielstein JT, Beutel G, Fleig S, Steinhoff J, Meyer TN, Hafer C, et al. Best supportive care and therapeutic plasma exchange with or without eculizumab in shiga-toxin-producing e. coli O104:H4 induced haemolytic-uraemic syndrome: an analysis of the German STEC-HUS registry. *Nephrol Dial Transplant* (2012) 27:3807–15. doi: 10.1093/ndt/gfs394

43. Coldewey SM, Neu C, Baumbach P, Scherag A, Goebel B, Ludewig K, et al. Identification of cardiovascular and molecular prognostic factors for the medium-term and long-term outcomes of sepsis (ICROS): protocol for a prospective monocentric cohort study. *BMJ Open* (2020) 10:e036527. doi: 10.1136/bmjopen-2019-036527

44. Hochberg Y, Benjamini Y. More powerful procedures for multiple significance testing. *Stat Med* (1990) 9:811–8. doi: 10.1002/sim.4780090710

45. Murtagh F, Legendre P. Ward's hierarchical agglomerative clustering method: Which algorithms implement ward's criterion? *J Classif* (2014) 31:274–95. doi: 10.1007/s00357-014-9161-z

46. Lee P, Chandel NS, Simon MC. Cellular adaptation to hypoxia through hypoxia inducible factors and beyond. *Nat Rev Mol Cell Biol* (2020) 21:268–83. doi: 10.1038/s41580-020-0227-y

47. Matsuura R, Doi K, Komaru Y, Miyamoto Y, Yoshida T, Isegawa T, et al. Endogenous erythropoietin and hepatic dysfunction in acute kidney injury requiring renal replacement therapy. *Nephron* (2019) 142:10–6. doi: 10.1159/000496618

48. Morgera S, Heering P, Szentandrasi T, Niederau C, Grabensee B. Erythropoietin in patients with acute renal failure and continuous veno-venous haemofiltration. *Int Urol Nephrol* (1997) 29:245–50. doi: 10.1007/BF02551350

49. Tamion F, Le Cam-Duchez V, Menard JF, Girault C, Coquerel A, Bonmarchand G. Erythropoietin and renin as biological markers in critically ill patients. *Crit Care* (2004) 8:R328–35. doi: 10.1186/cc2902

50. Yamashita T, Noiri E, Hamasaki Y, Matsubara T, Ishii T, Yahagi N, et al. Erythropoietin concentration in acute kidney injury is associated with insulin-like growth factor-binding protein-1. *Nephrol (Carlton)* (2016) 21:693–9. doi: 10.1111/nep.12656

51. Frank C, Werber D, Cramer JP, Askar M, Faber M, an der Heiden M, et al. Epidemic profile of shiga-toxin-producing escherichia coli O104:H4 outbreak in Germany. *N Engl J Med* (2011) 365:1771–80. doi: 10.1056/NEJMoa1106483

52. Maxwell PH, Osmond MK, Pugh CW, Heryet A, Nicholls LG, Tan CC, et al. Identification of the renal erythropoietin-producing cells using transgenic mice. *Kidney Int* (1993) 44:1149–62. doi: 10.1038/ki.1993.362

53. Gunzer F, Hennig-Pauka I, Waldmann KH, Sandhoff R, Grone HJ, Kreipe HH, et al. Gnotobiotic piglets develop thrombotic microangiopathy after oral infection with enterohemorrhagic escherichia coli. *Am J Clin Pathol* (2002) 118:364–75. doi: 10.1309/UMW9-D06Q-M94Q-JGH2

54. Walsh PR, Johnson S. Treatment and management of children with haemolytic uraemic syndrome. *Arch Dis Child* (2018) 103:285–91. doi: 10.1136/archdischild-2016-311377

55. Semenza GL, Koury ST, Nejfelt MK, Gearhart JD, Antonarakis SE. Cell-type-specific and hypoxia-inducible expression of the human erythropoietin gene in transgenic mice. *Proc Natl Acad Sci United States America* (1991) 88:8725–9. doi: 10.1073/pnas.88.19.8725

56. Semenza GL, Nejfelt MK, Chi SM, Antonarakis SE. Hypoxia-inducible nuclear factors bind to an enhancer element located 3' to the human erythropoietin gene. *Proc Natl Acad Sci United States America* (1991) 88:5680–4. doi: 10.1073/pnas.88.13.5680

57. Corrado C, Fontana S. Hypoxia and HIF signaling: One axis with divergent effects. *Int J Mol Sci 21* (2020) 21(66):5611. doi: 10.3390/ijms21165611

58. Fishbane S, Coyne DW. How I treat renal anemia. *Blood* (2020) 136:783–9. doi: 10.1182/blood.2019004330

59. Mikhail A, Brown C, Williams JA, Mathrani V, Shrivastava R, Evans J, et al. Renal association clinical practice guideline on anaemia of chronic kidney disease. *BMC Nephrol* (2017) 18:345. doi: 10.1186/s12882-017-0688-1

60. Heitrich M, Garcia DM, Stoyanoff TR, Rodriguez JP, Todaro JS, Aguirre MV. Erythropoietin attenuates renal and pulmonary injury in polymicrobial induced-sepsis through EPO-r, VEGF and VEGF-R2 modulation. *BioMed Pharmacother* (2016) 82:606–13. doi: 10.1016/j.biopha.2016.05.045

61. Kwak J, Kim JH, Jang HN, Jung MH, Cho HS, Chang SH, et al. Erythropoietin ameliorates Ischemia/Reperfusion-induced acute kidney injury *via* inflammasome suppression in mice. *Int J Mol Sci 21* (2020) 21(10):3453. doi: 10.3390/ijms21103453

62. Ranjbaran M, Kadkhodaee M, Seifi B, Adelipour M, Azarian B. Erythropoietin attenuates experimental haemorrhagic shock-induced renal damage through an iNOS- dependent mechanism in male wistar rats. *Injury* (2017) 48:262–9. doi: 10.1016/j.injury.2017.01.010

63. Stoyanoff TR, Rodriguez JP, Todaro JS, Colavita JPM, Torres AM, Aguirre MV. Erythropoietin attenuates LPS-induced microvascular damage in a murine model of septic acute kidney injury. *BioMed Pharmacother* (2018) 107:1046–55. doi: 10.1016/j.biopha.2018.08.087

64. de Seigneux S, Ponte B, Weiss L, Pugin J, Romand JA, Martin PY, et al. Epoetin administrated after cardiac surgery: effects on renal function and inflammation in a randomized controlled study. *BMC Nephrol* (2012) 13:132. doi: 10.1186/1471-2369-13-132

65. Kim JH, Shim JK, Song JW, Song Y, Kim HB, Kwak YL. Effect of erythropoietin on the incidence of acute kidney injury following complex valvular heart surgery: a double blind, randomized clinical trial of efficacy and safety. *Crit Care* (2013) 17:R254. doi: 10.1186/cc13081

66. Guillemet L, Jamme M, Bougouin W, Geri G, Deye N, Vivien B, et al. Effects of early high-dose erythropoietin on acute kidney injury following cardiac arrest: exploratory *post hoc* analyses from an open-label randomized trial. *Clin Kidney J* (2020) 13:413–20. doi: 10.1093/ckj/sfz068

67. Sureshkumar KK, Hussain SM, Ko TY, Thai NL, Marcus RJ. Effect of high-dose erythropoietin on graft function after kidney transplantation: a randomized, double-blind clinical trial. *Clin J Am Soc Nephrol* (2012) 7:1498–506. doi: 10.2215/CJN.01360212

68. Endre ZH, Walker RJ, Pickering JW, Shaw GM, Frampton CM, Henderson SJ, et al. Early intervention with erythropoietin does not affect the outcome of acute kidney injury (the EARLYARF trial). *Kidney Int* (2010) 77:1020–30. doi: 10.1038/ki.2010.25

69. Oh SW, Chin HJ, Chae DW, Na KY. Erythropoietin improves long-term outcomes in patients with acute kidney injury after coronary artery bypass grafting. *J Korean Med Sci* (2012) 27:506–11. doi: 10.3346/jkms.2012.27.5.506

70. Zheng G, Lyons JG, Tan TK, Wang Y, Hsu TT, Min D, et al. Disruption of e-cadherin by matrix metalloproteinase directly mediates epithelial-mesenchymal transition downstream of transforming growth factor-beta1 in renal tubular epithelial cells. *Am J Pathol* (2009) 175:580–91. doi: 10.2353/ajpath.2009.080983

71. Gao L, Liu MM, Zang HM, Ma QY, Yang Q, Jiang L, et al. Restoration of e-cadherin by PPBICA protects against cisplatin-induced acute kidney injury by attenuating inflammation and programmed cell death. *Lab Invest* (2018) 98:911–23. doi: 10.1038/s41374-018-0052-5

72. Ni J, Hou X, Wang X, Shi Y, Xu L, Zheng X, et al. 3-deazaneplanocin a protects against cisplatin-induced renal tubular cell apoptosis and acute kidney injury by restoration of e-cadherin expression. *Cell Death Dis* (2019) 10:355. doi: 10.1038/s41419-019-1589-y

73. Wang F, Yuan Q, Chen F, Pang J, Pan C, Xu F, et al. Fundamental mechanisms of the cell death caused by nitrosative stress. *Front Cell Dev Biol* (2021) 9:742483. doi: 10.3389/fcell.2021.742483

74. Goligorsky MS, Brodsky SV, Noiri E. NO bioavailability, endothelial dysfunction, and acute renal failure: new insights into pathophysiology. *Semin Nephrol* (2004) 24:316–23. doi: 10.1016/j.semnephrol.2004.04.003

75. Korkmaz A, Kolankaya D. Inhibiting inducible nitric oxide synthase with rutin reduces renal ischemia/reperfusion injury. *Can J Surg* (2013) 56:6–14. doi: 10.1503/cjs.004811

76. Noiri E, Peresleni T, Miller F, Goligorsky MS. *In vivo* targeting of inducible NO synthase with oligodeoxynucleotides protects rat kidney against ischemia. *J Clin Invest* (1996) 97:2377–83. doi: 10.1172/JCI118681

77. Sharma K, Danoff TM, DePiero A, Ziyadeh FN. Enhanced expression of inducible nitric oxide synthase in murine macrophages and glomerular mesangial cells by elevated glucose levels: possible mediation *via* protein kinase c. *Biochem Biophys Res Commun* (1995) 207:80–8. doi: 10.1006/bbrc.1995.1156

78. Yang FL, Subeq YM, Chiu YH, Lee RP, Lee CJ, Hsu BG. Recombinant human erythropoietin reduces rhabdomyolysis-induced acute renal failure in rats. *Injury* (2012) 43:367–73. doi: 10.1016/j.injury.2011.11.013

79. Chen H, Luo B, Yang X, Xiong J, Liu Z, Jiang M, et al. Therapeutic effects of nonerythropoietic erythropoietin analog ARA290 in experimental autoimmune encephalomyelitis rat. *J Neuroimmunol* (2014) 268:64–70. doi: 10.1016/j.jneuroim.2014.01.006

80. Liu Y, Lu J, Wang X, Chen L, Liu S, Zhang Z, et al. Erythropoietin-derived peptide protects against acute lung injury after rat traumatic brain injury. *Cell Physiol Biochem* (2017) 41:2037–44. doi: 10.1159/000475434

81. Bhargava P, Schnellmann RG. Mitochondrial energetics in the kidney. *Nat Rev Nephrol* (2017) 13:629–46. doi: 10.1038/nrneph.2017.107

82. Kaplan BS, Gale D, Ipp T. Hyperlipidemia in the hemolytic-uremic syndrome. *Pediatrics* (1971) 47:776–9. doi: 10.1542/peds.47.4.776

83. Sun G, Yin Z, Liu N, Bian X, Yu R, Su X, et al. Gut microbial metabolite TMAO contributes to renal dysfunction in a mouse model of diet-induced obesity. *Biochem Biophys Res Commun* (2017) 493:964–70. doi: 10.1016/j.bbrc.2017.09.108

84. Tang WH, Wang Z, Kennedy DJ, Wu Y, Buffa JA, Agatisa-Boyle B, et al. Gut microbiota-dependent trimethylamine n-oxide (TMAO) pathway contributes to both development of renal insufficiency and mortality risk in chronic kidney disease. *Circ Res* (2015) 116:448–55. doi: 10.1161/CIRCRESAHA.116.305360

85. Chihanga T, Ma Q, Nicholson JD, Ruby HN, Edelmann RE, Devarajan P, et al. NMR spectroscopy and electron microscopy identification of metabolic and ultrastructural changes to the kidney following ischemia-reperfusion injury. *Am J Physiol Renal Physiol* (2018) 314(2)F154–66. doi: 10.1152/ajprenal.00363.2017

86. Won AJ, Kim S, Kim YG, Kim KB, Choi WS, Kacew S, et al. Discovery of urinary metabolomic biomarkers for early detection of acute kidney injury. *Mol Biosyst* (2016) 12:133–44. doi: 10.1039/C5MB00492F

87. Li J, Yang M, Yu Z, Tian J, Du S, Ding H. Kidney-secreted erythropoietin lowers lipidemia *via* activating JAK2-STAT5 signaling in adipose tissue. *EBioMedicine* (2019) 50:317–28. doi: 10.1016/j.ebiom.2019.11.007

4. Discussion

This thesis combines the establishment and in-depth characterization of clinically relevant murine models of HUS - a disease for which there is currently no specific drug - with the performance of an interventional study for the disease in question with different potential therapeutics.

4.1 Modeling Hemolytic-Uremic Syndrome: In-Depth Characterization of Distinct Murine Models Reflecting Different Features of Human Disease

4.1.1 Differences in mice and men – Challenges in HUS model establishment

The greatest challenge in the establishment of clinically relevant murine HUS models that reliably reflect the key features of the human disease lies in the differentially expression of the Gb3 receptor in the two different species: While the highest expression levels of Gb3 are found in human glomeruli (Obrig *et al.* 1993), in mice these receptors are concentrated on tubular epithelial cells. As a result, Stx induces mainly glomerular damage in HUS patients and tubular injury in rodent models.

However, high levels of biologically active Gb3 are also found on human proximal tubule epithelial cells (Obrig *et al.* 1993), resulting in tubular injury during HUS in patients. Even more important, the underlying pathomechanisms of glomerular damage in HUS patients and tubular injury in rodent models appear to be similar, as they are based on the ribotoxic effects of Stx, the procoagulant state of the endothelium resulting in microthrombi and thereby hypoxia and oxidative stress and the pronounced local immune response. In this thesis, a murine model was established that reflects many of the important pathomechanistic features and symptoms observed in HUS patients including I) acute kidney injury, II) hemolysis, III) microthrombi formation, IV) renal immune cell invasion, V) oxidative stress and VI) complement activation (Dennhardt *et al.* 2018). As other murine models of HUS either did not reproduce all these symptoms or did not assess them (Keepers *et al.* 2006, Sauter *et al.* 2008), the subacute model of murine HUS established in this thesis is of superior clinical relevance. However, some characteristic symptoms of human HUS could not be reproduced in this model either (Dennhardt *et al.* 2018): instead of anemia and thrombocytopenia, mild hemoconcentration was observed in mice with HUS. In the model proposed by Keepers *et al.*, transient anemia and thrombocytopenia were reported (Keepers *et al.* 2006), however, it is arguable if this reflects the actions of Stx

in mice or can be attributed to the LPS which was co-applied (Aslam *et al.* 2006). In fact, hemoconcentration is also observed in humans suffering from HUS and resembles a risk factor for poor prognosis (Loos *et al.* 2021). As volume expansion is a crucial part of therapy in humans, anemia and thrombocytopenia become apparent even after initial hemoconcentration while they might be masked in mice subjected to Stx. Although the models established in this thesis for the first time included volume replacement in murine models of HUS (Dennhardt *et al.* 2018), the intensive care support in mice cannot be equalized to the one provided in humans.

4.1.2 STEC infection versus Stx intoxication

The natural ways of acquiring STEC infections are the ingestion of contaminated water or food as well as smear infection. It therefore appears consequential to establish murine models of HUS by orally challenging mice with STEC bacteria. However, due to their microbiome, mice are naturally way less susceptible to STEC infection (Mohawk and O'Brien 2011). Murine infection models thereby mostly rely on the disruption of the facultative flora of mice prior to infection, e.g. via streptomycin treatment (Wadolkowski *et al.* 1990), protein-calorie malnutrition (Kurioka *et al.* 1998) or the use of gnotobiotic mice (Isogai *et al.* 1998). Although the route of infection in these models resembles the route of infection in HUS patients, they carry the drawback that the missing microbiome might influence the outcome of infection in these animals. However, in order to study colonization, potential vaccines against STECs and assess the effectivity of antibiotics in HUS, models of actual infection are necessary.

A hybrid model of infection and Stx intoxication has been established by genetically engineering *Citrobacter rodentium*, a bacterium that is naturally infecting mice (Luperchio and Schauer 2001), to express Stx2 (Mallick *et al.* 2012). Oral ingestion of this modified bacterium induces HUS-like symptoms in mice (Mallick *et al.* 2012). Although this model overcomes the difficulties of using gnotobiotic mice or the usage of mice with a destroyed microbiome which might influence these animals' capability to deal with infections, this model also has shortcomes: Stx2 is the most prominent virulence factor of EHECs, however it is not the only one capable of damaging the endothelium during HUS pathogenesis. Several other virulence factors were isolated from various EHEC strains, such as EHEC hemolysin (Aldick *et al.* 2007), cytolethal distending toxin V (Bielaszewska *et al.* 2005) or EHEC vacuolating cytotoxin

(Bielaszewska *et al.* 2009). These additional virulence factors are absent in a model based on *Citrobacter rodentium*.

Due to the non-invasive nature of EHEC, Stx first needs to cross the intestinal mucosal barrier to gain access to intestinal endothelial cells and thereby the circulation. To date, the exact mechanism is unknown, although several distinct ways have been proposed in the literature: I) holotoxin uptake via Gb3 receptors on intestinal epithelial (Jacewicz *et al.* 1995) or Paneth cells (Schuller *et al.* 2007), II) paracellular transport (Hurley *et al.* 2001), III) uptake by macropinocytosis (Malyukova *et al.* 2009) or IV) uptake within bacterial outer membrane vesicles (Kunsmann *et al.* 2015, Stahl *et al.* 2015). Once in the bloodstream, Stx is immediately bound by neutrophils, monocytes, platelets or erythrocytes via Gb3 or other receptors (Brigotti *et al.* 2006, Stahl *et al.* 2009, te Loo *et al.* 2000). The exact mechanism of transport to the kidney and release of Stx is still unknown; however, recent studies indicate that Stx-carrying immune cells are able to shed Stx-loaded microvesicles that are targeted to the kidneys probably due to the high local expression of Gb3 receptors (Kunsmann *et al.* 2015, Stahl *et al.* 2015). Therefore, different administration routes for Stx were proposed in murine models of Stx intoxication. These models are important as they allow to study the role of Stx in the pathophysiology of HUS in isolation. Interestingly, Stx applied orally to mice led to the death of these animals and induced organ damage (Rasooly *et al.* 2010). However, large amounts of toxin are needed for these models and the reproducibility might be difficult as in contrast to EHEC bacteria which are excellently protected from the acidic milieu of the stomach (Coldewey *et al.* 2007), a substantial portion of the protein toxin might be degraded on its passage through the gastrointestinal tract. Other models rely on intraperitoneal delivery of the toxin, either in combination with LPS (Keepers *et al.* 2006) or divided into several sublethal doses (Sauter *et al.* 2008).

In conclusion, whether to choose a STEC infection or Stx intoxication model depends not only on the laboratory condition but in first line on the research question supposed to be answered. As this thesis aimed to establish a model to analyze pathomechanisms of HUS and to perform an interventional study testing different therapeutics, a model relying on Stx intoxication appeared to be the most promising approach. In contrast to other models of intoxication based on oral or intraperitoneal application of Stx, intravenous injection of Stx to the tail vein was chosen as it provides the highest and most rapid bioavailability (Dennhardt *et al.* 2018).

4.1.3 Controversial role of endotoxins in HUS pathogenesis

The involvement of LPS in the pathogenesis of HUS is highly controversial. During infection, EHEC bacteria colonize the gut and tightly adhere to the apical site of enterocytes by the formation of so called attaching and effacing (A/E) lesions (Stevens and Frankel 2014). Via these lesions and the type-III-secretion system, bacterial proteins are introduced into host cells (Stevens and Frankel 2014). Although bacteremia is reported only sporadically (Mariani-Kurkdjian *et al.* 2014) and LPS was never detected in HUS patients' blood samples, antibodies against EHEC-strain specific LPS are frequently detected in HUS patients and utilized in HUS diagnosis (Rastawicki *et al.* 2020). There are contradictory reports from different animal models and species regarding the need of LPS co-application to induce HUS-like symptoms: in mice, some symptoms were only inducible by Stx and LPS co-application (Keepers *et al.* 2006) and in rats glomerular damage also appears to depend on LPS more than Stx (Silberstein *et al.* 2011). Surprisingly, in rabbits, even the application of LPS alone is sufficient to induce HUS-like symptoms (Fong and King-Hrycaj 1983). In baboons, at least the toxicity of Stx1 appears to depend on LPS co-administration (Siegler *et al.* 2001). Based on the ambiguous role of LPS in HUS pathogenesis both in animals and humans, the models established in this thesis refrain from the co-administration of LPS allowing the assessment of Stx effects solely.

4.2 Targeting the innate repair receptor axis via erythropoietin or pyroglutamate helix B surface peptide attenuates hemolytic-uremic syndrome in mice

4.2.1 Alternative therapeutic strategies under investigation

As mentioned before, the use of antibiotics is highly controversial as it may increase the production and release of Stx. Furthermore, there is a high prevalence of multi drug resistant diarrheagenic *E. coli* strains in general and STEC strains specifically ranging between 60% and over 80% (Jafari *et al.* 2021, Zhang *et al.* 2018). This further complicates antibiotic treatment of HUS and underlines the need for innovative treatment concepts. Several treatment strategies have already been studied with varying successes. These strategies focus on two main concepts: removal or neutralization of Stx and prevention of host tissue damage.

An approach for the neutralization of Stx was demonstrated by Sauter *et al.* in mice with experimental HUS: By applying a monoclonal anti-Stx2 antibody 4 days after the induction of HUS by Stx injection, complete recovery was induced (Sauter *et al.* 2008). The safety of a humanized monoclonal anti-Stx2 antibody (urtoxazumab) was assessed in healthy adult volunteers and pediatric HUS patients (Lopez *et al.* 2010), however its potential effects on clinical outcome have not been analyzed in patients yet. For the removal of Stx, a chromosorb matrix was coupled with Stx-binding sites of Gb3 receptors (Synsorb-Pk). In a phase I study, oral application of Synsorb-Pk in healthy adults was well-tolerated and safe (Armstrong *et al.* 1995). However, in a multicenter randomized control trial including 145 pediatric patients with D+HUS, Synsorb-Pk treatment failed to prove a therapeutic benefit as disease severity was comparable in the placebo group and the group who received the drug orally (Trachtman *et al.* 2003). The drawback of Stx-neutralization strategies is the fact that therapy needs to be started immediately after onset of diarrhea to prevent that Stx enters the circulation and reaches its primary targets in the kidneys.

An intermediate approach is the impairment of cellular uptake and/or intracellular Stx trafficking to prevent its ribotoxic effects. Although this approach has shown promising results in a rat model of HUS (Silberstein *et al.* 2011), in order to be effective in HUS patients, this treatment also needs to be started as early as possible setting a close therapeutic window.

As multiple pathways are involved in the pathogenesis of HUS, the potential of treatable target seems to be high. However, none of these molecular therapeutic approaches could be implemented into the clinical routine yet. The complement C5 inhibitor eculizumab, that – although being a game-changer for patient prognosis in aHUS – is still controversially discussed in STEC-HUS (Mahat *et al.* 2019). Eculizumab was first studied to be implemented in the therapy of STEC-HUS during the 2011 outbreak in Germany where no beneficial short-term effects were observed (Kielstein *et al.* 2012). However, the authors stated that due to the crisis situation, the study could not be designed as a randomized control trial and the time-point of eculizumab application might not have been ideal for positive treatment effects (Kielstein *et al.* 2012). At the same time, France also experienced a smaller outbreak of HUS with 9 patients who were treated with eculizumab early after diagnosis (0-4 days) (Delmas *et al.* 2014). Of note, all patients recovered rapidly (Delmas *et al.* 2014). In the following

years, eculizumab was applied to pediatric HUS patients with severe neurological involvement (Pape *et al.* 2015, Percheron *et al.* 2018). Pape *et al.* highlighted again that late treatment once symptoms were established was less efficient (Pape *et al.* 2015) while the multicenter retrospective study by Percheron *et al.* found that eculizumab was favourable especially in those patients whose complement system was persistently deregulated (Percheron *et al.* 2018). In 2015, another outbreak of HUS occurred associated with a live-stock market in Istanbul (Agbas *et al.* 2018). Of the 22 pediatric patients, 9 were treated with eculizumab, however, at a follow-up no differences in outcome between those patients and those receiving best standard care were observable (Agbas *et al.* 2018). Monet-Didailler *et al.* performed a single-center matched cohort study in pediatric HUS patients without finding differences between eculizumab-treated and control patients at the 1-month and 12-month follow-up (Monet-Didailler *et al.* 2020). The authors did observe trends towards better long-term outcomes in the eculizumab-treated patients at their last follow-up, however none of these trends were significant (Monet-Didailler *et al.* 2020). Overall, these studies indicate that some HUS patients might profit from eculizumab treatment, however, a randomized control trial is clearly warranted in order to identify in which extent and how these patients are characterized.

Preclinical studies focusing on interference with one pathway of tissue-damage in HUS pathogenesis often suffer from the problem that pre-treatment of the animals before HUS induction usually is remarkably successful, but once the treatment is performed after the induction of HUS, the positive effects are abolished. For example, this was observed in a study by Gomez *et al.*, where pre-treatment with anti-oxidants reduced platelet activation, renal damage and increased survival in mice challenged with Stx2 (Gomez *et al.* 2013). Unfortunately, once the anti-oxidants were applied as a post-treatment, the survival benefits were abolished (Gomez *et al.* 2013).

The potential advantage of EPO and pHBSP as therapeutics lies in the fact that instead of affecting only one pathway in the multifactorial pathogenesis of HUS, they mediate tissue-protection via a variety of different signaling pathways resulting in anti-apoptotic, proliferative, anti-inflammatory, anti-fibrotic and anti-oxidative effects of the two compounds. The anti-oxidative and anti-nitrosative effects observed in this thesis led to an increase in survival although the treatment was started after the induction of HUS.

4.2.2 Renoprotective and anti-inflammatory potential of EPO and pHBSP in other conditions

In preclinical trials, EPO had shown renoprotective effects in a variety of diseases in different species. For example, EPO treatment attenuates septic AKI in mice (Coldewey *et al.* 2013), ischemia/reperfusion injury to murine kidneys (Kwak *et al.* 2020), hyperglycaemia-induced AKI in rats (Guan *et al.* 2020) and post resuscitation AKI in piglets (Pantazopoulos *et al.* 2016). However, when looking into clinical trials, the renoprotective properties of EPO appear to be less outstanding: A meta-analysis performed on clinical trials testing the renoprotective effects of erythropoiesis-stimulating agents in patients with kidney conditions including AKI, kidney transplantation and chronic kidney disease (CKD) showed that outcome was improved in a few trials, although overall no significant renoprotection was observed (Elliott *et al.* 2017). In contrast, meta-analysis of 9 randomized clinical trials using EPO for correction of anemia in CKD reported a significantly elevated risk of all-cause mortality (Phrommintikul *et al.* 2007) indicating that careful hemodynamic management is crucial when EPO is administered to HUS patients. Furthermore, it must be kept in mind that in these studies, EPO and ESAs were dosed primarily to induce erythropoiesis and correct anemia. Due to the differences in concentration dependency of EPO-R and IRR, other dosage regimens will be prerequisite to truly evaluate the renoprotective potential of EPO in any given disease.

As pHBSP has not yet been officially approved as a drug and clinical phase II trials were performed with a focus on neuropathy (Culver *et al.* 2017), only preclinical data on renoprotection can be reviewed. Rats undergoing 30 min of ischemia followed by 48 hours of reperfusion could be protected from acute kidney injury by intraperitoneal application of pHBSP 6 hours into reperfusion (Patel *et al.* 2012). Another study on ischemia/reperfusion injury in rats found that early application of pHBSP (1 hour into reperfusion) was more effective in the prevention of AKI than late application (4 hours into reperfusion) (van Rijt *et al.* 2013). Furthermore, pHBSP was also able to reduce early allograft injury in a rat model of renal allograft by reducing macrophage invasion and NF-κB activation (Guan *et al.* 2020).

Altogether, the promising preclinical effects of both compounds are well in line with the positive effects of EPO and pHBSP on the outcome of mice with HUS observed in this thesis, even though there was no direct nephroprotection.

4.2.3 Clinical aspects of anemia in HUS and its treatment

The progression of STEC infections to HUS is often rapid and associated with the development of profound anemia and clinical deterioration in under 24 hours (Bitzan 2009). Pathophysiologically, MAHA is caused by the shredding of erythrocytes passing thrombi and fibrin meshes in the microcirculation. MAHA associated with HUS is usually severe which is underlined by hemoglobin (Hb) levels under 10 mg/dl in over 90% of patients (Mele *et al.* 2014). In parallel, lactate dehydrogenase (LDH) is usually increased (>460 U/l) (Mele *et al.* 2014). Intravascular hemolysis is further indicated by hyperbilirubinemia and low or even undetectable haptoglobin (Mele *et al.* 2014). In the peripheral blood smear, an increase of reticulocytes and shistocytes is observed (Mele *et al.* 2014). Once the Hb drops under 7 mg/dl, red blood cell (RBC) transfusions are initiated (Bitzan 2009). A vast majority of 93% of pediatric and up to 80% of adult HUS patients requires RBC transfusion while hospitalized (Joseph *et al.* 2018, Mody *et al.* 2015). However, even though RBC transfusions are the mainstay of the treatment of HUS-associated MAHA, they are not free of risks. In contrary, they can even induce or aggravate AKI via several pathomechanisms, a phenomenon well-described in the context of cardiac surgery (Merchant *et al.* 2019). The main risk factor identified in AKI after cardiac surgery was hemolysis induced by shear stress during passage of the extracorporeal circuit (Steiner *et al.* 2015), as thereby the concentration of free Hb and pro-inflammatory cytokines is increased (Bennett-Guerrero *et al.* 2007). Similar effects might occur in the renal microcirculation of HUS patients which is constricted by microthrombi. These potentially dangerous effects might be mitigated when instead of transfusing a large number of RBCs relatively fast the physiological production of RBCs is enhanced by treatment with recombinant EPO. Treatment with EPO is routinely performed in anemia associated with chemotherapy against cancer, zidovidune treatment against HIV-infection and CKD as well as to reduce the need for RBC transfusions in major surgery (FDA Reference ID: 4160848; EMEA/H/C/000726). Surprisingly, EPO therapy is not approved for HUS-associated anemia and although off-label use comprises up to 50% of all EPO prescriptions (Guan *et al.* 2020), there is only the national German medical guideline for the treatment of childhood HUS that mentions the possibility to apply EPO for anemia treatment (Leitlinienprogramm Pädiatrie (Gesellschaft für Pädiatrische Nephrologie e.V. (GPN) 2022). Furthermore, the recommendation remains vague, simply stating that “EPO can be considered” without a clarification in which cases and which dosage and without citation of relevant

literature (Leitlinienprogramm Pädiatrie (Gesellschaft für Pädiatrische Nephrologie e.V. (GPN) 2022).

The reason for the hesitancy towards EPO treatment in HUS most probably lies in the fact that evidence from the literature is sparse and controversial. There are two case reports from the mid-90s to early 2000s, where EPO was successfully applied to manage anemia in the context of secondary, mitomycin C-induced HUS (Catalano *et al.* 2002, O'Brien *et al.* 1994). In STEC-HUS, a pilot trial performed by Pape and colleagues reported a reduced need for RBC transfusions in children treated with EPO (Pape *et al.* 2009). Contrasting to this pilot trial, a larger case-control study by Balestracci *et al.* found no differences in the need for RBC transfusions in children treated with or without EPO (Balestracci *et al.* 2015). However, the results of both trials are difficult to compare as they were using different EPO dosages and in case of the Pape trial, RBC transfusions were performed when Hb was ≤ 5, while in the other study transfusions were already started at an Hb ≤ 7 (Balestracci *et al.* 2015, Pape *et al.* 2009). Next to these conflicting studies, there is a case report from Korea, where a Jehova's witness child received EPO instead of RBC transfusion resulting not only in the attenuation of anemia but also in kidney function improvement (Woo da *et al.* 2016). A pilot randomized controlled trial comparing standard care (RBC transfusion when Hb ≤ 7 mg/dl) with EPO (50 IU/kg BW three times a week) recruiting 12 patients per arm could not find beneficial effects of EPO regarding the need of RBCs, however, the authors stated themselves that a larger patient cohort would be needed to verify these results (Balestracci *et al.* 2022). Until then, the results generated in this thesis hopefully might encourage the off-label use of EPO in the treatment of MAHA in HUS.

4.3 Limitations

Although it could be demonstrated in this thesis that repeated intravenous injections of Stx are sufficient to induce experimental HUS in mice covering most of the symptoms occurring in patients, the effects of EPO and pHBSP treatment should also be studied in an animal model using EHEC infection. This is especially interesting in the light of a recent study demonstrating that EPO has not only tissue-protective effects but also promotes macrophage-mediated phagocytosis and killing of *E. coli* and *Staphylococcus aureus* and thereby accelerates resolution of infection (Liang *et al.* 2021).

This thesis can only provide the preclinical groundwork for further studies assessing the therapeutic potential of EPO and pHBSP and does not replace controlled randomized trials in the clinical setting. However, in a situation where clinical evidence is low and conflicting, the results provided in this thesis can support the clinical decision for anemia treatment with EPO. The results regarding the improvement in survival and the reduction of oxidative stress provided here are indeed very promising, however, preclinical studies often suffer from a poor translational potential. A randomized clinical control trial will be needed to truly assess the value of the findings in this thesis for HUS patients. Due to the sporadic nature of the disease, such trials are hard to perform, however, the promising results presented here as well as the fact that due to the orphan disease status drug approval for pHBSP would be alleviated might provide motivation to perform such studies against the odds.

4.4 Outlook

The murine models established and characterized in this thesis will allow the examination of further therapeutic strategies and underlying pathomechanisms of HUS. For instance, the subacute model of HUS has already been implemented to study the role of the canonical and non-canonical NF-κB signaling pathways (Sobbe *et al.* 2020) or heme and heme degradation products (Pirschel *et al.* 2022) in this disease.

pHBSP treatment significantly improved survival of mice with experimental HUS by attenuating oxidative and nitrosative stress in the kidneys, protecting tubular epithelial barriers and partially reducing the expression of KIM-1. These positive effects alone would already warrant further examination of pHBSP as a potential therapeutic and efforts to translate the experimental results into the clinics. However, as it has already been demonstrated in a transplantation study performed in pigs, pHBSP also has beneficial effects in the prevention of post-transplantation fibrosis (van Rijt *et al.* 2013). About one third of HUS survivors suffer from long-term sequelae such as high blood pressure and chronic kidney disease (Garg *et al.* 2003, Rosales *et al.* 2012, Vaterodt *et al.* 2018). As fibrotic processes play a major role in the transition of AKI to CKD, pHBSP might not only able to mitigate disease progression and improve survival in the acute phase of the disease but also in the prevention and treatment of severe long-term sequelae. The same might hold true for EPO treatment in HUS, as many studies have shown beneficial effects of EPO on renal fibrosis both *in vitro* and *in vivo* (Bai *et al.* 2017, Chen *et al.* 2010, Geng *et al.* 2015). However, the treatment regimen must

be carefully adjusted, as Shi *et al.* demonstrated recently that excess EPO signaling worsens tubulointerstitial fibrosis in the acute stage of AKI (Shi *et al.* 2018).

Although the use of antibiotics in the treatment of HUS is still controversial, EPO might offer some new perspectives as it has been shown that a combinational therapy of EPO with ciprofloxacin improves clearance of *E. coli* in a murine model of self-limited peritonitis (Liang *et al.* 2021). Ciprofloxacin appears to increase the release of Stx from *E. coli* and is thereby detrimental in the therapy of STEC-HUS (McGannon *et al.* 2010), however, the combination of this or more safe antibiotics with EPO might improve their therapeutic efficacy in the future. As these positive effects of EPO on antibiosis and microbial clearance might be mediated via the IRR, it appears of great interest to assess if pHBSP might have similar beneficial effects.

4.5 Conclusion

In conclusion, this thesis provides the scientific community with two distinct preclinical murine models of HUS that were characterized in great detail and established to serve the need for clinically relevant animal models. For the first time, volume replacement therapy was applied in a murine model of HUS and a scoring system was proposed that is easily applicable in every laboratory. Furthermore, the proposed models of HUS were already applied in this thesis to perform an interventional preclinical study assessing the therapeutic potential of EPO and its non-hematopoietic peptide analog pHBSP. Hereby, the groundwork for the consideration of EPO and pHBSP in the therapy in HUS has been laid out. Both compounds have distinct benefits, while the positive effects of pHBSP on HUS outcome and oxidative stress response were more pronounced, EPO might not only improve renal oxidative stress but also attenuate MAHA at the same time. The promising results of this thesis prompt for the performance of further preclinical and clinical trials to eventually pave the way for the two compounds from bench to bedside.

5. References

Agapidou A, Vakalopoulou S, Papadopoulou T, Chadjiaggelidou C, Garypidou V. 2014. Successful Treatment of Severe Anemia using Erythropoietin in a Jehovah Witness with Non-Hodgkin Lymphoma. Hematol Rep, 6 (4):5600.

Agbas A, Goknar N, Akinci N, Yildirim ZY, Tasdemir M, Benzer M, Gokce I, Candan C, Kucuk N, Uzuner S, Ozcelik G, Demirkol D, Sever L, Caliskan S. 2018. Outbreak of Shiga toxin-producing *Escherichia-coli*-associated hemolytic uremic syndrome in Istanbul in 2015: outcome and experience with eculizumab. Pediatr Nephrol, 33 (12):2371-2381.

Ahmet I, Tae HJ, Juhaszova M, Riordon DR, Boheler KR, Sollott SJ, Brines M, Cerami A, Lakatta EG, Talan MI. 2011. A small nonerythropoietic helix B surface peptide based upon erythropoietin structure is cardioprotective against ischemic myocardial damage. Mol Med, 17 (3-4):194-200.

Aldick T, Bielaszewska M, Zhang W, Brockmeyer J, Schmidt H, Friedrich AW, Kim KS, Schmidt MA, Karch H. 2007. Hemolysin from Shiga toxin-negative Escherichia coli O26 strains injures microvascular endothelium. Microbes Infect, 9 (3):282-290.

Allegra A, Buemi M, Corica F, Aloisi C, Frisina N. 1999. Erythropoietin administration induces an increase of serum levels of soluble E-selectin and soluble intercellular adhesion molecule 1. Nephron, 82 (4):361-362.

Amran MY, Fujii J, Kolling GL, Villanueva SY, Kainuma M, Kobayashi H, Kameyama H, Yoshida S. 2013. Proposal for effective treatment of Shiga toxin-producing Escherichia coli infection in mice. Microb Pathog, 65:57-62.

Anagnostou A, Lee ES, Kessimian N, Levinson R, Steiner M. 1990. Erythropoietin has a mitogenic and positive chemotactic effect on endothelial cells. Proc Natl Acad Sci U S A, 87 (15):5978-5982.

Armstrong GD, Rowe PC, Goodyer P, Orrbine E, Klassen TP, Wells G, MacKenzie A, Lior H, Blanchard C, Auclair F, et al. 1995. A phase I study of chemically synthesized verotoxin (Shiga-like toxin) Pk-trisaccharide receptors attached to chromosorb for preventing hemolytic-uremic syndrome. J Infect Dis, 171 (4):1042-1045.

Aslam R, Speck ER, Kim M, Crow AR, Bang KW, Nestel FP, Ni H, Lazarus AH, Freedman J, Semple JW. 2006. Platelet Toll-like receptor expression modulates lipopolysaccharide-induced thrombocytopenia and tumor necrosis factor-alpha production in vivo. Blood, 107 (2):637-641.

Bai J, Xiao X, Zhang X, Cui H, Hao J, Han J, Cao N. 2017. Erythropoietin Inhibits Hypoxia-Induced Epithelial-To-Mesenchymal Transition via Upregulation of miR-200b in HK-2 Cells. Cell Physiol Biochem, 42 (1):269-280.

Balestracci A, Martin SM, Toledo I, Alvarado C, Wainsztein RE. 2015. Early erythropoietin in post-diarrheal hemolytic uremic syndrome: a case-control study. Pediatr Nephrol, 30 (2):339-344.

Balestracci A, Capone MA, Meni Battaglia L, Toledo I, Martin SM, Beaudoin L, Balbaryski J, Gomez L. 2022. Erythropoietin in children with hemolytic uremic syndrome: a pilot randomized controlled trial. Pediatr Nephrol, 37 (10):2383-2392.

Bauer A, Loos S, Wehrmann C, Horstmann D, Donnerstag F, Lemke J, Hillebrand G, Lobel U, Pape L, Haffner D, Bindt C, Ahlenstiel T, Melk A, Lehnhardt A, Kemper MJ, Oh J, Hartmann H. 2014. Neurological involvement in children with *E. coli*

O104:H4-induced hemolytic uremic syndrome. Pediatr Nephrol, 29 (9):1607-1615.

Bauwens A, Bielaszewska M, Kemper B, Langehanenberg P, von Bally G, Reichelt R, Mulac D, Humpf HU, Friedrich AW, Kim KS, Karch H, Muthing J. 2011. Differential cytotoxic actions of Shiga toxin 1 and Shiga toxin 2 on microvascular and macrovascular endothelial cells. Thromb Haemost, 105 (3):515-528.

Bazan JF. 1990. Structural design and molecular evolution of a cytokine receptor superfamily. Proc Natl Acad Sci U S A, 87 (18):6934-6938.

Bennett-Guerrero E, Veldman TH, Doctor A, Telen MJ, Ortel TL, Reid TS, Mulherin MA, Zhu H, Buck RD, Califf RM, McMahon TJ. 2007. Evolution of adverse changes in stored RBCs. Proc Natl Acad Sci U S A, 104 (43):17063-17068.

Bielaszewska M, Sinha B, Kuczius T, Karch H. 2005. Cytolethal distending toxin from Shiga toxin-producing *Escherichia coli* O157 causes irreversible G2/M arrest, inhibition of proliferation, and death of human endothelial cells. Infect Immun, 73 (1):552-562.

Bielaszewska M, Bauwens A, Greune L, Kemper B, Dobrindt U, Geelen JM, Kim KS, Schmidt MA, Karch H. 2009. Vacuolisation of human microvascular endothelial cells by enterohaemorrhagic *Escherichia coli*. Thromb Haemost, 102 (6):1080-1092.

Bilenker JH, Demers R, Porter DL, Wasserstein AG, Peters E, Manaker S. 2002. Recombinant human erythropoietin usage in a large academic medical center. Am J Manag Care, 8 (8):742-747.

Bitzan M. 2009. Treatment options for HUS secondary to *Escherichia coli* O157:H7. Kidney Int Suppl, (112):S62-66.

Boerlin P, McEwen SA, Boerlin-Petzold F, Wilson JB, Johnson RP, Gyles CL. 1999. Associations between virulence factors of Shiga toxin-producing Escherichia coli and disease in humans. J Clin Microbiol, 37 (3):497-503.

Boesch S, Nachbauer W, Mariotti C, Sacca F, Filla A, Klockgether T, Klopstock T, Schols L, Jacobi H, Buchner B, vom Hagen JM, Nanetti L, Manicom K. 2014. Safety and tolerability of carbamylated erythropoietin in Friedreich's ataxia. Mov Disord, 29 (7):935-939.

Brigotti M, Caprioli A, Tozzi AE, Tazzari PL, Ricci F, Conte R, Carnicelli D, Procaccino MA, Minelli F, Ferretti AV, Paglialonga F, Edefonti A, Rizzoni G. 2006. Shiga toxins present in the gut and in the polymorphonuclear leukocytes circulating in the blood of children with hemolytic-uremic syndrome. J Clin Microbiol, 44 (2):313-317.

Brines M, Cerami A. 2012. The receptor that tames the innate immune response. Mol Med, 18:486-496.

Brines M, Dunne AN, van Velzen M, Proto PL, Ostenson CG, Kirk RI, Petropoulos IN, Javed S, Malik RA, Cerami A, Dahan A. 2015. ARA 290, a nonerythropoietic peptide engineered from erythropoietin, improves metabolic control and neuropathic symptoms in patients with type 2 diabetes. Mol Med, 20:658-666.

Brines M, Grasso G, Fiordaliso F, Sfacteria A, Ghezzi P, Fratelli M, Latini R, Xie QW, Smart J, Su-Rick CJ, Pobre E, Diaz D, Gomez D, Hand C, Coleman T, Cerami A. 2004. Erythropoietin mediates tissue protection through an erythropoietin and common beta-subunit heteroreceptor. Proc Natl Acad Sci U S A, 101 (41):14907-14912.

Brines M, Patel NS, Villa P, Brines C, Mennini T, De Paola M, Erbayraktar Z, Erbayraktar S, Sepodes B, Thiemermann C, Ghezzi P, Yamin M, Hand CC, Xie QW, Coleman T, Cerami A. 2008. Nonerythropoietic, tissue-protective peptides

derived from the tertiary structure of erythropoietin. Proc Natl Acad Sci U S A, 105 (31):10925-10930.

Byrne L, Jenkins C, Launders N, Elson R, Adak GK. 2015. The epidemiology, microbiology and clinical impact of Shiga toxin-producing Escherichia coli in England, 2009-2012. Epidemiol Infect, 143 (16):3475-3487.

Carr PD, Gustin SE, Church AP, Murphy JM, Ford SC, Mann DA, Woltring DM, Walker I, Ollis DL, Young IG. 2001. Structure of the complete extracellular domain of the common beta subunit of the human GM-CSF, IL-3, and IL-5 receptors reveals a novel dimer configuration. Cell, 104 (2):291-300.

Catalano C, Gianesini C, Fabbian F. 2002. Erythropoietin is beneficial in mitomycin-induced hemolytic-uremic syndrome. Nephron, 91 (2):324-326.

Chen CL, Chou KJ, Lee PT, Chen YS, Chang TY, Hsu CY, Huang WC, Chung HM, Fang HC. 2010. Erythropoietin suppresses epithelial to mesenchymal transition and intercepts Smad signal transduction through a MEK-dependent mechanism in pig kidney (LLC-PK1) cell lines. Exp Cell Res, 316 (7):1109-1118.

Chiurchiu C, Firrincieli A, Santostefano M, Fusaroli M, Remuzzi G, Ruggenenti P. 2003. Adult nondiarrhea hemolytic uremic syndrome associated with Shiga toxin *Escherichia coli* O157:H7 bacteremia and urinary tract infection. Am J Kidney Dis, 41 (1):e4 1 - e4 4.

Chong Y, Fitzhenry R, Heuschkel R, Torrente F, Frankel G, Phillips AD. 2007. Human intestinal tissue tropism in *Escherichia coli* O157 : H7--initial colonization of terminal ileum and Peyer's patches and minimal colonic adhesion *ex vivo*. Microbiology, 153 (Pt 3):794-802.

Clackson T, Wells JA. 1995. A hot spot of binding energy in a hormone-receptor interface. Science, 267 (5196):383-386.

Coldewey SM, Hartmann M, Schmidt DS, Engelking U, Ukena SN, Gunzer F. 2007. Impact of the *rpoS* genotype for acid resistance patterns of pathogenic and probiotic *Escherichia coli*. BMC Microbiol, 7:21.

Coldewey SM, Khan AI, Kapoor A, Collino M, Rogazzo M, Brines M, Cerami A, Hall P, Sheaff M, Kieswich JE, Yaqoob MM, Patel NS, Thiemermann C. 2013. Erythropoietin attenuates acute kidney dysfunction in murine experimental sepsis by activation of the beta-common receptor. Kidney Int, 84 (3):482-490.

Coleman TR, Westenfelder C, Togel FE, Yang Y, Hu Z, Swenson L, Leuvenink HG, Ploeg RJ, d'Uscio LV, Katusic ZS, Ghezzi P, Zanetti A, Kaushansky K, Fox NE, Cerami A, Brines M. 2006. Cytoprotective doses of erythropoietin or carbamylated erythropoietin have markedly different procoagulant and vasoactive activities. Proc Natl Acad Sci U S A, 103 (15):5965-5970.

Constantinescu AR, Bitzan M, Weiss LS, Christen E, Kaplan BS, Cnaan A, Trachtman H. 2004. Non-enteropathic hemolytic uremic syndrome: causes and short-term course. Am J Kidney Dis, 43 (6):976-982.

Culver DA, Dahan A, Bajorunas D, Jeziorska M, van Velzen M, Aarts L, Tavee J, Tannemaat MR, Dunne AN, Kirk RI, Petropoulos IN, Cerami A, Malik RA, Brines M. 2017. Cibinetide Improves Corneal Nerve Fiber Abundance in Patients With Sarcoidosis-Associated Small Nerve Fiber Loss and Neuropathic Pain. Invest Ophthalmol Vis Sci, 58 (6):BIO52-BIO60.

Cummings KC, Mohle-Boetani JC, Werner SB, Vugia DJ. 2002. Population-based trends in pediatric hemolytic uremic syndrome in California, 1994-1999: substantial underreporting and public health implications. Am J Epidemiol, 155 (10):941-948.

Davies M, Barrett AJ, Travis J, Sanders E, Coles GA. 1978. The degradation of human glomerular basement membrane with purified lysosomal proteinases: evidence

for the pathogenic role of the polymorphonuclear leucocyte in glomerulonephritis. Clin Sci Mol Med, 54 (3):233-240.

Delmas Y, Vendrely B, Clouzeau B, Bachir H, Bui HN, Lacraz A, Helou S, Bordes C, Reffet A, Llanas B, Skopinski S, Rolland P, Gruson D, Combe C. 2014. Outbreak of Escherichia coli O104:H4 haemolytic uraemic syndrome in France: outcome with eculizumab. Nephrol Dial Transplant, 29 (3):565-572.

Dennhardt S, Pirschel W, Wissuwa B, Daniel C, Gunzer F, Lindig S, Medyukhina A, Kiehntopf M, Rudolph WW, Zipfel PF, Gunzer M, Figge MT, Amann K, Coldewey SM. 2018. Modeling Hemolytic-Uremic Syndrome: In-Depth Characterization of Distinct Murine Models Reflecting Different Features of Human Disease. Front Immunol, 9:1459.

Dundas S, Todd WT, Stewart AI, Murdoch PS, Chaudhuri AK, Hutchinson SJ. 2001. The central Scotland *Escherichia coli* O157:H7 outbreak: risk factors for the hemolytic uremic syndrome and death among hospitalized patients. Clin Infect Dis, 33 (7):923-931.

EFSA E. 2021. The European Union One Health 2020 Zoonoses Report. 6971. EFSA Journal.

Elliott S, Tomita D, Endre Z. 2017. Erythropoiesis stimulating agents and reno-protection: a meta-analysis. BMC Nephrol, 18 (1):14.

Endo Y, Mitsui K, Motizuki M, Tsurugi K. 1987. The mechanism of action of ricin and related toxic lectins on eukaryotic ribosomes. The site and the characteristics of the modification in 28 S ribosomal RNA caused by the toxins. J Biol Chem, 262 (12):5908-5912.

Exeni R, Donato H, Rendo P, Antonuccio M, Rapetti MC, Grimoldi I, Exeni A, de Galvagni A, Trepacka E, Amore A. 1998. Low levels of serum erythropoietin in children with endemic hemolytic uremic syndrome. Pediatr Nephrol, 12 (3):226-230.

Exeni RA, Fernandez-Brando RJ, Santiago AP, Fiorentino GA, Exeni AM, Ramos MV, Palermo MS. 2018. Pathogenic role of inflammatory response during Shiga toxin-associated hemolytic uremic syndrome (HUS). Pediatr Nephrol, 33 (11):2057-2071.

Fernandez GC, Te Loo MW, van der Velden TJ, van der Heuvel LP, Palermo MS, Monnens LL. 2003. Decrease of thrombomodulin contributes to the procoagulant state of endothelium in hemolytic uremic syndrome. Pediatr Nephrol, 18 (10):1066-1068.

Fernandez GC, Lopez MF, Gomez SA, Ramos MV, Bentancor LV, Fernandez-Brando RJ, Landoni VI, Dran GI, Meiss R, Isturiz MA, Palermo MS. 2006. Relevance of neutrophils in the murine model of haemolytic uraemic syndrome: mechanisms involved in Shiga toxin type 2-induced neutrophilia. Clin Exp Immunol, 146 (1):76-84.

Fernandez GC, Gomez SA, Ramos MV, Bentancor LV, Fernandez-Brando RJ, Landoni VI, Lopez L, Ramirez F, Diaz M, Alduncin M, Grimoldi I, Exeni R, Isturiz MA, Palermo MS. 2007. The functional state of neutrophils correlates with the severity of renal dysfunction in children with hemolytic uremic syndrome. Pediatr Res, 61 (1):123-128.

Fitzpatrick MM, Shah V, Filler G, Dillon MJ, Barratt TM. 1992. Neutrophil activation in the haemolytic uraemic syndrome: free and complexed elastase in plasma. Pediatr Nephrol, 6 (1):50-53.

Fong JS, King-Hrycaj BD. 1983. Impaired and exhausted platelets in modified generalized Shwartzman reaction: an analogue of hemolytic uremic syndrome associated with endotoxemia. J Lab Clin Med, 102 (6):847-857.

Forsyth KD, Simpson AC, Fitzpatrick MM, Barratt TM, Levinsky RJ. 1989. Neutrophil-mediated endothelial injury in haemolytic uraemic syndrome. Lancet, 2 (8660):411-414.

Frank C, Werber D, Cramer JP, Askar M, Faber M, an der Heiden M, Bernard H, Fruth A, Prager R, Spode A, Wadl M, Zoufaly A, Jordan S, Kemper MJ, Follin P, Muller L, King LA, Rosner B, Buchholz U, Stark K, Krause G, Team HUSI. 2011. Epidemic profile of Shiga-toxin-producing Escherichia coli O104:H4 outbreak in Germany. N Engl J Med, 365 (19):1771-1780.

Garcia A, Marini RP, Catalfamo JL, Knox KA, Schauer DB, Rogers AB, Fox JG. 2008. Intravenous Shiga toxin 2 promotes enteritis and renal injury characterized by polymorphonuclear leukocyte infiltration and thrombosis in Dutch Belted rabbits. Microbes Infect, 10 (6):650-656.

Garcia A, Marini RP, Feng Y, Vitsky A, Knox KA, Taylor NS, Schauer DB, Fox JG. 2002. A naturally occurring rabbit model of enterohemorrhagic *Escherichia coli*-induced disease. J Infect Dis, 186 (11):1682-1686.

Garcia A, Bosques CJ, Wishnok JS, Feng Y, Karalius BJ, Butterton JR, Schauer DB, Rogers AB, Fox JG. 2006. Renal injury is a consistent finding in Dutch Belted rabbits experimentally infected with enterohemorrhagic *Escherichia coli*. J Infect Dis, 193 (8):1125-1134.

Garg AX, Suri RS, Barrowman N, Rehman F, Matsell D, Rosas-Arellano MP, Salvadori M, Haynes RB, Clark WF. 2003. Long-term renal prognosis of diarrhea-associated hemolytic uremic syndrome: a systematic review, meta-analysis, and meta-regression. JAMA, 290 (10):1360-1370.

Gasser C, Gautier E, Steck A, Siebenmann RE, Oechslin R. 1955. [Hemolytic-uremic syndrome: bilateral necrosis of the renal cortex in acute acquired hemolytic anemia]. Schweiz Med Wochenschr, 85 (38-39):905-909.

Geng XC, Hu ZP, Lian GY. 2015. Erythropoietin ameliorates renal interstitial fibrosis via the inhibition of fibrocyte accumulation. Mol Med Rep, 11 (5):3860-3865.

Gerber A, Karch H, Allerberger F, Verweyen HM, Zimmerhackl LB. 2002. Clinical course and the role of shiga toxin-producing *Escherichia coli* infection in the hemolytic-uremic syndrome in pediatric patients, 1997-2000, in Germany and Austria: a prospective study. J Infect Dis, 186 (4):493-500.

Gomez SA, Abrey-Recalde MJ, Panek CA, Ferrarotti NF, Repetto MG, Mejias MP, Fernandez GC, Vanzulli S, Isturiz MA, Palermo MS. 2013. The oxidative stress induced *in vivo* by Shiga toxin-2 contributes to the pathogenicity of haemolytic uraemic syndrome. Clin Exp Immunol, 173 (3):463-472.

Goode B, O'Reilly C, Dunn J, Fullerton K, Smith S, Ghneim G, Keen J, Durso L, Davies M, Montgomery S. 2009. Outbreak of *escherichia coli* O157: H7 infections after Petting Zoo visits, North Carolina State Fair, October-November 2004. Arch Pediatr Adolesc Med, 163 (1):42-48.

Guan XZ, Wang LL, Pan X, Liu L, Sun XL, Zhang XJ, Wang DQ, Yu Y. 2020. Clinical Indications of Recombinant Human Erythropoietin in a Single Center: A 10-Year Retrospective Study. Front Pharmacol, 11:1110.

Gunzer F, Hennig-Pauka I, Waldmann KH, Sandhoff R, Grone HJ, Kreipe HH, Matussek A, Mengel M. 2002. Gnotobiotic piglets develop thrombotic microangiopathy after oral infection with enterohemorrhagic *Escherichia coli*. Am J Clin Pathol, 118 (3):364-375.

Heinisch BB, Vcelar B, Kapiotis S, Blann A, Wolzt M, Siller-Matula JM, Jilma B. 2012. The effect of erythropoietin on platelet and endothelial activation markers: a prospective trial in healthy volunteers. Platelets, 23 (5):352-358.

Hilton DJ, Watowich SS, Katz L, Lodish HF. 1996. Saturation mutagenesis of the WSXWS motif of the erythropoietin receptor. J Biol Chem, 271 (9):4699-4708.

Hudson JQ, Sameri RM. 2002. Darbepoetin alfa, a new therapy for the management of anemia of chronic kidney disease. Pharmacotherapy, 22 (9 Pt 2):141S-149S.

Hurley BP, Thorpe CM, Acheson DW. 2001. Shiga toxin translocation across intestinal epithelial cells is enhanced by neutrophil transmigration. Infect Immun, 69 (10):6148-6155.

Ikeda M, Ito S, Honda M. 2004. Hemolytic uremic syndrome induced by lipopolysaccharide and Shiga-like toxin. Pediatr Nephrol, 19 (5):485-489.

Inward CD, Howie AJ, Fitzpatrick MM, Rafaat F, Milford DV, Taylor CM. 1997. Renal histopathology in fatal cases of diarrhoea-associated haemolytic uraemic syndrome. British Association for Paediatric Nephrology. Pediatr Nephrol, 11 (5):556-559.

Ishikawa N, Kamitsuji H, Murakami T, Nakayama A, Umeki Y. 2000. Plasma levels of granulocyte elastase-alpha1-proteinase inhibitor complex in children with hemolytic uremic syndrome caused by verotoxin-producing *Escherichia coli*. Pediatr Int, 42 (6):637-641.

Isogai E, Isogai H, Kimura K, Hayashi S, Kubota T, Fujii N, Takeshi K. 1998. Role of tumor necrosis factor alpha in gnotobiotic mice infected with an *Escherichia coli* O157:H7 strain. Infect Immun, 66 (1):197-202.

Jacewicz MS, Acheson DW, Mobassaleh M, Donohue-Rolfe A, Balasubramanian KA, Keusch GT. 1995. Maturational regulation of globotriaosylceramide, the Shiga-like toxin 1 receptor, in cultured human gut epithelial cells. J Clin Invest, 96 (3):1328-1335.

Jafari E, Oloomi M, Bouzari S. 2021. Characterization of antimicrobial susceptibility, extended-spectrum beta-lactamase genes and phylogenetic groups of Shigatoxin producing *Escherichia coli* isolated from patients with diarrhea in Iran. Ann Clin Microbiol Antimicrob, 20 (1):24.

Jelkmann W. 1998. Proinflammatory cytokines lowering erythropoietin production. J Interferon Cytokine Res, 18 (8):555-559.

Jelkmann W. 2004. Molecular biology of erythropoietin. Intern Med, 43 (8):649-659.

Jenssen GR, Hovland E, Bjerre A, Bangstad HJ, Nygard K, Vold L. 2014. Incidence and etiology of hemolytic-uremic syndrome in children in Norway, 1999-2008--a retrospective study of hospital records to assess the sensitivity of surveillance. BMC Infect Dis, 14:265.

Jerse AE, Gicquelais KG, Kaper JB. 1991. Plasmid and chromosomal elements involved in the pathogenesis of attaching and effacing *Escherichia coli*. Infect Immun, 59 (11):3869-3875.

Joseph A, Rafat C, Zafrani L, Mariani-Kurkdjian P, Veyradier A, Hertig A, Rondeau E, Mariotte E, Azoulay E. 2018. Early Differentiation of Shiga Toxin-Associated Hemolytic Uremic Syndrome in Critically Ill Adults With Thrombotic Microangiopathy Syndromes. Crit Care Med, 46 (9):e904-e911.

Kakoullis L, Papachristodoulou E, Chra P, Panos G. 2019. Shiga toxin-induced haemolytic uraemic syndrome and the role of antibiotics: a global overview. J Infect, 79 (2):75-94.

Karmali MA, Steele BT, Petric M, Lim C. 1983. Sporadic cases of haemolytic-uraemic syndrome associated with faecal cytotoxin and cytotoxin-producing *Escherichia coli* in stools. Lancet, 1 (8325):619-620.

Karmali MA, Petric M, Lim C, Fleming PC, Arbus GS, Lior H. 1985. The association between idiopathic hemolytic uremic syndrome and infection by verotoxin-producing *Escherichia coli*. J Infect Dis, 151 (5):775-782.

Keepers TR, Psotka MA, Gross LK, Obrig TG. 2006. A murine model of HUS: Shiga toxin with lipopolysaccharide mimics the renal damage and physiologic response of human disease. J Am Soc Nephrol, 17 (12):3404-3414.

Kielstein JT, Beutel G, Fleig S, Steinhoff J, Meyer TN, Hafer C, Kuhlmann U, Bramstedt J, Panzer U, Vischedyk M, Busch V, Ries W, Mitzner S, Mees S, Stracke S, Nurnberger J, Gerke P, Wiesner M, Sucke B, Abu-Tair M, Kribben A, Klause N, Schindler R, Merkel F, Schnatter S, Dorresteijn EM, Samuelsson O, Brunkhorst R, Collaborators of the DS-HUSr. 2012. Best supportive care and therapeutic plasma exchange with or without eculizumab in Shiga-toxin-producing E. coli O104:H4 induced haemolytic-uraemic syndrome: an analysis of the German STEC-HUS registry. Nephrol Dial Transplant, 27 (10):3807-3815.

Kitamura H, Isaka Y, Takabatake Y, Imamura R, Suzuki C, Takahara S, Imai E. 2008. Nonerythropoietic derivative of erythropoietin protects against tubulointerstitial injury in a unilateral ureteral obstruction model. Nephrol Dial Transplant, 23 (5):1521-1528.

Koury MJ, Sawyer ST, Brandt SJ. 2002. New insights into erythropoiesis. Curr Opin Hematol, 9 (2):93-100.

Kunsmann L, Ruter C, Bauwens A, Greune L, Gluder M, Kemper B, Fruth A, Wai SN, He X, Lloubes R, Schmidt MA, Dobrindt U, Mellmann A, Karch H, Bielaszewska M. 2015. Virulence from vesicles: Novel mechanisms of host cell injury by *Escherichia coli* O104:H4 outbreak strain. Sci Rep, 5:13252.

Kurioka T, Yunou Y, Kita E. 1998. Enhancement of susceptibility to Shiga toxin-producing *Escherichia coli* O157:H7 by protein calorie malnutrition in mice. Infect Immun, 66 (4):1726-1734.

Kwak J, Kim JH, Jang HN, Jung MH, Cho HS, Chang SH, Kim HJ. 2020. Erythropoietin Ameliorates Ischemia/Reperfusion-Induced Acute Kidney Injury via Inflammasome Suppression in Mice. Int J Mol Sci, 21 (10).

Lacombe C, Mayeux P. 1999. The molecular biology of erythropoietin. Nephrol Dial Transplant, 14 Suppl 2:22-28.

Lai PH, Everett R, Wang FF, Arakawa T, Goldwasser E. 1986. Structural characterization of human erythropoietin. J Biol Chem, 261 (7):3116-3121.

Leitlinienprogramm Pädiatrie (Gesellschaft für Pädiatrische Nephrologie e.V. (GPN) DGfK-uJeVD, AWMF). 2022. Hämolytisch-Urämisches Syndrom im Kindesalter https://www.awmf.org/leitlinien/detail/ll/166-002.html: AWMF.

Liang F, Guan H, Li W, Zhang X, Liu T, Liu Y, Mei J, Jiang C, Zhang F, Luo B, Zhang Z. 2021. Erythropoietin Promotes Infection Resolution and Lowers Antibiotic Requirements in *E. coli*- and *S. aureus*-Initiated Infections. Front Immunol, 12:658715.

Lill JK, Thiebes S, Pohl JM, Bottek J, Subramaniam N, Christ R, Soun C, Gueler F, Zwanziger D, Hoffmann F, von Eggeling F, Bracht T, Sitek B, Hickey MJ, Hofnagel O, Engel DR. 2021. Tissue-resident macrophages mediate neutrophil recruitment and kidney injury in shiga toxin-induced hemolytic uremic syndrome. Kidney Int.

Livnah O, Stura EA, Johnson DL, Middleton SA, Mulcahy LS, Wrighton NC, Dower WJ, Jolliffe LK, Wilson IA. 1996. Functional mimicry of a protein hormone by a peptide agonist: the EPO receptor complex at 2.8 A. Science, 273 (5274):464-471.

Livnah O, Johnson DL, Stura EA, Farrell FX, Barbone FP, You Y, Liu KD, Goldsmith MA, He W, Krause CD, Pestka S, Jolliffe LK, Wilson IA. 1998. An antagonist peptide-EPO receptor complex suggests that receptor dimerization is not sufficient for activation. Nat Struct Biol, 5 (11):993-1004.

Loesch A, Tang H, Cotter MA, Cameron NE. 2010. Sciatic nerve of diabetic rat treated with epoetin delta: effects on C-fibers and blood vessels including pericytes. Angiology, 61 (7):651-668.

Loirat C, Fakhouri F, Ariceta G, Besbas N, Bitzan M, Bjerre A, Coppo R, Emma F, Johnson S, Karpman D, Landau D, Langman CB, Lapeyraque AL, Licht C, Nester C, Pecoraro C, Riedl M, van de Kar NC, Van de Walle J, Vivarelli M, Fremeaux-Bacchi V, International HUS. 2016. An international consensus approach to the management of atypical hemolytic uremic syndrome in children. Pediatr Nephrol, 31 (1):15-39.

Loos S, Oh J, van de Loo L, Kemper MJ, Blohm M, Schild R. 2021. Hemoconcentration and predictors in Shiga toxin-producing *E. coli*-hemolytic uremic syndrome (STEC-HUS). Pediatr Nephrol.

Lopez EL, Contrini MM, Glatstein E, Gonzalez Ayala S, Santoro R, Allende D, Ezcurra G, Teplitz E, Koyama T, Matsumoto Y, Sato H, Sakai K, Hoshide S, Komoriya K, Morita T, Harning R, Brookman S. 2010. Safety and pharmacokinetics of urtoxazumab, a humanized monoclonal antibody, against Shiga-like toxin 2 in healthy adults and in pediatric patients infected with Shiga-like toxin-producing *Escherichia coli*. Antimicrob Agents Chemother, 54 (1):239-243.

Luperchio SA, Schauer DB. 2001. Molecular pathogenesis of *Citrobacter rodentium* and transmissible murine colonic hyperplasia. Microbes Infect, 3 (4):333-340.

Lynn RM, O'Brien SJ, Taylor CM, Adak GK, Chart H, Cheasty T, Coia JE, Gillespie IA, Locking ME, Reilly WJ, Smith HR, Waters A, Willshaw GA. 2005. Childhood hemolytic uremic syndrome, United Kingdom and Ireland. Emerg Infect Dis, 11 (4):590-596.

Macdougall IC. 2005. CERA (Continuous Erythropoietin Receptor Activator): a new erythropoiesis-stimulating agent for the treatment of anemia. Curr Hematol Rep, 4 (6):436-440.

Mahat U, Matar RB, Rotz SJ. 2019. Use of complement monoclonal antibody eculizumab in Shiga toxin producing *Escherichia coli* associated hemolytic uremic syndrome: A review of current evidence. Pediatr Blood Cancer, 66 (11):e27913.

Mallick EM, McBee ME, Vanguri VK, Melton-Celsa AR, Schlieper K, Karalius BJ, O'Brien AD, Butterton JR, Leong JM, Schauer DB. 2012. A novel murine infection model for Shiga toxin-producing *Escherichia coli*. J Clin Invest, 122 (11):4012-4024.

Malyukova I, Murray KF, Zhu C, Boedeker E, Kane A, Patterson K, Peterson JR, Donowitz M, Kovbasnjuk O. 2009. Macropinocytosis in Shiga toxin 1 uptake by human intestinal epithelial cells and transcellular transcytosis. Am J Physiol Gastrointest Liver Physiol, 296 (1):G78-92.

Manton N, Smith NM, Byard RW. 2000. Unexpected childhood death due to hemolytic uremic syndrome. Am J Forensic Med Pathol, 21 (1):90-92.

Mariani-Kurkdjian P, Lemaitre C, Bidet P, Perez D, Boggini L, Kwon T, Bonacorsi S. 2014. Haemolytic-uraemic syndrome with bacteraemia caused by a new hybrid *Escherichia coli* pathotype. New Microbes New Infect, 2 (4):127-131.

Masuda S, Okano M, Yamagishi K, Nagao M, Ueda M, Sasaki R. 1994. A novel site of erythropoietin production. Oxygen-dependent production in cultured rat astrocytes. J Biol Chem, 269 (30):19488-19493.

Matise I, Sirinarumitr T, Bosworth BT, Moon HW. 1999. Ultrastructure and DNA fragmentation analysis of arterioles in swine infected with Shiga toxin-producing *Escherichia coli*. Adv Exp Med Biol, 473:163-171.

Matthews DJ, Topping RS, Cass RT, Giebel LB. 1996. A sequential dimerization mechanism for erythropoietin receptor activation. Proc Natl Acad Sci U S A, 93 (18):9471-9476.

Mayer CL, Leibowitz CS, Kurosawa S, Stearns-Kurosawa DJ. 2012. Shiga toxins and the pathophysiology of hemolytic uremic syndrome in humans and animals. Toxins (Basel), 4 (11):1261-1287.

Mayer CL, Parello CS, Lee BC, Itagaki K, Kurosawa S, Stearns-Kurosawa DJ. 2015. Pro-Coagulant Endothelial Dysfunction Results from EHEC Shiga Toxins and Host Damage-Associated Molecular Patterns. Front Immunol, 6:155.

McGannon CM, Fuller CA, Weiss AA. 2010. Different classes of antibiotics differentially influence shiga toxin production. Antimicrob Agents Chemother, 54 (9):3790-3798.

McKee ML, O'Brien AD. 1995. Investigation of enterohemorrhagic *Escherichia coli* O157:H7 adherence characteristics and invasion potential reveals a new attachment pattern shared by intestinal *E. coli*. Infect Immun, 63 (5):2070-2074.

MDS 2022. 02.05. Boletín integrado de vigilancia N560 SE30 2021 https://bancos.salud.gob.ar/recurso/boletin-integrado-de-vigilancia-n560-se30-2021.

Mele C, Remuzzi G, Noris M. 2014. Hemolytic uremic syndrome. Semin Immunopathol, 36 (4):399-420.

Menkis AH, Martin J, Cheng DC, Fitzgerald DC, Freedman JJ, Gao C, Koster A, Mackenzie GS, Murphy GJ, Spiess B, Ad N. 2012. Drug, devices, technologies, and techniques for blood management in minimally invasive and conventional cardiothoracic surgery: a consensus statement from the International Society for Minimally Invasive Cardiothoracic Surgery (ISMICS) 2011. Innovations (Phila), 7 (4):229-241.

Merchant AM, Neyra JA, Minhajuddin A, Wehrmann LE, Mills RA, Gualano SK, Kumbhani DJ, Huffman LC, Jessen ME, Fox AA. 2019. Packed red blood cell transfusion associates with acute kidney injury after transcatheter aortic valve replacement. BMC Anesthesiol, 19 (1):99.

Michael M, Elliott EJ, Craig JC, Ridley G, Hodson EM. 2009. Interventions for hemolytic uremic syndrome and thrombotic thrombocytopenic purpura: a systematic review of randomized controlled trials. Am J Kidney Dis, 53 (2):259-272.

Mirza S, Chen J, Murphy JM, Young IG. 2010. The role of interchain heterodisulfide formation in activation of the human common beta and mouse betaIL-3 receptors. J Biol Chem, 285 (32):24759-24768.

Mody RK, Gu W, Griffin PM, Jones TF, Rounds J, Shiferaw B, Tobin-D'Angelo M, Smith G, Spina N, Hurd S, Lathrop S, Palmer A, Boothe E, Luna-Gierke RE, Hoekstra RM. 2015. Postdiarrheal hemolytic uremic syndrome in United States children: clinical spectrum and predictors of in-hospital death. J Pediatr, 166 (4):1022-1029.

Mohawk KL, O'Brien AD. 2011. Mouse models of *Escherichia coli* O157:H7 infection and shiga toxin injection. J Biomed Biotechnol, 2011:258185.

Monet-Didailler C, Chevallier A, Godron-Dubrasquet A, Allard L, Delmas Y, Contin-Bordes C, Brissaud O, Llanas B, Harambat J. 2020. Outcome of children with Shiga toxin-associated haemolytic uraemic syndrome treated with eculizumab: a matched cohort study. Nephrol Dial Transplant, 35 (12):2147-2153.

Nairz M, Schroll A, Moschen AR, Sonnweber T, Theurl M, Theurl I, Taub N, Jamnig C, Neurauter D, Huber LA, Tilg H, Moser PL, Weiss G. 2011. Erythropoietin contrastingly affects bacterial infection and experimental colitis by inhibiting nuclear factor-kappaB-inducible immune pathways. Immunity, 34 (1):61-74.

Nitschke M, Sayk F, Hartel C, Roseland RT, Hauswaldt S, Steinhoff J, Fellermann K, Derad I, Wellhoner P, Buning J, Tiemer B, Katalinic A, Rupp J, Lehnert H, Solbach W, Knobloch JK. 2012. Association between azithromycin therapy and duration of bacterial shedding among patients with Shiga toxin-producing enteroaggregative *Escherichia coli* O104:H4. JAMA, 307 (10):1046-1052.

O'Brien ME, Casey S, Treleaven J, Powles TJ. 1994. Use of erythropoietin in the management of the haemolytic uraemic syndrome induced by mitomycin C/tamoxifen. Eur J Cancer, 30A (6):894-895.

Obrig TG, Louise CB, Lingwood CA, Boyd B, Barley-Maloney L, Daniel TO. 1993. Endothelial heterogeneity in Shiga toxin receptors and responses. J Biol Chem, 268 (21):15484-15488.

Ochoa F, Oltra G, Gerhardt E, Hermes R, Cohen L, Damiano AE, Ibarra C, Lago NR, Zotta E. 2012. Microalbuminuria and early renal response to lethal dose Shiga toxin type 2 in rats. Int J Nephrol Renovasc Dis, 5:29-36.

Ohara T, Kojio S, Taneike I, Nakagawa S, Gondaira F, Tamura Y, Gejyo F, Zhang HM, Yamamoto T. 2002. Effects of azithromycin on shiga toxin production by *Escherichia coli* and subsequent host inflammatory response. Antimicrob Agents Chemother, 46 (11):3478-3483.

Panda A, Tatarov I, Melton-Celsa AR, Kolappaswamy K, Kriel EH, Petkov D, Coksaygan T, Livio S, McLeod CG, Nataro JP, O'Brien AD, DeTolla LJ. 2010. *Escherichia coli* O157:H7 infection in Dutch belted and New Zealand white rabbits. Comp Med, 60 (1):31-37.

Pantazopoulos C, Iacovidou N, Kouskouni E, Pliatsika P, Papalois A, Kaparos G, Barouxis D, Vasileiou P, Lelovas P, Kotsilianou O, Pantazopoulos I, Gkiokas G, Garosa C, Faa G, Xanthos T. 2016. Effect of Erythropoietin on Postresuscitation Renal Function in a Swine Model of Ventricular Fibrillation. Biomed Res Int, 2016:3567275.

Pape L, Hartmann H, Bange FC, Suerbaum S, Bueltmann E, Ahlenstiel-Grunow T. 2015. Eculizumab in Typical Hemolytic Uremic Syndrome (HUS) With Neurological Involvement. Medicine (Baltimore), 94 (24):e1000.

Pape L, Ahlenstiel T, Kreuzer M, Drube J, Froede K, Franke D, Ehrich JH, Haubitz M. 2009. Early erythropoietin reduced the need for red blood cell transfusion in childhood hemolytic uremic syndrome: a randomized prospective pilot trial. Pediatr Nephrol, 24 (5):1061-1064.

Patel NS, Nandra KK, Brines M, Collino M, Wong WF, Kapoor A, Benetti E, Goh FY, Fantozzi R, Cerami A, Thiemermann C. 2011. A nonerythropoietic peptide that mimics the 3D structure of erythropoietin reduces organ injury/dysfunction and inflammation in experimental hemorrhagic shock. Mol Med, 17 (9-10):883-892.

Patel NS, Kerr-Peterson HL, Brines M, Collino M, Rogazzo M, Fantozzi R, Wood EG, Johnson FL, Yaqoob MM, Cerami A, Thiemermann C. 2012. Delayed administration of pyroglutamate helix B surface peptide (pHBSP), a novel nonerythropoietic analog of erythropoietin, attenuates acute kidney injury. Mol Med, 18:719-727.

Percheron L, Gramada R, Tellier S, Salomon R, Harambat J, Llanas B, Fila M, Allain-Launay E, Lapeyraque AL, Leroy V, Adra AL, Berard E, Bourdat-Michel G, Chehade H, Eckart P, Merieau E, Pietrement C, Sellier-Leclerc AL, Fremeaux-Bacchi V, Dimeglio C, Garnier A. 2018. Eculizumab treatment in severe pediatric STEC-HUS: a multicenter retrospective study. Pediatr Nephrol, 33 (8):1385-1394.

Philo JS, Aoki KH, Arakawa T, Narhi LO, Wen J. 1996. Dimerization of the extracellular domain of the erythropoietin (EPO) receptor by EPO: one high-affinity and one low-affinity interaction. Biochemistry, 35 (5):1681-1691.

Phrommintikul A, Haas SJ, Elsik M, Krum H. 2007. Mortality and target haemoglobin concentrations in anaemic patients with chronic kidney disease treated with erythropoietin: a meta-analysis. Lancet, 369 (9559):381-388.

Piastra M, Ruggiero A, Langer A, Caresta E, Chiaretti A, Pulitano S, Polidori G, Riccardi R. 2004. Pulmonary hemorrhage complicating a typical hemolytic-uremic syndrome. Respiration, 71 (5):537-541.

Pirschel W, Mestekemper AN, Wissuwa B, Krieg N, Kroller S, Daniel C, Gunzer F, Tolosano E, Bauer M, Amann K, Heinemann SH, Coldewey SM. 2022. Divergent roles of haptoglobin and hemopexin deficiency for disease progression of Shiga-toxin-induced hemolytic-uremic syndrome in mice. Kidney Int.

Ramos MV, Mejias MP, Sabbione F, Fernandez-Brando RJ, Santiago AP, Amaral MM, Exeni R, Trevani AS, Palermo MS. 2016. Induction of Neutrophil Extracellular Traps in Shiga Toxin-Associated Hemolytic Uremic Syndrome. J Innate Immun, 8 (4):400-411.

Rasooly R, Do PM, Griffey SM, Vilches-Moure JG, Friedman M. 2010. Ingested Shiga toxin 2 (Stx2) causes histopathological changes in kidney, spleen, and thymus tissues and mortality in mice. J Agric Food Chem, 58 (16):9281-9286.

Rastawicki W, Smietanska K, Rokosz-Chudziak N, Wolkowicz T. 2020. Antibody response to lipopolysaccharides and recombinant proteins of Shiga toxin (STX)-producing *Escherichia coli* (STEC) in children with haemolytic uraemic syndrome in Poland. Lett Appl Microbiol, 70 (6):440-446.

Richardson SE, Rotman TA, Jay V, Smith CR, Becker LE, Petric M, Olivieri NF, Karmali MA. 1992. Experimental verocytotoxemia in rabbits. Infect Immun, 60 (10):4154-4167.

Richmond TD, Chohan M, Barber DL. 2005. Turning cells red: signal transduction mediated by erythropoietin. Trends Cell Biol, 15 (3):146-155.

RKI. 2012. Infektionsepidemiologisches Jahrbuch meldepflichtiger Krankheiten für 2011. https://www.rki.de/DE/Content/Infekt/Jahrbuch/Jahrbuch_2011.html: Robert Koch Institut.

RKI. 2021. Infektionsepidemiologisches Jahrbuch meldepflichtiger Krankheiten für 2020. https://www.rki.de/DE/Content/Infekt/Jahrbuch/Jahrbuch_2020.html: Robert Koch Institut.

Robertson CS, Garcia R, Gaddam SS, Grill RJ, Cerami Hand C, Tian TS, Hannay HJ. 2013. Treatment of mild traumatic brain injury with an erythropoietin-mimetic peptide. J Neurotrauma, 30 (9):765-774.

Robitaille P, Gonthier M, Grignon A, Russo P. 1997. Pancreatic injury in the hemolytic-uremic syndrome. Pediatr Nephrol, 11 (5):631-632.

Roche JK, Keepers TR, Gross LK, Seaner RM, Obrig TG. 2007. CXCL1/KC and CXCL2/MIP-2 are critical effectors and potential targets for therapy of *Escherichia coli* O157:H7-associated renal inflammation. Am J Pathol, 170 (2):526-537.

Rosales A, Hofer J, Zimmerhackl LB, Jungraithmayr TC, Riedl M, Giner T, Strasak A, Orth-Holler D, Wurzner R, Karch H, German-Austrian HUSSG. 2012. Need for long-term follow-up in enterohemorrhagic *Escherichia coli*-associated hemolytic uremic syndrome due to late-emerging sequelae. Clin Infect Dis, 54 (10):1413-1421.

Rutjes NW, Binnington BA, Smith CR, Maloney MD, Lingwood CA. 2002. Differential tissue targeting and pathogenesis of verotoxins 1 and 2 in the mouse animal model. Kidney Int, 62 (3):832-845.

Saulle E, Riccioni R, Coppola S, Parolini I, Diverio D, Riti V, Mariani G, Laufer S, Sargiacomo M, Testa U. 2009. Colocalization of the VEGF-R2 and the common IL-3/GM-CSF receptor beta chain to lipid rafts leads to enhanced p38 activation. Br J Haematol, 145 (3):399-411.

Sauter KA, Melton-Celsa AR, Larkin K, Troxell ML, O'Brien AD, Magun BE. 2008. Mouse model of hemolytic-uremic syndrome caused by endotoxin-free Shiga toxin 2 (Stx2) and protection from lethal outcome by anti-Stx2 antibody. Infect Immun, 76 (10):4469-4478.

Schuller S, Heuschkel R, Torrente F, Kaper JB, Phillips AD. 2007. Shiga toxin binding in normal and inflamed human intestinal mucosa. Microbes Infect, 9 (1):35-39.

Shi M, Flores B, Li P, Gillings N, McMillan KL, Ye J, Huang LJ, Sidhu SS, Zhong YP, Grompe MT, Streeter PR, Moe OW, Hu MC. 2018. Effects of erythropoietin receptor activity on angiogenesis, tubular injury, and fibrosis in acute kidney injury: a "U-shaped" relationship. Am J Physiol Renal Physiol, 314 (4):F501-F516.

Siegler RL, Pysher TJ, Lou R, Tesh VL, Taylor FB, Jr. 2001. Response to Shiga toxin-1, with and without lipopolysaccharide, in a primate model of hemolytic uremic syndrome. Am J Nephrol, 21 (5):420-425.

Siegler RL, Obrig TG, Pysher TJ, Tesh VL, Denkers ND, Taylor FB. 2003. Response to Shiga toxin 1 and 2 in a baboon model of hemolytic uremic syndrome. Pediatr Nephrol, 18 (2):92-96.

Silberstein C, Lucero MS, Zotta E, Copeland DP, Lingyun L, Repetto HA, Ibarra C. 2011. A glucosylceramide synthase inhibitor protects rats against the cytotoxic effects of shiga toxin 2. Pediatr Res, 69 (5 Pt 1):390-394.

Sobbe IV, Krieg N, Dennhardt S, Coldewey SM. 2020. Involvement of NF-kappaB1 and the Non-Canonical NF-kappaB Signaling Pathway in the Pathogenesis of Acute Kidney Injury in Shiga-Toxin-2-Induced Hemolytic-Uremic Syndrome in Mice. Shock.

Soysal N, Mariani-Kurkdjian P, Smail Y, Liguori S, Gouali M, Loukiadis E, Fach P, Bruyand M, Blanco J, Bidet P, Bonacorsi S. 2016. Enterohemorrhagic *Escherichia coli* Hybrid Pathotype O80:H2 as a New Therapeutic Challenge. Emerg Infect Dis, 22 (9):1604-1612.

Stahl AL, Sartz L, Nelsson A, Bekassy ZD, Karpman D. 2009. Shiga toxin and lipopolysaccharide induce platelet-leukocyte aggregates and tissue factor release, a thrombotic mechanism in hemolytic uremic syndrome. PLoS One, 4 (9):e6990.

Stahl AL, Arvidsson I, Johansson KE, Chromek M, Rebetz J, Loos S, Kristoffersson AC, Bekassy ZD, Morgelin M, Karpman D. 2015. A novel mechanism of bacterial toxin transfer within host blood cell-derived microvesicles. PLoS Pathog, 11 (2):e1004619.

Stearns-Kurosawa DJ, Collins V, Freeman S, Debord D, Nishikawa K, Oh SY, Leibowitz CS, Kurosawa S. 2011. Rescue from lethal Shiga toxin 2-induced renal failure with a cell-permeable peptide. Pediatr Nephrol, 26 (11):2031-2039.

Stearns-Kurosawa DJ, Oh SY, Cherla RP, Lee MS, Tesh VL, Papin J, Henderson J, Kurosawa S. 2013. Distinct renal pathology and a chemotactic phenotype after enterohemorrhagic *Escherichia coli* shiga toxins in non-human primate models of hemolytic uremic syndrome. Am J Pathol, 182 (4):1227-1238.

Steiner ME, Ness PM, Assmann SF, Triulzi DJ, Sloan SR, Delaney M, Granger S, Bennett-Guerrero E, Blajchman MA, Scavo V, Carson JL, Levy JH, Whitman G, D'Andrea P, Pulkrabek S, Ortel TL, Bornikova L, Raife T, Puca KE, Kaufman RM, Nuttall GA, Young PP, Youssef S, Engelman R, Greilich PE, Miles R, Josephson CD, Bracey A, Cooke R, McCullough J, Hunsaker R, Uhl L, McFarland JG, Park Y, Cushing MM, Klodell CT, Karanam R, Roberts PR, Dyke C, Hod EA, Stowell CP. 2015. Effects of red-cell storage duration on patients undergoing cardiac surgery. N Engl J Med, 372 (15):1419-1429.

Stevens MP, Frankel GM. 2014. The Locus of Enterocyte Effacement and Associated Virulence Factors of Enterohemorrhagic *Escherichia coli*. Microbiol Spectr, 2 (4):EHEC-0007-2013.

Sugatani J, Komiyama N, Mochizuki T, Hoshino M, Miyamoto D, Igarashi T, Hoshi S, Miwa M. 2002. Urinary concentrating defect in rats given Shiga toxin: elevation in urinary AQP2 level associated with polyuria. Life Sci, 71 (2):171-189.

Syed RS, Reid SW, Li C, Cheetham JC, Aoki KH, Liu B, Zhan H, Osslund TD, Chirino AJ, Zhang J, Finer-Moore J, Elliott S, Sitney K, Katz BA, Matthews DJ, Wendoloski JJ, Egrie J, Stroud RM. 1998. Efficiency of signalling through cytokine receptors depends critically on receptor orientation. Nature, 395 (6701):511-516.

Tarr PI, Gordon CA, Chandler WL. 2005. Shiga-toxin-producing *Escherichia coli* and haemolytic uraemic syndrome. Lancet, 365 (9464):1073-1086.

Taylor FB, Jr., Tesh VL, DeBault L, Li A, Chang AC, Kosanke SD, Pysher TJ, Siegler RL. 1999. Characterization of the baboon responses to Shiga-like toxin: descriptive study of a new primate model of toxic responses to Stx-1. Am J Pathol, 154 (4):1285-1299.

te Loo DM, Monnens LA, van Der Velden TJ, Vermeer MA, Preyers F, Demacker PN, van Den Heuvel LP, van Hinsbergh VW. 2000. Binding and transfer of verocytotoxin by polymorphonuclear leukocytes in hemolytic uremic syndrome. Blood, 95 (11):3396-3402.

Thayu M, Chandler WL, Jelacic S, Gordon CA, Rosenthal GL, Tarr PI. 2003. Cardiac ischemia during hemolytic uremic syndrome. Pediatr Nephrol, 18 (3):286-289.

Togel FE, Ahlstrom JD, Yang Y, Hu Z, Zhang P, Westenfelder C. 2016. Carbamylated Erythropoietin Outperforms Erythropoietin in the Treatment of AKI-on-CKD and Other AKI Models. J Am Soc Nephrol, 27 (11):3394-3404.

Trachtman H, Cnaan A, Christen E, Gibbs K, Zhao S, Acheson DW, Weiss R, Kaskel FJ, Spitzer A, Hirschman GH, Investigators of the HUSSPMCT. 2003. Effect of an oral Shiga toxin-binding agent on diarrhea-associated hemolytic uremic syndrome in children: a randomized controlled trial. JAMA, 290 (10):1337-1344.

Tsuda E, Kawanishi G, Ueda M, Masuda S, Sasaki R. 1990. The role of carbohydrate in recombinant human erythropoietin. Eur J Biochem, 188 (2):405-411.

Ueba H, Brines M, Yamin M, Umemoto T, Ako J, Momomura S, Cerami A, Kawakami M. 2010. Cardioprotection by a nonerythropoietic, tissue-protective peptide mimicking the 3D structure of erythropoietin. Proc Natl Acad Sci U S A, 107 (32):14357-14362.

van Rijt WG, Nieuwenhuijs-Moeke GJ, van Goor H, Jespersen B, Ottens PJ, Ploeg RJ, Leuvenink HG. 2013. ARA290, a non-erythropoietic EPO derivative, attenuates renal ischemia/reperfusion injury. J Transl Med, 11:9.

Vaterodt L, Holle J, Huseman D, Muller D, Thumfart J. 2018. Short- and Long-Term Renal Outcome of Hemolytic-Uremic Syndrome in Childhood. Front Pediatr, 6:220.

Wadolkowski EA, Burris JA, O'Brien AD. 1990. Mouse model for colonization and disease caused by enterohemorrhagic *Escherichia coli* O157:H7. Infect Immun, 58 (8):2438-2445.

Watowich SS. 2011. The erythropoietin receptor: molecular structure and hematopoietic signaling pathways. J Investig Med, 59 (7):1067-1072.

Wöchtl B, Gunzer F, Gerner W, Gasse H, Koch M, Bago Z, Ganter M, Weissenbock H, Dinhopl N, Coldewey SM, von Altrock A, Waldmann KH, Saalmuller A, Zimmermann K, Steinmann J, Kehrmann J, Klein-Hitpass L, Blom J, Ehricht R, Engelmann I, Hennig-Pauka I. 2017. Comparison of clinical and immunological findings in gnotobiotic piglets infected with *Escherichia coli* O104:H4 outbreak strain and EHEC O157:H7. Gut Pathog, 9:30.

Woo da E, Lee JM, Kim YK, Park YH. 2016. Recombinant Human Erythropoietin Therapy for a Jehovah's Witness Child With Severe Anemia due to Hemolytic-Uremic Syndrome. Korean J Pediatr, 59 (2):100-103.

Yamamoto ET, Mizuno M, Nishikawa K, Miyazawa S, Zhang L, Matsuo S, Natori Y. 2005. Shiga toxin 1 causes direct renal injury in rats. Infect Immun, 73 (11):7099-7106.

Zangari T, Melton-Celsa AR, Panda A, Smith MA, Tatarov I, De Tolla L, O'Brien AD. 2014. Enhanced virulence of the *Escherichia coli* O157:H7 spinach-associated outbreak strain in two animal models is associated with higher levels of Stx2 production after induction with ciprofloxacin. Infect Immun, 82 (12):4968-4977.

Zhang SX, Zhou YM, Tian LG, Chen JX, Tinoco-Torres R, Serrano E, Li SZ, Chen SH, Ai L, Chen JH, Xia S, Lu Y, Lv S, Teng XJ, Xu W, Gu WP, Gong ST, Zhou XN, Geng LL, Hu W. 2018. Antibiotic resistance and molecular characterization of diarrheagenic *Escherichia coli* and non-typhoidal *Salmonella* strains isolated from infections in Southwest China. Infect Dis Poverty, 7 (1):53.

Zhang YL, Radhakrishnan ML, Lu X, Gross AW, Tidor B, Lodish HF. 2009. Symmetric signaling by an asymmetric 1 erythropoietin: 2 erythropoietin receptor complex. Mol Cell, 33 (2):266-274.

Zhao YL, Cen XB, Ito M, Yokoyama K, Takagi K, Kitaichi K, Nadai M, Ohta M, Takagi K, Hasegawa T. 2002. Shiga-like toxin II derived from *Escherichia coli* O157:H7 modifies renal handling of levofloxacin in rats. Antimicrob Agents Chemother, 46 (5):1522-1528.

6. Appendix

List of publications

1) De Lucia D, Lucio OM, Musio B, Bender A, Listing M, Dennhardt S, Koeberle A, Garscha U, Rizzo R, Manfredini S, Werz O, Ley SV. Design, synthesis and evaluation of semi-synthetic triazole-containing caffeic acid analogs as 5-lipoxygenase inhibitors. Eur J Med Chem. 2015 Aug 28;101:573-83. doi: 10.1016/j.ejmech.2015.07.011. Epub 2015 Jul 15. Erratum in: Eur J Med Chem. 2015 Oct 20;103:223-5. PMID: 26197161.

2) Swain SM, Sahoo N, Dennhardt S, Schönherr R, Heinemann SH. Ca(2+)/calmodulin regulates Kvβ1.1-mediated inactivation of voltage-gated K(+) channels. Sci Rep. 2015 Oct 21;5:15509. doi: 10.1038/srep15509. PMID: 26487174; PMCID: PMC4614385.

3) Gerstmeier J, Newcomer ME, Dennhardt S, Romp E, Fischer J, Werz O, Garscha U. 5-Lipoxygenase-activating protein rescues activity of 5-lipoxygenase mutations that delay nuclear membrane association and disrupt product formation. FASEB J. 2016 May;30(5):1892-900. doi: 10.1096/fj.201500210R. Epub 2016 Feb 3. PMID: 26842853; PMCID: PMC4836370.

4) Dennhardt S*, Pirschel W*, Wissuwa B, Daniel C, Gunzer F, Lindig S, Medyukhina A, Kiehntopf M, Rudolph WW, Zipfel PF, Gunzer M, Figge MT, Amann K, Coldewey SM. Modeling Hemolytic-Uremic Syndrome: In-Depth Characterization of Distinct Murine Models Reflecting Different Features of Human Disease. Front Immunol. 2018 Jun 25;9:1459. doi: 10.3389/fimmu.2018.01459. PMID: 29988557; PMCID: PMC6026657. *Authors contributed equally.

5) *Dennhardt S, *Finke KR, Huwiler A, Coldewey SM. Sphingosine-1-phosphate promotes barrier-stabilizing effects in human microvascular endothelial cells via AMPK-dependent mechanisms. Biochim Biophys Acta Mol Basis Dis. 2019 Apr 1;1865(4):774-781. doi: 10.1016/j.bbadis.2018.12.022. Epub 2019 Jan 17. Erratum in: Biochim Biophys Acta Mol Basis Dis. 2020 Oct 1;1866(10):165892. PMID: 30660683. *Authors contributed equally.

6) Sobbe IV, Krieg N, Dennhardt S, Coldewey SM. Involvement of NF-κB1 and the Non-Canonical NF-κB Signaling Pathway in the Pathogenesis of Acute Kidney Injury in Shiga-Toxin-2-Induced Hemolytic-Uremic Syndrome in Mice. Shock. 2020 May 18. doi: 10.1097/SHK.0000000000001558. Epub ahead of print. PMID: 32433206.

7) Dennhardt S*, Finke KR*, Huwiler A, Coldewey SM. Corrigendum to "Sphingosine-1-phosphate promotes barrier-stabilizing effects in human microvascular endothelial cells via AMPK-dependent mechanisms" [Biochim. Biophys. Acta Mol. Basis Dis. 2019 Apr 1;1865(4):774-781]. Biochim Biophys Acta Mol Basis Dis. 2020 Oct 1;1866(10):165892. doi: 10.1016/j.bbadis.2020.165892. Epub 2020 Jul 4. Erratum for: Biochim Biophys Acta Mol Basis Dis. 2019 Apr 1;1865(4):774-781. PMID: 32631629. *Authors contributed equally.

8) Dennhardt S, Pirschel W, Wissuwa B, Imhof D, Daniel C, Kielstein JT, Hennig-Pauka I, Amann K, Gunzer F, Coldewey SM. Targeting the innate repair receptor axis via erythropoietin or pyroglutamate helix B surface peptide attenuates hemolytic-uremic syndrome in mice. Front Immunol. 2022 Sep 23;13:1010882. doi: 10.3389/fimmu.2022.1010882. PMID: 36211426; PMCID: PMC9537456.

Curriculum vitae

Die Seite “Curriculum vitae” enthält persönliche Daten und ist daher nicht Bestandteil dieser Veröffentlichung.

Partizipation an wissenschaftlichen Kongressen

11.-13.09.2019	Weimar Sepsis Update 2019; The non-canonical NF-κB signaling pathway is involved in the pathogenesis of Shiga-toxin-induced hemolytic-uraemic syndrome in mice; Sophie Dennhardt, Isabelle Victoria Sobbe, Nadine Krieg, Bianka Wissuwa, Sina M. Coldewey (abstract, poster, oral presentation)
15.-16.02.2019	33. Wissenschaftliche Arbeitstage der Anästhesie Würzburg (WAT); Sphingosin-1-Phosphat vermittelt über AMPK-abhängige Mechanismen in humanen mikrovaskulären Endothelzellen Barriere-stabilisierende Effekte; Karl R. Finke, Sophie Dennhardt, Andrea Huwiler, Sina M. Coldewey (abstract)
19.-21.02.2018	70. Jahrestagung der Deutschen Gesellschaft für Hygiene und Mikrobiologie (DGHM) Bochum; Development of murine models mimicking key symptoms of diarrhea-positive hemolytic-uraemic syndrome; Sophie Dennhardt, Wiebke Pirschel, Bianka Wissuwa, Christoph Daniel, Florian Gunzer, Sandro Lindig, Wolfram W. Rudolph, Kerstin Amann, Sina M. Coldewey (abstract, oral presentation)
13.-15.09.2017	XVIIth Congress of the European Shock Society Paris; Hallmarks of human hemolytic-uraemic syndrome mimicked in a murine model mediated by Shiga toxin; Sophie Dennhardt, Wiebke Pirschel, Bianka Wissuwa, Christoph Daniel, Florian Gunzer, Sandro Lindig, Wolfram W. Rudolph, Kerstin Amann, Sina M. Coldewey (abstract, poster)

Author Contribution Statement

Manuskript Nr. I

Kurzreferenz: Dennhardt *et al.* (2018), Front Immunol

Beitrag des Doktoranden / der Doktorandin

Beitrag des Doktoranden / der Doktorandin zu Abbildungen, die experimentelle Daten wiedergeben (nur für Originalartikel):

Abbildung # 1	☐	100% (die in dieser Abbildung wiedergegebenen Daten entstammen vollständig experimentellen Arbeiten, die der Kandidat/die Kandidatin durchgeführt hat)
	☐	0% (die in dieser Abbildung wiedergegebenen Daten basieren ausschließllich auf Arbeiten anderer Koautoren)
	☒	Etwaiger Beitrag des Doktoranden / der Doktorandin zur Abbildung: 20 % Kurzbeschreibung des Beitrages: *Auswertung der Daten inkl. statistischer Analyse, Interpretation der Daten, Erstellen der Grafik*
Abbildung # 2	☐	100% (die in dieser Abbildung wiedergegebenen Daten entstammen vollständig experimentellen Arbeiten, die der Kandidat/die Kandidatin durchgeführt hat)
	☐	0% (die in dieser Abbildung wiedergegebenen Daten basieren ausschließllich auf Arbeiten anderer Koautoren)

	☒	Etwaiger Beitrag des Doktoranden / der Doktorandin zur Abbildung: 80 % Kurzbeschreibung des Beitrages: *Durchführung Tierversuche (i.v.-Injektionen zur HUS-Induktion, Volumengabe, Scoring, Blut- und Organentnahme), Auswertung der Daten inkl. statistischer Analyse, Interpretation der Daten, Erstellen der Grafik*
Abbildung # 3	☐	100% (die in dieser Abbildung wiedergegebenen Daten entstammen vollständig experimentellen Arbeiten, die der Kandidat/die Kandidatin durchgeführt hat)
	☐	0% (die in dieser Abbildung wiedergegebenen Daten basieren ausschließllich auf Arbeiten anderer Koautoren)
	☒	Etwaiger Beitrag des Doktoranden / der Doktorandin zur Abbildung: 90 % Kurzbeschreibung des Beitrages: *Durchführung Tierversuche (i.v.-Injektionen zur HUS-Induktion, Volumengabe, Scoring, Blut- und Organentnahme), Auswertung der Daten inkl. statistischer Analyse, Interpretation der Daten, Erstellen der Grafik*
Abbildung # 4	☐	100% (die in dieser Abbildung wiedergegebenen Daten entstammen vollständig experimentellen Arbeiten, die der Kandidat/die Kandidatin durchgeführt hat)
	☐	0% (die in dieser Abbildung wiedergegebenen Daten basieren ausschließllich auf Arbeiten anderer Koautoren)

	☒	Etwaiger Beitrag des Doktoranden / der Doktorandin zur Abbildung: 90 % Kurzbeschreibung des Beitrages: *Durchführung Tierversuche (i.v.-Injektionen zur HUS-Induktion, Volumengabe, Scoring, Blut- und Organentnahme), Etablierung und Durchführung Hämolyse-Assay, Auswertung der Daten inkl. statistischer Analyse, Interpretation der Daten, Erstellen der Grafik*
Abbildung # 5	☐	100% (die in dieser Abbildung wiedergegebenen Daten entstammen vollständig experimentellen Arbeiten, die der Kandidat/die Kandidatin durchgeführt hat)
	☐	0% (die in dieser Abbildung wiedergegebenen Daten basieren ausschließllich auf Arbeiten anderer Koautoren)
	☒	Etwaiger Beitrag des Doktoranden / der Doktorandin zur Abbildung: 30 % Kurzbeschreibung des Beitrages: *Durchführung Tierversuche (i.v.-Injektionen zur HUS-Induktion, Volumengabe, Scoring, Blut- und Organentnahme), Auswertung der Daten Panel A- C inkl. statistischer Analyse, Interpretation der Daten, Erstellen der Grafik*
Abbildung # 6	☐	100% (die in dieser Abbildung wiedergegebenen Daten entstammen vollständig experimentellen Arbeiten, die der Kandidat/die Kandidatin durchgeführt hat)
	☐	0% (die in dieser Abbildung wiedergegebenen Daten basieren ausschließllich auf Arbeiten anderer Koautoren)

	☒	Etwaiger Beitrag des Doktoranden / der Doktorandin zur Abbildung: 40 % Kurzbeschreibung des Beitrages: *Durchführung Tierversuche (i.v.-Injektionen zur HUS-Induktion, Volumengabe, Scoring, Blut- und Organentnahme), Auswertung der Daten Panel A-F inkl. statistischer Analyse, Interpretation der Daten, Erstellen der Grafik*
Abbildung # 7-9	☐	100% (die in dieser Abbildung wiedergegebenen Daten entstammen vollständig experimentellen Arbeiten, die der Kandidat/die Kandidatin durchgeführt hat)
	☐	0% (die in dieser Abbildung wiedergegebenen Daten basieren ausschließllich auf Arbeiten anderer Koautoren)
	☒	Etwaiger Beitrag des Doktoranden / der Doktorandin zur Abbildung: 20 % Kurzbeschreibung des Beitrages: *Durchführung Tierversuche (i.v.-Injektionen zur HUS-Induktion, Volumengabe, Scoring, Blut- und Organentnahme), Interpretation der Daten, Erstellen der Grafik*
Abbildung # 10	☐	100% (die in dieser Abbildung wiedergegebenen Daten entstammen vollständig experimentellen Arbeiten, die der Kandidat/die Kandidatin durchgeführt hat)
	☐	0% (die in dieser Abbildung wiedergegebenen Daten basieren ausschließllich auf Arbeiten anderer Koautoren)

	☒	Etwaiger Beitrag des Doktoranden / der Doktorandin zur Abbildung: 50 % Kurzbeschreibung des Beitrages: *Durchführung Tierversuche (i.v.-Injektionen zur HUS-Induktion, Volumengabe, Scoring, Blut- und Organentnahme), Assistenz bei RNA-Isolation, Auswertung der Daten Panel B-F, Interpretation der Daten, Erstellen der Grafik*
Tabelle # 1-2	☐	100% (die in dieser Abbildung wiedergegebenen Daten entstammen vollständig experimentellen Arbeiten, die der Kandidat/die Kandidatin durchgeführt hat)
	☐	0% (die in dieser Abbildung wiedergegebenen Daten basieren ausschließllich auf Arbeiten anderer Koautoren)
	☒	Etwaiger Beitrag des Doktoranden / der Doktorandin zur Abbildung: 90 % Kurzbeschreibung des Beitrages: *Durchführung Tierversuche (i.v.-Injektionen zur HUS-Induktion, Volumengabe, Scoring, Blut- und Organentnahme), Assistenz bei RNA-Isolation, Auswertung der Daten mittels DAVID, Interpretation der Daten, Erstellen der Tabellen*

Manuskript Nr. II

Kurzreferenz: Dennhardt *et al.* (2022), Front Immunol

Beitrag des Doktoranden / der Doktorandin

Beitrag des Doktoranden / der Doktorandin zu Abbildungen, die experimentelle Daten wiedergeben (nur für Originalartikel):

Abbildung # 1	☐	100% (die in dieser Abbildung wiedergegebenen Daten entstammen vollständig experimentellen Arbeiten, die der Kandidat/die Kandidatin durchgeführt hat)
	☐	0% (die in dieser Abbildung wiedergegebenen Daten basieren ausschließllich auf Arbeiten anderer Koautoren)
	☒	Etwaiger Beitrag des Doktoranden / der Doktorandin zur Abbildung: 60 % Kurzbeschreibung des Beitrages: *Auswertung der ELISA- und Patientendaten inkl. statistischer Analyse, Interpretation der Daten, Erstellen der Grafik*
Abbildung # 2	☐	100% (die in dieser Abbildung wiedergegebenen Daten entstammen vollständig experimentellen Arbeiten, die der Kandidat/die Kandidatin durchgeführt hat)
	☐	0% (die in dieser Abbildung wiedergegebenen Daten basieren ausschließllich auf Arbeiten anderer Koautoren)
	☒	Etwaiger Beitrag des Doktoranden / der Doktorandin zur Abbildung: 70 % Kurzbeschreibung des Beitrages:

		Durchführung Mausversuche (i.v.-Injektionen zur HUS-Induktion, Volumengabe, Scoring, Blut- und Organentnahme), Auswertung der Daten inkl. statistischer Analyse, Interpretation der Daten, Erstellen der Grafik
Abbildung # 3	☐	100% (die in dieser Abbildung wiedergegebenen Daten entstammen vollständig experimentellen Arbeiten, die der Kandidat/die Kandidatin durchgeführt hat)
	☐	0% (die in dieser Abbildung wiedergegebenen Daten basieren ausschließllich auf Arbeiten anderer Koautoren)
	☒	Etwaiger Beitrag des Doktoranden / der Doktorandin zur Abbildung: 90 % Kurzbeschreibung des Beitrages: *Durchführung Tierversuche (i.v.-Injektionen zur HUS-Induktion, Volumengabe, Scoring, Blut- und Organentnahme), Auswertung der Daten inkl. statistischer Analyse, Interpretation der Daten, Erstellen der Grafik*
Abbildung # 4	☐	100% (die in dieser Abbildung wiedergegebenen Daten entstammen vollständig experimentellen Arbeiten, die der Kandidat/die Kandidatin durchgeführt hat)
	☐	0% (die in dieser Abbildung wiedergegebenen Daten basieren ausschließllich auf Arbeiten anderer Koautoren)
	☒	Etwaiger Beitrag des Doktoranden / der Doktorandin zur Abbildung: 60 % Kurzbeschreibung des Beitrages: *Durchführung Tierversuche (i.v.-Injektionen zur HUS-Induktion, Volumengabe, Scoring, Blut- und Organentnahme), Auswertung der*

		Daten Panel A-C inkl. statistischer Analyse, Interpretation der Daten, Erstellen der Grafik
Abbildung # 5	☐	100% (die in dieser Abbildung wiedergegebenen Daten entstammen vollständig experimentellen Arbeiten, die der Kandidat/die Kandidatin durchgeführt hat)
	☐	0% (die in dieser Abbildung wiedergegebenen Daten basieren ausschließllich auf Arbeiten anderer Koautoren)
	☒	Etwaiger Beitrag des Doktoranden / der Doktorandin zur Abbildung: 20 % Kurzbeschreibung des Beitrages: *Durchführung Tierversuche (i.v.-Injektionen zur HUS-Induktion, Volumengabe, Scoring, Blut- und Organentnahme), Interpretation der Daten, Erstellen der Grafik*
Abbildung # 6	☐	100% (die in dieser Abbildung wiedergegebenen Daten entstammen vollständig experimentellen Arbeiten, die der Kandidat/die Kandidatin durchgeführt hat)
	☐	0% (die in dieser Abbildung wiedergegebenen Daten basieren ausschließllich auf Arbeiten anderer Koautoren)
	☒	Etwaiger Beitrag des Doktoranden / der Doktorandin zur Abbildung: 50 % Kurzbeschreibung des Beitrages: *Durchführung Tierversuche (i.v.-Injektionen zur HUS-Induktion, Volumengabe, Scoring, Blut- und Organentnahme), statistische Analyse, Interpretation der Daten, Erstellen der Grafik*

Abbildung # 7	☐	100% (die in dieser Abbildung wiedergegebenen Daten entstammen vollständig experimentellen Arbeiten, die der Kandidat/die Kandidatin durchgeführt hat)
	☐	0% (die in dieser Abbildung wiedergegebenen Daten basieren ausschließllich auf Arbeiten anderer Koautoren)
	☒	Etwaiger Beitrag des Doktoranden / der Doktorandin zur Abbildung: 50 % Kurzbeschreibung des Beitrages: *Durchführung Tierversuche (i.v.-Injektionen zur HUS-Induktion, Volumengabe, Scoring, Blut- und Organentnahme), Auswertung der Daten inkl. statistische Analyse Panel A, Interpretation der Daten, Erstellen der Grafik*
Abbildung # 8	☐	100% (die in dieser Abbildung wiedergegebenen Daten entstammen vollständig experimentellen Arbeiten, die der Kandidat/die Kandidatin durchgeführt hat)
	☐	0% (die in dieser Abbildung wiedergegebenen Daten basieren ausschließllich auf Arbeiten anderer Koautoren)
	☒	Etwaiger Beitrag des Doktoranden / der Doktorandin zur Abbildung: 30 % Kurzbeschreibung des Beitrages: *Durchführung Tierversuche (i.v.-Injektionen zur HUS-Induktion, Volumengabe, Scoring, Blut- und Organentnahme), Interpretation der Daten*

Tabelle # 1	☐	100% (die in dieser Abbildung wiedergegebenen Daten entstammen vollständig experimentellen Arbeiten, die der Kandidat/die Kandidatin durchgeführt hat)
	☐	0% (die in dieser Abbildung wiedergegebenen Daten basieren ausschließllich auf Arbeiten anderer Koautoren)
	☒	Etwaiger Beitrag des Doktoranden / der Doktorandin zur Abbildung: 20 % Kurzbeschreibung des Beitrages: *Zusammenstellung und Interpretation der Daten*
Tabelle # 2	☐	100% (die in dieser Abbildung wiedergegebenen Daten entstammen vollständig experimentellen Arbeiten, die der Kandidat/die Kandidatin durchgeführt hat)
	☐	0% (die in dieser Abbildung wiedergegebenen Daten basieren ausschließllich auf Arbeiten anderer Koautoren)
	☒	Etwaiger Beitrag des Doktoranden / der Doktorandin zur Abbildung: 20 % Kurzbeschreibung des Beitrages: *Zusammenstellung und Interpretation der Daten*
Tabelle # 3	☐	100% (die in dieser Abbildung wiedergegebenen Daten entstammen vollständig experimentellen Arbeiten, die der Kandidat/die Kandidatin durchgeführt hat)
	☐	0% (die in dieser Abbildung wiedergegebenen Daten basieren ausschließllich auf Arbeiten anderer Koautoren)

☒ Etwaiger Beitrag des Doktoranden / der Doktorandin zur Abbildung: 90 %

Kurzbeschreibung des Beitrages:

Durchführung Tierversuche (i.v.-Injektionen zur HUS-Induktion, Volumengabe, Scoring, Blut- und Organentnahme), Zusammenstellung und Interpretation der Daten, statistische Analyse

Acknowledgements

First and foremost, my heartfelt thanks goes to Prof. Dr. Dr. Sina Coldewey, not only for entrusting me with the interesting topic of this thesis and mentoring me, but also for being someone who never turned away from any problem, no matter if work-related or not. Thank you for offering me this chance and also believing in me when I did not.

I am thankful to Prof. Dr. Regine Heller for taking the role of my second supervisor and letting me stay in her lab to refine my immunoblotting skills.

Of course, I am also deeply thankful for all the fruitful cooperations without which this thesis would not have been possible. Namely, I would like to thank Prof. Dr. Florian Gunzer for the provision of Stx and Prof. Dr. Diana Imhof for the synthesis of pHBSP, but also, I am grateful to all other co-authors involved in the manuscripts that are the base for this thesis.

I would like to thank Dr. Bianka Wissuwa for her support and guidance in how to negotiate the obstacles in animal experiments and their documentation and the long, often after-work-hour discussions and talks that kept me on track. Thanks to Wiebke Pirschel for her assistance in the performance of animal experiments and the performance of histology and immunohistochemistry. A huge thank you also goes to our lab technician Dipl.-Ing. Jacqueline Fischer for the tireless performance of ELISAs, technical hints and (sometimes last-minute) replenishment of lab supplies and chemicals. I would also like to thank all other former and present colleagues in the lab for fruitful discussions, inspiring coffee breaks and helping hands or uplifting words when they were needed.

Heartfelt thanks also goes out to my family, especially my parents Kathrin and Jens and my little sister Luise. Although they did not always have a clue what I was doing in the lab at all, they did all their best to always support me in reaching my goals. (Thanks mom for forbidding me to become a lab technician in 10^{th} grade).

I would also like to thank my partner Jojo for the motivation and understandment during the last phase of paper submission and dissertation preparation. Of course, I also thank my friends, especially Kiko for emotional support during the pandemic, and Charlie for uplifting nerd evenings with soul food when I needed them most.

Ehrenwörtliche Erklärung

Hiermit erkläre ich, dass mir die Promotionsordnung der Medizinischen Fakultät der Friedrich-Schiller-Universität bekannt ist,

ich die Dissertation selbst angefertigt habe und alle von mir benutzten Hilfsmittel, persönlichen Mitteilungen und Quellen in meiner Arbeit angegeben sind,

mich folgende Personen bei der Auswahl und Auswertung des Materials sowie bei der Herstellung des Manuskripts unterstützt haben: Prof. Dr. med. Sina Coldewey, PhD,

die Hilfe eines Promotionsberaters nicht in Anspruch genommen wurde und dass Dritte weder unmittelbar noch mittelbar geldwerte Leistungen von mir für Arbeiten erhalten haben, die im Zusammenhang mit dem Inhalt der vorgelegten Dissertation stehen,

dass ich die Dissertation noch nicht als Prüfungsarbeit für eine staatliche oder andere wissenschaftliche Prüfung eingereicht habe und

dass ich die gleiche, eine in wesentlichen Teilen ähnliche oder eine andere Abhandlung nicht bei einer anderen Hochschule als Dissertation eingereicht habe.

Jena, den ……

_____

Sophie Dennhardt